

https://dspace.org/

Voltage uprating of existing high voltage substations when transient voltage stress and available withstand strength are coordinated

Schutte, Peet

2017

http://hdl.handle.net/10539/23546

Schutte, Peet (2017) Voltage uprating of existing high voltage substations when transient voltage stress and available withstand strength are coordinated, University of the Witwatersrand, <http://hdl.handle.net/10539/23546>

Downloaded from a DSpace repository. https://dspace.org/

MASTER'S DISSERTATION

VOLTAGE UPRATING OF EXISTING HIGH VOLTAGE SUBSTATIONS WHEN TRANSIENT VOLTAGE STRESS AND AVAILABLE WITHSTAND STRENGTH ARE COORDINATED



Author:
P.J Schutte

Supervisor:
Dr. J.M van Coller

A dissertation submitted to the Faculty of Engineering and the Built Environment, University of the Witwatersrand, Johannesburg, in fulfilment of the requirements for the degree of Master of Science in Engineering

in the

High Voltage Research Group
School of Electrical and Information Engineering

Johannesburg, June 2017

South Africa

DECLARATION

I hereby declare that this dissertation is my own unaided work. It is being submitted to the Degree of Master of Science to the University of the Witwatersrand, Johannesburg. It has not been submitted before for any degree or examination to any other University.

…….....

Petrus Johannes Schutte

…… day of …….. year ……..

ABSTRACT

Servitude availability in space-constrained built-up areas within the Johannesburg or Central Load Network (CLN) poses every-day challenges for power system engineers. Strengthening the backbone 88/275 kV transmission system within the CLN becomes even more difficult when multi-circuit transmission lines are required for increased power transfer capabilities. When uprating is considered to increase the power transfer capability, the withstand levels of existing external insulation demands an optimisation to find a new stress versus strength balance that allows reliable operation of substations at higher voltages. The research includes primarily an investigative simulation study to evaluate the current Eskom available design clearances in terms of their withstand capability when subjected to over-voltage transients. Two voltage range classes were evaluated and the results are discussed. For voltage range 1, it was found that the over-voltage stress was low enough to allow for a higher nominal operating voltage while maintaining the existing clearances. For voltage range 2, existing clearances are also found to be conservative and smaller safety margins will most likely be acceptable. From a transient analysis evaluation, voltage uprating is considered as a very attractive option to increase the power transfer capability of existing substations. Current Eskom clearances for 88 kV and 275 kV are expected to perform well during transients generated in uprated systems. Electrode grading to improve the field gradients in the substation will require attention to increase gap factors. Additional surge arresters are considered to be a cost effective solution to control over-voltages throughout the whole uprated substation. The physical modification of substations to replace strung conductors with tubular conductors, ensuring sufficient outage time to refurbish and rebuild with new equipment will be the most challenging part of uprating existing substations.

ACKNOWLEDGEMENTS

The completion of this work could not have been possible without the expertise and patient guidance of Mr Chris van der Merwe. I am grateful to have learned from you and appreciate the countless interactions and guidance. Your ability to transfer knowledge is remarkable and it is always a pleasure to work with you.

A special mention to Braam Groenewald who has introduced me to this topic of research, Mark Peffer for the mentorship and good example of integrity, and Phineas Tlhatlhetji for giving me the opportunity and expecting only the best of me.

To my academic mentor Dr. J.M van Coller of the University of the Witwatersrand, thank you for your support and guidance. In addition, a special acknowledgment to the Eskom Power Plant Engineering Institute (EPPEI) for the opportunity.

Finally yet importantly, I thank my family and spouse Christine Schutte for the support and encouragement to finish the research and strive for excellence.

SUMMARY

For fast-front over-voltages in voltage range 1, the results have shown that even with a very conservative approach the probability of the gap flashing over is very small. From the simulations, it was clear that for the protective margin to decrease below 25 % and diminish the available margin of protection the substation configuration will be required to be very impractical. The conclusion is to coordinate the selection of insulation for the protection of the non-recoverable insulation. Busbar arresters will assist with the required additional energy dissipation for severe fast transient over-voltages initiated by a back-flashover close to the substation. Busbar arresters will also limit over-voltages to the maximum allowable protective margin of 25 %, where very long conductor distances separate equipment from installed arresters at the line entrances and transformers.

For slow-front over-voltages in range 1 it was found that the protective distance of the surge arrester during switching surges extends beyond the substation busbars. This is due to the slow surge steepness. The over-voltage stress is expected not to exceed the arrester protective level when switching surges enter the substation. The Gallet – Leroy equation yields a switching impulse withstand value of 344 kV for the airgap when the gap factors are in the range of 1.0 for phase-to-earth and 1.16 for phase-to-phase. This implies that the electrode configuration with a gap factor of 1.0 and 1.16 decreases the airgap withstand strength to its minimum. The 1 m clearance will essentially have a 90 % probability of withstanding a switching surge with a peak of 344 kV. It is clear that switching surges generated in a 132 kV system will not stress the external insulation to a point where it should be considered as a risk.

The results for voltage range 2 switching studies yielded switching impulse withstand level (SIWL) values of 1019 kV for the phase-to-earth 2.35 m gap. When considering that the arrester limits the voltage to 642 kV, the margin of protection is in the range of 58.7 %. With the minimum protective margin required to be 25 %, and the phase-to-earth / phase-to-phase ratio required to be 1.5, the gap factors were adjusted to obtain a minimum expected SIWL for the standard air clearances. It was found that when the gap factors are 1.14 and 1.41 for phase-to-earth and phase-to-phase electrode configuration respectively, the SIWL values were 800 kV and 1200 kV. This suggests that at sea level, gap factors are not required to be larger than 1.14 and 1.41 to maintain a 25 % margin of protection for existing gaps. When at an altitude of 1800 m and above sea level, the withstand level is effectively reduced due to the air density being lower. When the gap factors are increased to 1.3 and 1.67 for phase-to-earth and phase-to-phase electrode configuration, the same withstand levels of 800 kV and 1200 kV with a 25 % protective margin are realised.

From a transient analysis evaluation, voltage uprating is considered as a very attractive option to increase the power transfer capability of existing substations. Current Eskom clearances for 88 kV and 275 kV are expected to perform well during transients generated in uprated systems. Electrode grading to improve the field gradients in the substation will require attention to increase gap factors. Additional surge arresters are considered to be a cost effective solution to control over-voltages throughout the whole uprated substation.

TABLE OF CONTENTS

1 INTRODUCTION 3

1.1 Background 3

1.2 Scope 5

1.3 Research questions 5
1.3.1 Evaluation of current Eskom clearance standard 5
1.3.2 Impact of additional surge limiting devices on expected over-voltages 5
1.3.3 Main challenges when considering uprating of substations 5

1.4 Research justification 5

1.5 Research approach 6

1.6 Chapter summary 7

2 LITERATURE STUDY 8

2.1 Introduction to insulation coordination and voltage uprating 8
2.1.1 Substation insulation coordination 9
2.1.2 Types of insulation 10
2.1.3 Standard atmospheric conditions 10
2.1.4 Standard wave shapes 10
2.1.5 Standardised LIWL, SIWL and clearances adopted in South Africa 12

2.2 Origins of switching transients 13
2.2.1 Capacitor bank energisation 17
2.2.2 Back-to-back capacitor switching 18
2.2.3 Transmission line closing and reclosing 20
2.2.4 Outrush transients 26
2.2.5 Switching of single core coaxial cables 27

2.3 Voltage stress classification 29
2.3.1 Main over-voltage classes 29
2.3.2 Fast-front over-voltages 30
2.3.3 Slow-front switching over-voltages 37
2.3.4 Temporary over-voltages 40
2.3.5 Determination of voltage stress 41

2.4 Limiting voltage stress 41

2.5 Dielectric strength of external insulation 42
2.5.1 Breakdown mechanisms of recoverable insulation 42
2.5.2 Airgap strength when subjected to power frequency voltages 46
2.5.3 Airgap strength when subjected to slow-front switching over-voltages 47
2.5.4 Airgap strength when subjected to fast-front lightning over-voltages 49
2.5.5 Contamination 50

2.6 Design clearances 52
2.6.1 Clearances based on lightning impulse 53
2.6.2 Clearances based on switching impulses 55

2.7 Metal-oxide varistor surge arresters 61
2.7.1 General Characteristic of the metal-oxide arrester 62
2.7.2 Arrester Classes 62
2.7.3 Energy Handling and discharge characteristics 62

2.7.4 Protective Margin 63
2.7.5 8/20 µs and 30/60 µs Discharge Voltage 63
2.7.6 Arrester Protective Distance 63

3 CALCULATIONS AND SIMULATIONS 65

3.1 Methodology for slow-front over-voltage studies 65

3.2 Methodology for fast-front over-voltage studies 67
3.2.1 Withstand levels and protective margin 68

3.3 Uprating 88 kV to 132 kV 68
3.3.1 Slow-front transient analysis 70
3.3.2 Fast-front transient analysis 74

3.4 Uprating 275 kV to 400 kV 77
3.4.1 Slow-front transient analysis 77

3.5 Other considerations 83
3.5.1 Increased Electromagnetic field strength 83
3.5.2 Altitude correction 83

4 RESULTS 84

4.1 Uprating 88 kV to 132 kV Results 84
4.1.1 Switching study 84
4.1.2 Lightning study 86

4.2 Uprating 275 kV to 400 kV results 93
4.2.1 Switching over-voltage stress simulation 93
4.2.2 Determination and selection of switching impulse withstand levels 106
4.2.3 Risk of failure based on specific switching impulse withstand level 108
4.2.4 Sending and receiving end clearance calculation 111

5 CONCLUSION 113

5.1 Voltage range 1: 88 kV uprated to 132 kV - transient analysis 113
5.1.1 Fast-front transients 113
5.1.2 Slow-front transients 114

5.2 Voltage range 2: 275 kV uprated to 400 kV - switching transient analysis 115

5.3 Recommendations and future work 116

6 REFERENCES 117

7 APPENDICES 119

7.1 Voltage range 1 and 2 statistical switching study ATP model 119

7.2 Voltage range 2 back-flashover ATP model 119

LIST OF FIGURES

Figure 2-1: Lightning impulse wave shape 11
Figure 2-2: Switching impulse wave shape 11
Figure 2-3: Conceptual illustration network equivalent 16
Figure 2-4: Capacitor bank inrush current 17
Figure 2-5: Capacitor Transient over-voltage (phase-to-earth) 18
Figure 2-6: Inrush current during back-to-back capacitor bank energisation 19
Figure 2-7: Back-to-back energisation of capacitor bank 20
Figure 2-8: Travelling wave [10] 23
Figure 2-9: Travelling wave behaviour at a point of discontinuity [10] 23
Figure 2-10: Sending and receiving end transient showing the travel time 25
Figure 2-11: Comparison of transient over-voltage during closing and reclosing 26
Figure 2-12: Capacitor bank outrush current 27
Figure 2-13: Transient inrush current when capacitor is energised 28
Figure 2-14: Transient over-voltage of capacitor 28
Figure 2-15: Negative downward impulse front definitions [25] 34
Figure 2-16: Probability of peak lightning currents [22],[25] 36
Figure 2-17: Semi-statistical analysis for determining the risk of failure 39
Figure 2-18 : Volt-Time characteristic of insulators for the standard lightning impulse 44
Figure 2-19: Power frequency CFO voltage and the impact of the gap factor 46
Figure 2-20: U - Curves for rod - plane gaps for slow-front over-voltages [30] 47
Figure 2-21: External Insulation CFO voltage approximation 48
Figure 2-22: CIGRE volt-time curve for line insulator flashover [30] 50
Figure 2-23: Insulator string CFO as a function of SSD [32] 51
Figure 2-24: Clearance based on LIWL as a function of the CFO gradient [30] 55
Figure 2-25: Arrester protective distance 64
Figure 3-1: Statistical switch distributions 66
Figure 3-2: 88 kV Feeder bay layout 69
Figure 3-3: Single-line diagram of substation with double busbar switching arrangement 70
Figure 3-4: 132 kV Interconnected transmission lines and substations 71
Figure 3-5: 108 kV Rated Voltage Maximum Current / Voltage characteristic curve 72
Figure 3-6: Statistical switch parameters 73
Figure 3-7: 88 kV Transmission line tower configuration 74
Figure 3-8: 132 kV Substation single-line diagram 75
Figure 3-9: 132 kV Substation simplified Scenario 2 75
Figure 3-10: Ramp type lightning current sources for simulation 76
Figure 3-11: 400 kV Interconnected transmission lines and substations 78
Figure 3-12: 312 kV Rated Voltage Maximum Current / Voltage characteristic curve 79
Figure 3-13: 275 kV Single circuit suspension tower 80
Figure 3-14: 275 kV Feeder bay layout for uprating to 400 kV 81
Figure 3-15: 275 kV Transformer bay layout for uprating to 400 kV 82
Figure 4-1: 88 kV standard clearance and SIWL for mid-point 85
Figure 4-2: 88 kV Standard clearance and SIWL for sending/receiving end 85
Figure 4-3: 88/132 kV back-flashover simulation model 86
Figure 4-4: Insulator voltage as a function of tower footing resistance 88
Figure 4-5: Tower top and phase A voltages indicating flashovers 89

Figure 4-6: Transient voltages propagating towards the substation 90
Figure 4-7: Line entrance arrester energy 92
Figure 4-8: Worst-case distributions for sending, mid-point and receiving end 97
Figure 4-9: Sending end worst case switching over-voltage 98
Figure 4-10: Sending end worst case switching over-voltage (with arresters) 98
Figure 4-11: Transmission line mid-point over-voltage distributions 100
Figure 4-12: Mid-point over-voltage distribution (including pre-insertion resistors) 101
Figure 4-13: Receiving end worst case switching over-voltage. 102
Figure 4-14: Receiving end worst case switching over-voltage (with arresters) 103
Figure 4-15: 275 kV Equivalent SIWL (based on standard clearances and specific gap factors) 106
Figure 4-16: 275 kV Equivalent SIWL (smallest gap factors to obtain worst case) 107
Figure 4-17: Over-voltage stress versus strength (5 GVA 50 km Sending end) 109
Figure 4-18: Over-voltage stress versus strength (20 GVA 400 km Receiving end) 110
Figure 4-19: Clearance as a function of the gap factor at 800 kV SIWL 111
Figure 7-1: Statistical switching study ATP model. 119
Figure 7-2: Back-flashover ATP model. 119

LIST OF TABLES

Table 2-1: Standard clearances (based on silicon-carbide arresters) [15] 13
Table 2-2: Capacitor bank switching philosophy comparison 20
Table 2-3: DC Trapped charge decay after 3 seconds [19] 22
Table 2-4: Closing and reclosing circuit breaker times and over-voltage values 26
Table 2-5: Critical over-voltages [17] 29
Table 2-6: Maximum over-voltage factors during interruption of magnetising currents [19] . 40
Table 2-7: Standard Eskom clearances CFO voltage approximations 48
Table 2-8: Standard Eskom voltage levels and clearance based on LIWL [17],[18] 54
Table 2-9: Typical phase-earth gap factors recommended by IEC [17] 56
Table 2-10: IEC recommended gap factors for phase-to-earth switching impulse [17] 57
Table 2-11: Typical phase-phase gap factors recommended by IEC [17] 58
Table 2-12: Switching surge parameters for phase-to-earth according to IEEE [18] 58
Table 2-13: Switching surge factors for phase-to-phase configurations IEEE [18] 59
Table 2-14: Basic withstand levels from IEC and IEEE [17], [18] 59
Table 2-15: The recommended minimum clearances according to the IEEE guide [9] 60
Table 2-16: Coefficient of variation comparison 60
Table 3-1: 88 kV bay layout dimensions 68
Table 3-2: 88 kV Busbar parameters 68
Table 3-3: 132 kV substation equipment distances 69
Table 3-4: Study 1 Positive sequence source parameters 71
Table 3-5: 108 kV Rated voltage surge arrester parameters 71
Table 3-6: 108 kV Rated arrester voltage/current characteristic 72
Table 3-7: 88 kV Single circuit transmission line parameters 74
Table 3-8: Lightning current source parameters 76
Table 3-9: Study 1 Positive sequence source parameters 78
Table 3-10: 312 kV Rated voltage surge arrester parameters 78
Table 3-11: 312 kV rated arrester characteristic for current impulse $U30/60\ \mu s$ 79
Table 3-12: 275 kV Single circuit transmission line parameters 81
Table 3-13: 275 kV bay layout dimensions 83
Table 4-1: Switching over-voltage distributions 84
Table 4-2: Eskom standard clearances for 88 kV and 132 kV substations 84
Table 4-3: Required SIWL for 88 kV airgaps when uprating to 132 kV 86
Table 4-4: Calculated and simulated tower top voltages 87
Table 4-5: Substation peak over-voltages in the substation for Source 4 91
Table 4-6: Sensitivity of arrester protective distance on transformer 2 CB 91
Table 4-7: Configuration 1 over-voltage distributions 93
Table 4-8: Configuration 2 over-voltage distributions 94
Table 4-9: Configuration 3 over-voltage distributions 95
Table 4-10: Configuration 4 over-voltage distributions 96
Table 4-11: Sending end worst-case over-voltage scenario 97
Table 4-12: Sending end arrester energy analysis 99
Table 4-13: Maximum transmission line mid-point distributions 99
Table 4-14: Risk of flashover at transmission line mid-point 100
Table 4-15: Receiving end worst case over-voltage scenario 102
Table 4-16: Receiving End Arrester Energy Analysis 103
Table 4-17: Single phase-to-earth fault over-voltage evaluation 104

Table 4-18: Surge arrester protective distance for slow-front switching surges 105
Table 4-19: Eskom standard clearances for 275 kV and 400 kV substations 107
Table 4-20: Standard 275 kV clearances and representative SIWL's. 108
Table 4-21: Sending end risk calculation based on 4 different SIWL's 108
Table 4-22: Receiving end risk calculation based on 4 different SIWL's 110
Table 4-23: The impact of altitude correction on preferred clearance 112

1 INTRODUCTION

1.1 Background

Servitude availability in space-constrained built-up areas within the Johannesburg or Central Load Network (CLN) poses every-day challenges for power system engineers. Strengthening the backbone 88/275 kV transmission system within the CLN becomes even more difficult when multi-circuit transmission lines are required for increased power transfer capabilities.

The need arises to investigate the feasibility of uprating the nominal voltage of existing substations. The field of insulation coordination within high voltage substations presents guidance for electrical engineers on adequately selecting the insulation to withstand the stresses the system is subjected to. Unfortunately, the standards that have been adopted are outdated and all designs are currently based on these guidelines [1]. Minimum electrical and operating clearances should be revised with regards to the use of modern metal-oxide surge arrester technology. Phase-to-earth and phase-to-phase clearances depend on a number of combined probabilistic calculations, but also include safety factors and other considerations mentioned in the literature [2]. Minimum clearances, surge protection devices and the approach of selecting the insulation for high voltage systems have evolved dramatically in the past 50 years.

Regarding transmission line capacity upgrading, a vast amount of literature is available. The methods and opportunities available to upgrade the capacity of transmission lines are well described in the literature [3] [4]. Instances where the capacity upgrading in transmission lines has been evaluated proved that thorough insulation coordination studies are required to establish the feasibility of voltage uprating [5]. Usually the substation is not the primary concern when evaluating the capacity upgrading. Substation upgrading or uprating is usually triggered by the transmission line infrastructure constraints. Transmission line uprating or upgrading methods are well understood and documented [6].

Substation voltage uprating is not so well documented in the literature. The safety aspects [7] and performance [8] of uprated substations has been documented but the literature lacks the design experience.

Avoiding unnecessarily large levels of conservatism (safety margins) will yield an optimised substation design. The revision of appropriate standards will inherently open the door to a more economical solution. Large levels of conservatism are found in substations with nominal voltage below 242 kV. It was found that lowering the insulation level one or two steps, similar levels of conservatism of higher voltage ranges are achieved [9].

According to A. R. Hileman, Substation insulation coordination includes mainly the specification of the following [10]:

1. Equipment insulation strength in terms of the Lightning Impulse withstand Level (LIWL) and the Switching impulse withstand Level (SIWL).
2. Phase-to-earth and phase-to-phase clearances.
3. Requirement of surge arresters and the specification thereof.
4. Requirement of protective gaps.
5. Shielding against lightning strikes.
6. Lightning performance of transmission lines connected to the substation.

It is well-known that apparatus-based electrical clearances have been verified by extensive laboratory testing and have existed for several years. Due to the complexity of substations as a whole, typical combinations of hardware assemblies, clamps, bus conductors, conductor stringers, droppers and insulators, have not been tested as extensively.

The AIEE Substations Committee published a guide [11] for minimum electrical clearances for substations. The guide was published in 1954 and presented clearances based mainly on phase-to-ground clearances and lightning over-voltage flashover (1.3 m rod gap [10]) at selected Basic Lightning Impulse withstand levels. The clearance values did however account for altitude correction and, before any safety margin adjustment, reflected a breakdown gradient for air of 600-850 kV/m.

The IEEE Substations Committee published the first reports on minimum electrical clearances based on switching surge phenomena [12]. The electrical clearances listed within this document were published for reference to operating voltages exceeding 242 kV. In 1972 the Committee published updated clearances based on switching surge requirements [13].

In 1975 Georges Gallet [14] et al. presented the well-known and generally accepted expression describing the positive switching impulse strength of air insulation. The concept of gap factor, k_g was also introduced during this time and was valid for airgap configurations between 1 m and at least 30 m.

The current standard insulation clearances for Air-Insulated-Substations (AIS) used by Eskom are based on the old Electrical Engineering Directive 14/1/5-1 [1]. This document was based on the British Standards of the time. All the clearances were based on lightning impulse withstand values. The literature clearly states that clearances for nominal voltages exceeding 132 kV are determined by switching surge phenomena. In addition to this, metal-oxide surge arresters were not yet in existence during the time of the compilation of the recommended clearances. All these clearance values were based on gapped-type silicon-carbide arresters. Metal-oxide arresters limit over-voltages to 1.8 p.u compared to the 2.6 p.u typical of gapped-type arresters.

The need to investigate the uprating of existing transmission lines and substations is therefore driven by the increasing load growth and limited availability of servitudes. Voltage uprating involves increasing the nominal voltage while maintaining the original insulation level. Voltage sensitive equipment will have to be replaced but the aim would be to retain the existing infrastructure in the substation. It is understood that there would certainly be additional strategies to be considered to increase the withstand capability of the whole system. Additional surge arresters in strategic positions and increased shielding strategies against lightning strikes will have to be evaluated to increase the withstand capability of the substations.

1.2 Scope

This research covers air-insulated substations with nominal operating voltage of 88 kV (phase-to-phase) and above. It aims to address the need for voltage uprating of existing substations to improve the power transfer capability of the interconnected transmission network.

The emphasis of the study is to establish the expected transient over-voltage stresses an air-insulated substation might experience. This primarily includes transients initiated by switching and lightning. Temporary over-voltages and electromagnetic field effects are not included within the study.

Although guidelines are available for compact design, current outdated guidelines in terms of clearances are still being followed. The aim is not to revise current standards within the utility, but to provide clarity on the approach of compact substation design when transient over-voltages are considered. A detailed over-voltage stress analysis is included as the one of the primary inputs to calculate the risk of insulation failure. When the voltage stresses and available external withstand strength are coordinated, the outcome is expected to produce a reliable solution for voltage uprating.

The research will allow the substation design engineer to be aware of the transient design criteria related to voltage uprating, with safety as a priority and to maintain an acceptable level of system reliability.

1.3 Research questions

1.3.1 Evaluation of current Eskom clearance standard

Referring to international recommended guidelines, external insulation withstand capability analysis and the expected maximum voltage stresses in an uprated substation, how conservative are the current Eskom Standard substation clearances for 88 kV and 275 kV?

1.3.2 Impact of additional surge limiting devices on expected over-voltages

What is the impact on the expected voltage stresses within uprated 88 kV and 275 kV substations when additional surge limiting devices are included in key positions?

1.3.3 Main challenges when considering uprating of substations

When coordinating the voltage stress and strength with regards to internal and external air insulation, what are the main challenges in terms of transients to overcome when evaluating the possibility of uprating substations in voltage range 1 (88 kV to 132 kV) and voltage range 2 (275 kV to 400 kV)?

1.4 Research justification

Eskom needs to strengthen the 88/275 kV network in and around the Johannesburg area. Due to land and servitude availability, it is almost impossible to construct new transmission lines and substations. The need arises to consider the uprating of the nominal voltage of existing substations and transmission lines.

Very conservative electrical clearances for insulation coordination in transmission substations have produced in some cases very large and overdesigned substation layouts. Substation compacting can be achieved following international guidelines on minimum

clearances but all of these guidelines are standardised clearances for specific withstand levels or nominal voltages [2].

To optimise the insulation requirements to allow successful voltage uprating, the voltage stresses in the substation need to be evaluated. Additionally, the withstand capability of the airgaps currently available as minimum clearances within the substation need to be studied. The selection of insulation levels to withstand the voltages stresses regarding equipment is also standardised within Eskom, and the results of this research will clearly define how conservative the current approach is.

1.5 Research approach

The Substation Layout Design Guide [15] (internal Eskom technical guide on substation design) clearly defines the insulation coordination approach Eskom has adopted. The minimum clearances for phase-to-earth and phase-to-phase voltages are also specified as a guideline.

The evaluation of basic insulation coordination concepts, supported by the literature will set the platform to investigate a more optimised approach to allow for the feasibility of nominal voltage uprating of substations.

Existing High and Extra High Voltage substation configurations will be studied. The main purpose will be to determine where the risk of insulation breakdown might be high. The study will include the consideration of mitigation strategies to increase the protection and withstand capability of the system against surge over-voltages.

For uprating 88 kV to 132 kV, a representative substation configuration is subjected to fast-front over-voltage. Over-voltages in the substation at different locations are evaluated to determine the arrester protective distance and margin. The substation is subjected to worst-case fast-front surges to investigate whether or not the available clearance is sufficient for uprating. The impact of adding more surge arresters at strategic locations within substations will be determined with transient simulations. Although switching over-voltages are not of primary concern in this voltage range, statistical switching studies will serve as the best method to analyse the risk of insulation failure.

For uprating 275 kV to 400 kV, a standard 275 kV transmission line tower geometry is considered. For the substation arrangement, an Eskom 275 kV feeder and transformer bay arrangement is considered to evaluate the available clearances. For this study, an extensive statistical study will yield the best results for evaluation. Transient simulations are required to be evaluated statistically to gather information of representative over-voltage distributions and to determine the risk of insulation failure. Over-voltage distributions at the sending, receiving and mid-point of the transmission line are obtained with and without surge limiting devices. Worst-case scenarios are extracted from the distributions to evaluate the energy demand on the arresters at the sending and receiving ends of the line. Additional surge limiting methods are studied to minimise the mid-point over-voltages. Standard Eskom clearances are converted into switching impulse withstand levels to evaluate optimum electrode configurations to minimise the risk of flashover. The system configurations will include primarily the energisation of transmission lines of different lengths with the combination of different source parameters. The scenarios to consider are to combine line lengths of 50, 100, 200 and 400 km with source short-circuit powers of 5, 10 and 20 GVA.

1.6 Chapter summary

- Chapter 1 Introduction

In this chapter, a background is given regarding the concept of voltage uprating and the need to investigate this. The scope of the research is defined and the research questions are captured. The research justification and approach are discussed.

- Chapter 2 Literature Study

In this chapter an overview of insulation coordination and voltage uprating is given. The Standard implemented in South Africa is discussed and background is given on how the Standard is used. Main over-voltage stress classes and how the stress can be limited is discussed. External air insulation strength is evaluated in the literature and a good overview is given on the withstand levels of airgaps. The substation design clearance is evaluated with reference to the IEEE and IEC standards to determine the best practice.

- Chapter 3 Calculations and Simulations

In this chapter, the methodologies for the relevant insulation coordination studies are described. Two-voltage range groups are discussed where the simulations are described in terms of the technical approach.

- Chapter 4 Results

In this chapter, all the results of the studies are captured. The main results for voltage range 1 include the switching and lightning studies. For voltage range 1, the results include detailed lightning studies of a back-flashover and a simplified switching study. For voltage range 2, only a switching study was performed and the results are captured. The study includes detailed configurations to determine the maximum expected over-voltage stress distributions, withstand level selection, risk of failure analysis and clearance calculations.

- Chapter 5 Discussion and conclusions

This chapter includes the main conclusions regarding the research and revisits the research questions. Both voltage ranges are discussed separately. Recommendations and future work are discussed.

2 LITERATURE STUDY

2.1 Introduction to insulation coordination and voltage uprating

Although the focus of this research primarily includes substation voltage uprating, it is impossible to separate the main concepts from transmission line uprating. Power system engineers encounter two major constraints regarding power transfer capability. Firstly, the transmission system thermal constraint, which includes the avoidance of over-heating and conductor current carrying capacity. Usually this constraint refers to the overloading of transmission lines in terms of current carrying capacity of the line and conductor bundles. For increasing the current carrying capacity, reference is made to the practice of thermal uprating. The second constraint is the transmission system voltage constraint. Steady state over-voltages form part of temporary over-voltages and can cause insulation failure, short-circuits, damage to equipment, etc. Maximum operating voltages are usually between 5 and 10 % above the nominal voltage. To increase the power transfer capability, uprating the nominal voltage should be considered as a viable solution.

It is important to evaluate both the substation and the transmission lines involved when voltage uprating is considered. Some of the usual technical criteria regarding voltage uprating include [16]:

- Analyse transmission line and substation clearances,
- Corona performance,
- Electric and magnetic fields,
- Right of way limitations and servitudes,
- Pollution criteria,
- Structural and mechanical strengths.

Techniques used to perform voltage uprating might include [16]:

- Addition of insulator units,
- Replacement of ceramic insulators with non-ceramics,
- Replacement or inclusion of V-strings rather than I-strings,
- Re-tensioning conductors to minimise sag,
- Raising, inserting new, moving of towers,
- Improving corona performance,

Most of the electrical engineering challenges regarding voltage uprating are related to insulation coordination. A number of definitions could define insulation coordination. First the goal should be defined. The goal of the insulation within a substation environment is fundamentally focused around limiting the risk of insulation breakdown. It is almost impossible to completely prevent the breakdown of insulation, but carefully selecting the insulation strength to improve the withstand capability of the system is directly linked to the probability of insulation breakdown.

Furthermore, when considering the anticipated over-voltages and the acceptable risk of failure, the selection of insulation strength could be defined more accurately. When surge protective devices are included into the selection criteria the goal is defined even more.

The expanded definition of insulation coordination is then given by [10]:

“Insulation coordination comprises the selection of the electric strength of equipment and its application, in relation to the voltages which can appear on the system for which the equipment is intended and taking into account the characteristics of available protective devices, so as to reduce to an economically and operationally acceptable level the probability that the resulting voltage stresses imposed on the equipment will cause damage to equipment insulation or affect continuity of service”

By a simplified definition it is “ the art of correlating equipment electrical insulation strengths with expected over-voltage stresses so as to result in an acceptable risk of failure while considering economics and operating criteria” [17].

The goal is then not only to select the strength of insulation, but also to optimise the selection to select the minimum insulation, or minimum clearance to minimise cost.

The process fundamentally includes the following:

- Reliability criteria selection,
- Determination of electrical stresses,
- Comparison of stresses and insulation strength characteristics,
- Selection of strength,
- Reduction of stress by means of protective devices.

After the selection of reliability criteria, the process simply involves extensive comparison between the stresses versus strength.

The sources of stress that should be considered mainly include:

1. Lightning over-voltages, created by lightning strikes,
2. Switching over-voltages, created by operating of circuit breakers or disconnectors or faults in the system.

2.1.1 Substation insulation coordination

The concept of insulation coordination was defined in the original context mainly to arrange the insulation levels of the components in the high voltage system in such a manner that if an insulation failure did occur, it would be confined to the place on the system where it would result in the least amount of damage, be least expensive to repair, and cause the smallest disturbance to the continuity of supply. The term has developed over the years and is used in a much broader sense today.

The scope of the research includes the insulation coordination optimisation of air-insulated substation (AIS) assemblies of structures supporting equipment and buses exposed to atmospheric conditions that use air as the external insulating medium.

To be more specific for the design of AIS substations the following should be considered:

- Equipment insulation strength,
- Phase-earth and phase-phase clearances,
- Surge arrester need (location, rating and quantity),
- Protective gap need (location, rating and quantity),
- Shield wires and masts for lightning protection (location, type).

It is important to note that the approach Eskom has adopted for substation design clearances is based on the old silicon-carbide gapped-type surge arrester protective characteristics. The ability of the silicon-carbide arresters to limit over-voltages cannot be compared to the more advanced metal-oxide varistor (MOV) type surge arresters. The reliability of the old technology was also a great concern and the failure rates were very high. The reliability of the surge arresters has a significant impact on the reliability of the substation. The two major improvements of the MOV arresters are the significant improvement of reliability and lower clamping voltages. It is evident that MOV surge arresters should be considered when the over-voltage stresses and insulation strengths are coordinated.

2.1.2 Types of insulation

The insulation could be separated into categories: Internal, external and also as self-restoring (also known as recoverable) and non-self-restoring (non-recoverable) [10].

External insulation refers to the distances between electrodes in open air and across surfaces of the solid insulation of equipment in contact with open air that are subjected to dielectric stresses and to the effects of atmospheric and other external conditions such as pollution.

Self-restoring insulation refers to a type of insulation that is capable of a complete recovery of its insulation properties after a disruptive discharge. Often this type of insulation is external insulation.

Non-self-restoring insulation loses its insulation properties or does not fully recover completely after a disruptive discharge. Internal insulation is generally a type of non-self-restoring insulation.

2.1.3 Standard atmospheric conditions

The insulation strength is based on the standard atmospheric conditions [10]:

1. Ambient air temperature of 20 ºC,
2. Air pressure of 101.3 kPa,
3. Absolute humidity of 11 grams of water/m^3 of air,
4. For rain tests 1 to 1.5 mm of water/minute,
5. Altitude: Sea level.

When the specific calculations are done for actual atmospheric conditions, the strength in terms of voltage is corrected to these standard values.

2.1.4 Standard wave shapes

The equipment insulation strength is defined by the basic lightning impulse insulation level (LIWL), and by the basic switching impulse insulation level (SIWL) [18].

The LIWL and SIWL could be better defined by the standard lightning and switching impulse wave shapes. These wave shapes are described by their time to crest and their time to half value of the tail. It is important to note that the definition of the time to crest for these two waveforms differs.

For the lightning impulse waveform a line is drawn between the two points t_{30} and t_{90}. That is, two points where the voltage is equal to 30% and 90% of the crest voltage. The point at

which this line intersects the zero voltage line is called the virtual origin and the wave shape is measured from this point at all times. A horizontal line is then drawn across the crest value so as to intersect the t_{30} - t_{90} line. The time from the virtual origin to the point of this intersection is called the time to crest, or the virtual time to crest t_f. The time to half value is the time between the virtual origin and the time where the voltage decreases to 50% of the crest value, t_T [10].

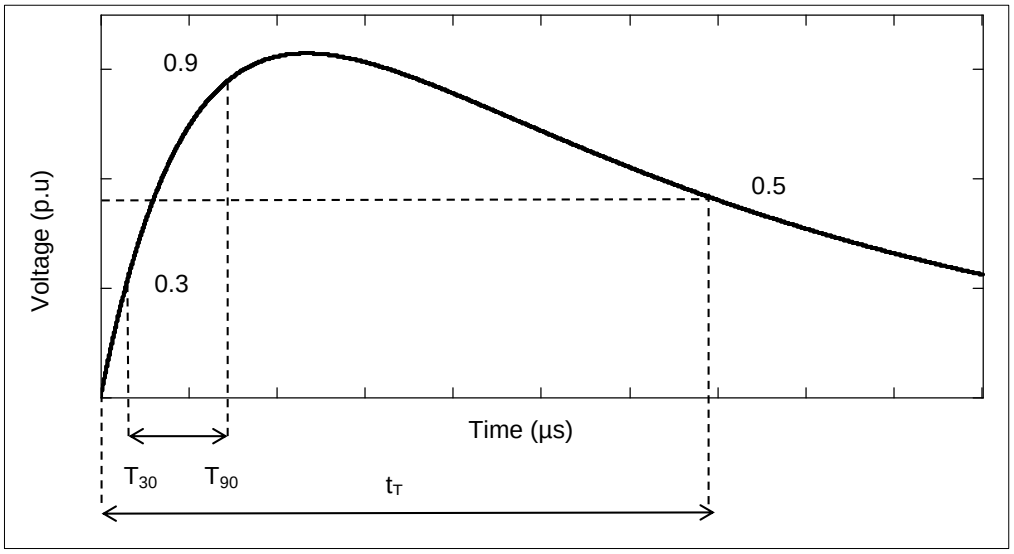


Figure 2-1: Lightning impulse wave shape

In general, wave shapes are described by the relationship between t_f and t_T. More specifically t_f/t_T µs. The standard lightning impulse wave shape is 1.2/50 µs shown in Figure 2-1.

For the switching impulse wave shape in Figure 2-2, the time to crest is measured from the actual time zero to the actual crest value of the impulse. The tail is defined by the time to half value, the time is also measured from the actual time zero and not the virtual time zero.

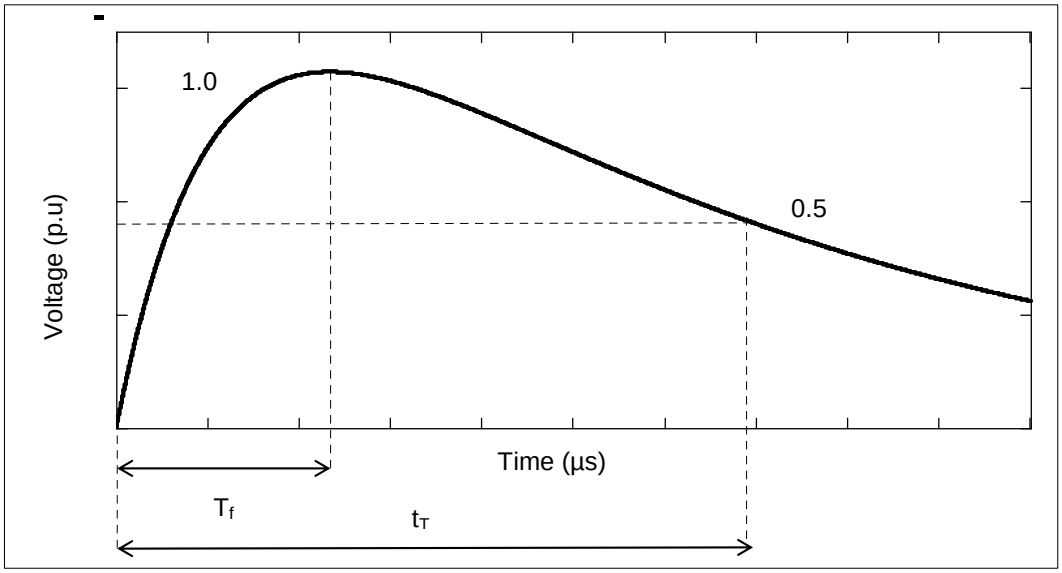


Figure 2-2: Switching impulse wave shape

The standard switching impulse wave shape is 250/2500 μs, again described by the relationship t_f/t_T μs [10].

2.1.5 Standardised LIWL, SIWL and clearances adopted in South Africa

Currently in South Africa, the substation insulation coordination only regards the LIWL as a determining factor when it comes to the standardised withstand levels and electrical clearances.

The LIWL is "the electrical strength of insulation expressed in terms of the crest value of the standard *lightning* impulse under standard atmospheric conditions." [10]

The LIWL is usually defined for dry conditions and the SIWL for wet conditions. The LIWL and SIWL are equal to the crest value of the standard impulse wave shapes mentioned in the previous paragraph.

The SIWL is "the electrical strength of insulation expressed in terms of the crest value of the standard *switching* impulse." [10]

Both the LIWL and SIWL may be expressed as either statistical or conventional. The statistical LIWL and SIWL are defined probabilistically. When the standard waveforms with a crest value equal to the LIWL or SIWL are applied, the probability of a flashover is 10%.

The insulation strength characteristic is represented by a cumulative Gaussian distribution. The mean of the distribution is defined by the critical flashover voltage (CFO). When the critical flashover voltage is applied to the insulation, a 50% probability of a flashover is realised. Aiming then for a 10% probability of a flashover, results in the definition that the LIWL and SIWL are 1.28 standard deviations below the CFO. The statistical LIWL and SIWL can be best described by the following equations [10]:

$$\text{LIWL} = CFO\left(1 - 1.28\frac{\sigma_f}{CFO}\right) \tag{2.1}$$

$$\text{SIWL} = CFO\left(1 - 1.28\frac{\sigma_f}{CFO}\right) \tag{2.2}$$

Sigma, σ_f, is the coefficient of variation. The standard coefficients of variation of lightning and switching impulse breakdown voltages differ. Sigma is in the range of 2 to 3% for lightning impulses, and for switching impulses ranges between 5 and 7% [10].

The conventional LIWL and SIWL are derived when the insulation withstands 1 – 3 impulse applications with a crest value equal to the LIWL or SIWL.

As mentioned before, in South Africa, electrical clearances are mainly based on the LIWL. This LIWL is calculated and standardised for design application.

The standardised electrical clearances are calculated as a function of the LIWL. The following equations describe the relatively poorly defined phase-to-earth (C_e) and phase-to-phase (C_p,) electrical clearances in millimetre [15].

$$C_e = 2.26(\text{LIWL}) - 20mm \tag{2.3}$$

$$C_p \begin{matrix} = 1.35.C_e\ (up\ to\ 650\ kV\ \text{LIWL}) \\ = 1.25.C_e\ (\text{LIWL} > 650\ kV) \end{matrix} \tag{2.4}$$

Referring to the equations it is clear that the clearances are mainly a function of the LIWL and a scaling factor. The factor to adjust from the phase-to-earth clearance to the phase-to-phase clearance is defined within the Electrical Engineering Directive EED 14/1/5-1 [1].

Currently in South Africa, substation clearances are based on assuming the use of silicon-carbide gapped-type surge arresters. The following table summarizes the electrical and working clearances applied in the substation design environment. The LIWL is then calculated and standardised as summarised in Table 2-1.

Table 2-1: Standard clearances (based on silicon-carbide arresters) [15]

Nominal Voltage (RMS phase-to-phase kV)	Maximum Voltage (RMS phase-to-phase kV)	Withstand Levels (kV)		Minimum Electrical Clearance (mm)		Minimum Working Clearance (m)	
		LIWL	SIWL	Phase-to-earth	Phase-to-phase	Vertical	Horizontal
88	100	380	-	1000	1350	3.5	2.1
132	145	550	-	1200	1650	3.7	2.3
275	300	1050	850	2350	2950	4.8	3.4
400	420	1425	1050	3200	4000	5.7	4.3

2.2 Origins of switching transients

Transient over-voltages in power systems may have an adverse effect on key equipment. This in turn affects the reliability of the system. Over-voltage transients are also a major determining factor when specifying the external insulation to obtain acceptable system reliability. Normally these transients are introduced during switching operations, fault clearing, and lightning strikes or due to equipment failure. Time-domain computer models are typically developed to evaluate these transients. The Electromagnetic Transient Program (EMTP) usually performs complex simulations of this kind [19].

Capacitor bank switching and transmission line switching are closely related in that both are essentially a capacitor being charged and discharged during switching. The majority of switching operations being energising and de-energising of capacitive elements such as capacitor banks, transmission lines and cables, leads to an emphasis put on these transients.

Consider a basic circuit containing an inductance L, capacitance C and resistance R. This circuit is in fact very common among power systems and can represent a transmission line, capacitor bank or cable network. The circuit contains two energy storage devices, an inductance storing magnetic energy (magnetic field) and a capacitance storing charge (electric field). When the switch is closed, an exchange of energy between the magnetic field, and the electric field takes place and as a result, an oscillation occurs. The frequency of this oscillation is a function of the inductance and capacitance of the circuit [20].

When a sinusoidal source voltage $E_{max}\sin(\omega t + \varphi)$ is switched on in a series RLC circuit at t = 0, Kirchhoff's voltage law leads to the following expression:

$$E_{max}\sin(\omega t+\varphi)=L\frac{di}{dt}+Ri+\frac{1}{C}\int i\,dt \tag{2.5}$$

To find the transient response of the circuit, solving the homogeneous differential equation is necessary.

$$0=\frac{d^2i}{dt^2}+\frac{R}{L}\frac{di}{dt}+\frac{1}{LC}i \tag{2.6}$$

The complete solution for the oscillating current is obtained where the current is expressed as a function i(t) [20].

$$i(t)=K+\frac{E_{max}}{\sqrt{R^2+\left(\frac{1}{\omega C}-\omega L\right)^2}}.sin\left[\omega t+\varphi+tan^{-1}\left(\frac{\left(\frac{1}{\omega C}-\omega L\right)}{R}\right)\right] \tag{2.7}$$

Where

$$K=e^{\propto t}[k_1\cos(\beta t)+k_2\sin(\beta t)] \tag{2.8}$$

$$\propto=-\left(\frac{R}{2L}\right) \tag{2.9}$$

$$\beta=\left[\left(\frac{1}{LC}\right)-\left(\frac{R}{2L}\right)^2\right]^{1/2} \tag{2.10}$$

$$\omega=2\pi f_s \tag{2.11}$$

The transient over-voltage is then a function of the high frequency oscillating current. The magnitude of the peak inrush oscillating current is approximated by the following expression:

$$i(t)=\frac{V(0)}{Z_0}\sin(2\pi f_s t) \tag{2.12}$$

Where V(0) is the difference between the source voltage and the initial voltage of the capacitor at the instant of energisation.

The characteristic impedance is as follows:

$$Z_0 = \sqrt{\frac{L}{C}} \tag{2.13}$$

The size of the capacitor determines the magnitude of the inrush current due to its effect on the characteristic impedance. The damping constant, characteristic impedance and natural frequency of the circuit can be calculated as a function of the inductance, capacitance and resistance of the circuit.

After the switch is closed the transient current flows at the natural frequency.

$$f_s = \frac{1}{2\pi\sqrt{LC}} \tag{2.14}$$

The transient inrush current consists of high magnitude, high frequency components initially and then decays over time. The damping of the system refers to the time constant that dictates the duration of the decay.

The steepness of the current referred to as di/dt, reaches high values just after energisation. When considering the voltage across the capacitor, it is clear that the transient originates due to the high di/dt components.

$$V_C = V_{source} - V_L - V_R \tag{2.15}$$

$$V_C(t) = E_{max}\sin(\omega t + \varphi) - L\frac{di(t)}{dt} - Ri(t) \tag{2.16}$$

$$\omega = 2\pi f_s \tag{2.17}$$

The voltage across the capacitor during the initial transient behaviour essentially oscillates due to the contribution of the voltage across the inductor. This contribution of the inductor is a function of the inductor size and the steepness of current passing through.

The steady state charging current is:

$$i_c = \frac{E_{max}}{Z} \tag{2.18}$$

Where

$$Z = \sqrt{R^2 + \left(\omega L + \frac{1}{\omega C}\right)^2} \tag{2.19}$$

Switching transients usually have very complex waveforms and require special attention when the insulation coordination process is followed. Insulation coordination studies with the assistance of computer simulations are required in most cases. System parameters are obtained and models are developed in detail to maximize the accuracy of the results. For

substation insulation coordination it is essential to understand the maximum values of over-voltage, and also the probability distributions of the total expected stresses the system is likely to experience.

For illustrative purposes regarding the capacitive switching transients, consider a power system consisting of a number of common elements usually connected at the substation. The substation is connected to a feeding network with an equivalent impedance and sinusoidal voltage source. This source impedance represents the total short-circuit power of the rest of the network. The substation busbar is connected to two capacitor banks, transmission line, single core cable, fault equivalent connection and a step-down transformer.

The magnitudes of the over-voltages must be known when considering voltage uprating. To understand the switching surge phenomena regarding capacitive switching, the following section provides background to the most common scenarios encountered. The different configurations are shown in Figure 2-3.

The source parameters are an equivalent resistance and inductance representing the short-circuit capability of the network. The source parameters are as follows: R1 = 6 Ω, L1 = 54 mH (13.6 kA single phase fault level).

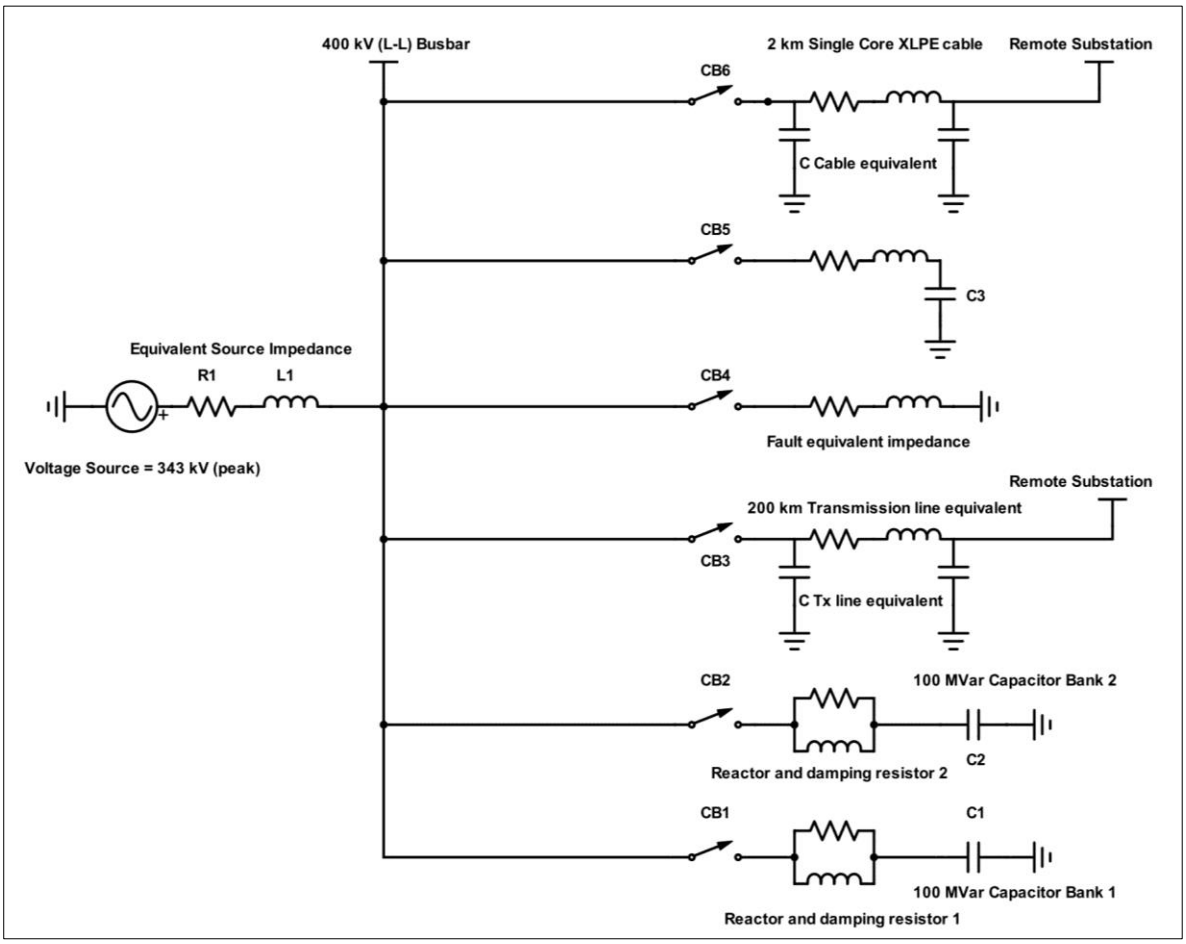


Figure 2-3: Conceptual illustration network equivalent

2.2.1 Capacitor bank energisation

Firstly, consider the energisation of Capacitor bank 1. CB1 is closed and during the instant of energisation the inrush current transient is initiated. For illustration purposes 2 x 400 kV 100 MVar capacitor banks are connected to the 400 kV busbar.

The capacitor bank parameters are as follows:

Capacitance C = 0.9 µF/phase

Reactor inductance L = 800 µH/phase

Damping resistor R = 10 Ω/phase

At the instant of energisation, a fully discharged capacitor bank acts like a short-circuit. The source bus voltage collapses when the circuit breaker closes and then recovers over time in an oscillatory manner. The worst-case scenario of circuit breaker timing is when the breaker closes at the peak of the source voltage. In the following scenario, the peak voltage is at t = 0, and the source voltage can be observed as a cosine function.

When closing CB1 at the peak source voltage (at t = 0), the exchange of energy storage between the feeding inductance and capacitor bank capacitance produces an oscillating inrush current.

The transient inrush current waveform reaches a maximum of almost 1.5 kA with a frequency of 722 Hz as shown in Figure 2-4.

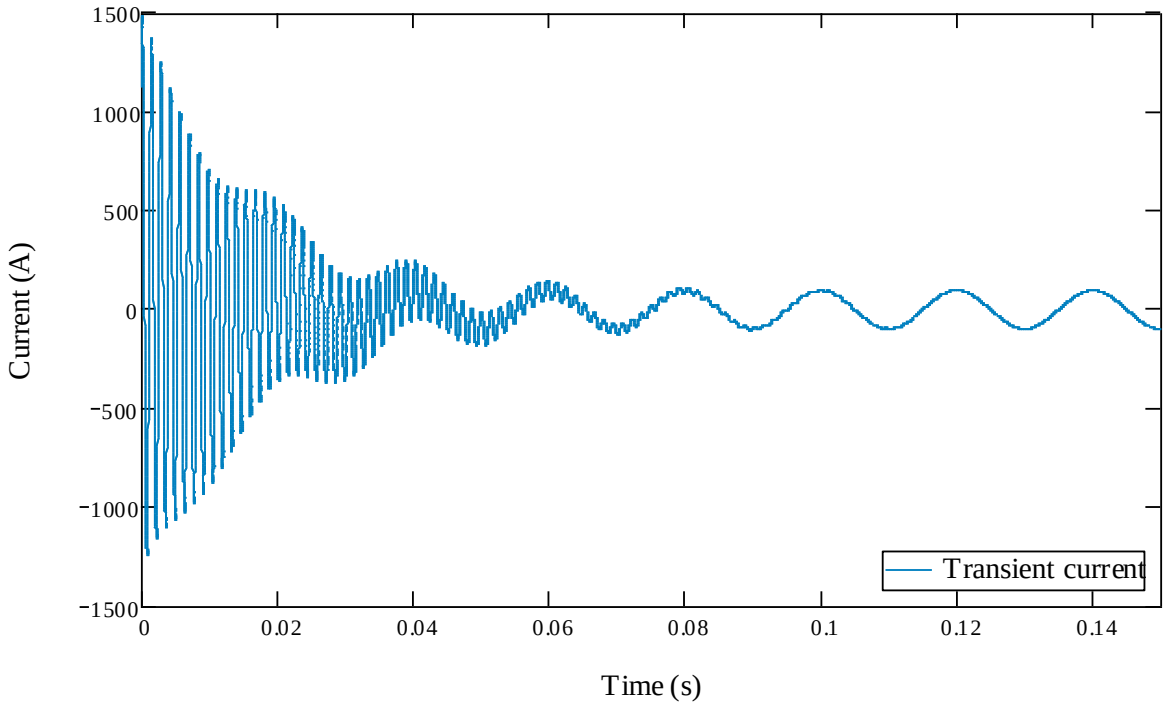


Figure 2-4: Capacitor bank inrush current

The transient current produces an over-voltage in the range of 1.9 p.u. The normal procedure is to earth the neutral of the capacitor bank and this earthing convention contributes to limiting the over-voltage on the healthy phases during earth faults.

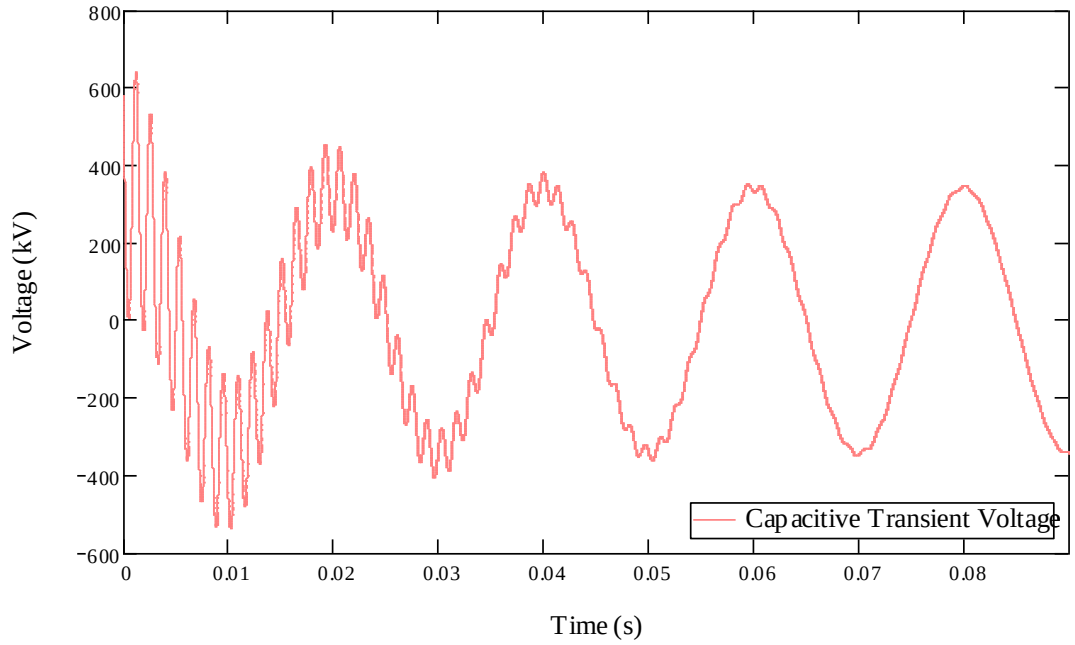


Figure 2-5: Capacitor Transient over-voltage (phase-to-earth)

The voltage oscillations as shown in Figure 2-5 can be dangerous and should be carefully evaluated. When a surge protection device is installed, it is important to select the device based on the total energy that it will be required to dissipate during these transients. During fault conditions, there is a probability that the fault current will only be cleared after 500 ms. This is when the backup protection operates and clears the fault. During this time, very high fault currents will flow depending on the source short-circuit strength. Depending on the earthing factor, the voltage of the healthy phases could rise and produce significant temporary over-voltages.

2.2.2 Back-to-back capacitor switching

During the energisation of a second capacitor (C_2) while one capacitor (C_1) is already in service, extremely high inrush currents are contributed to the energisation of C_2 by the capacitor in service. The inrush current into the capacitor being energised is also a high frequency transient oscillation. The frequency of the current is a function of the equivalent capacitance.

The equivalent capacitance (C_{EQ}) of two parallel capacitors with capacitance C_1 and C_2 is then given by the following expression:

$$C_{EQ} = C_1 + C_2 \tag{2.20}$$

$$f_s = \frac{1}{2\pi\sqrt{LC_{EQ}}} \tag{2.21}$$

$$i(t) = \frac{V(0)}{Z_{01}} \sin(2\pi f_s t) \tag{2.22}$$

$$Z_{01} = \sqrt{\frac{L}{C_{EQ}}} \tag{2.23}$$

The complexity of the higher order differential equations is too complex for manual calculations and it is better to use EMTP software for the evaluation of the transient behaviour.

In Figure 2-6 the high inrush current of approximately 5 kA appears briefly and transfers to the oscillatory transient charging current of value much lower. These rather high current transients can cause damage to the capacitors of the capacitor bank. The switching device is also subjected to severe stresses. During the disconnection of a capacitor bank, the interrupter opens its contacts where the current passes through the zero crossing. The voltage at this point is at its maximum, and remains at this voltage due to trapped charge. The source voltage is in steady state and the voltage across the disconnecting device can reach 2 p.u. When the interrupting device initiates its closing sequence, dielectric breakdown of the insulation between the interrupter terminals can lead to a prestrike. The prestrike consists of the dielectric breakdown of insulation just before the contacts touch during a closing operation. The suddenly created plasma channel contains very high currents and can cause the contact material to melt.

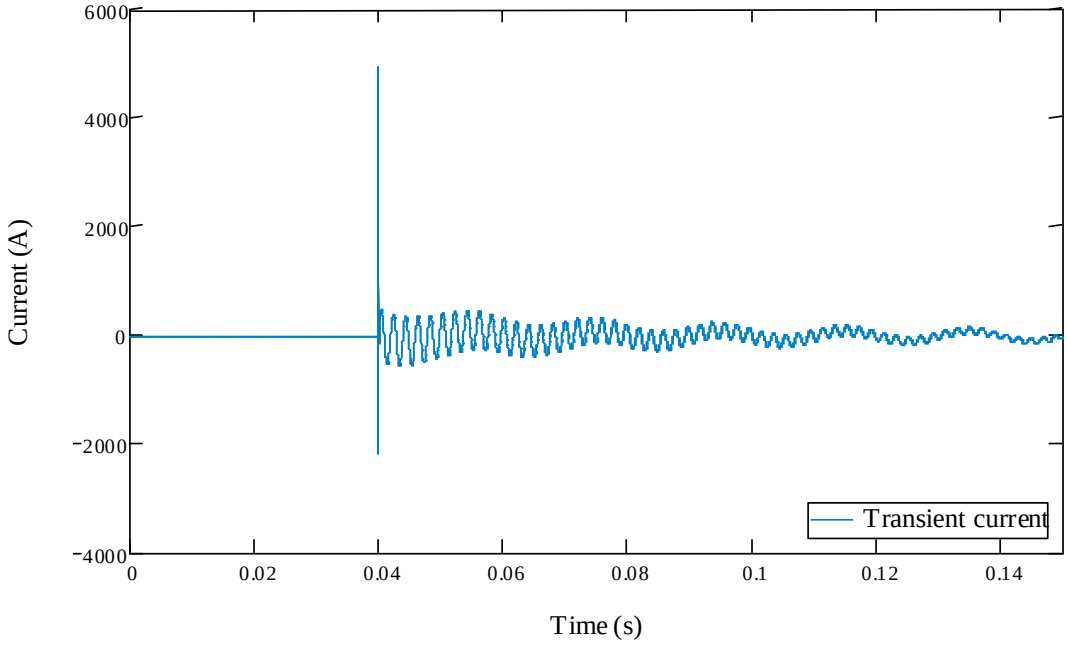


Figure 2-6: Inrush current during back-to-back capacitor bank energisation

With reference to the source voltage, it is best to switch during a zero crossing of the voltage. With additional capacitance connected to the busbar, the voltage does not collapse as severely when compared to the switching of a single capacitor bank. The results are listed in Table 2-2.

Table 2-2: Capacitor bank switching philosophy comparison

	Single capacitor bank	Back-to-back
Over-voltage peak (kV)	666	498
Inrush current peak (A)	1360	4910
Oscillation frequency (Hz)	722	510

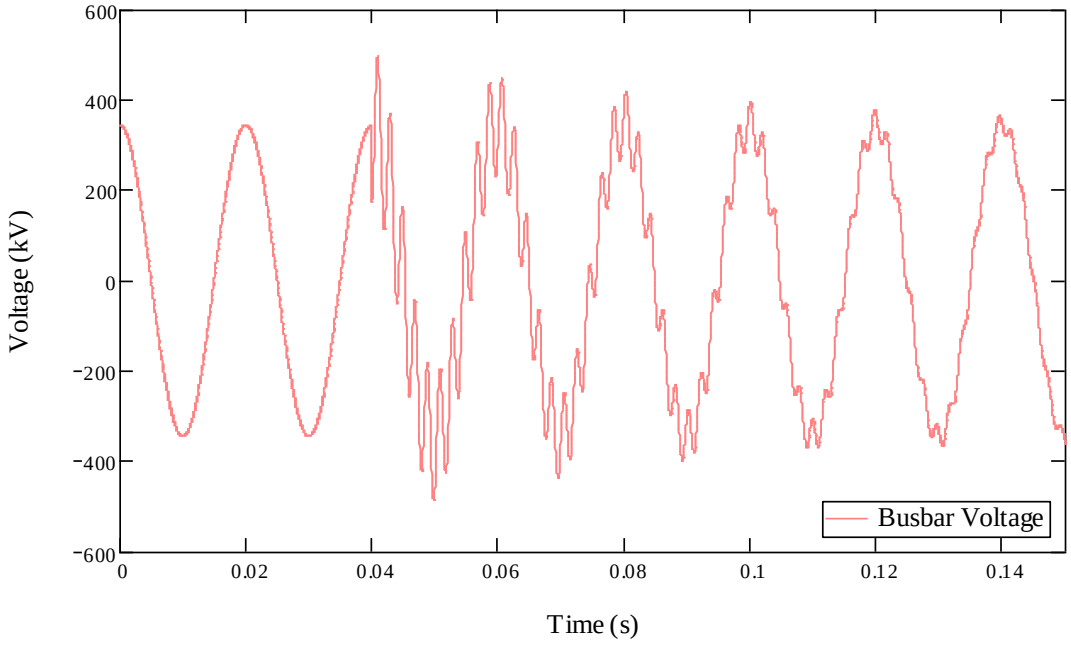


Figure 2-7: Back-to-back energisation of capacitor bank

As shown in Figure 2-7, the voltage dips, recovers, and then oscillates at a frequency of 510 Hz. In the case of back-to-back energisation, the over-voltage is not the main problem to overcome in the power system. The short duration high inrush currents could potentially be much more problematic.

2.2.3 Transmission line closing and reclosing

During a switching operation, a change in the state of the power system causes a disturbance. Transmission lines are electrically comparable to capacitive components such as capacitive loads when referring to the energisation behaviour. The generation of transient phenomena includes oscillatory over-voltages and are especially of concern where a significant change in impedance exists. The transients propagating along the transmission lines are generated through the capacitive charging but also include the travelling wave. Switching transients usually consist of very complex waveforms for which their fundamental frequency lies within the range of 100 Hz to 1000 Hz. The insulation of the system is stressed severely during certain switching operations and when voltage uprating is considered, these scenarios should be carefully evaluated [19].

There are a large number of parameters influencing the magnitude of over-voltages during transmission line switching. The following parameters have a strong influence on the total over-voltage magnitude when measured at the remote end of the line [19].

- Line length,
- Degree of shunt compensation,
- Line termination (open or terminated by a substation transformer),
- Presence of trapped charge,
- Closing resistors,
- Phase angles of circuit breaker closing,
- Total short-circuit power,
- Feeder network - inductive or complex.

According to the CIGRE working group 13.02 [19], worst-case switching scenarios include reclosing procedures. Trapped charge or residual voltage on the switched un-compensated line has a significant influence on the over-voltage magnitude. When clearing single-phase faults, single-phase auto reclosing is usually implemented. In this case, trapped charge is non-existent due to the faulted phase voltage short-circuit to earth and the healthy phases at nominal voltage (noted that there are higher voltages due to the neutral displacement during single phase-earth faults).

In the case where three-phase auto reclosing is implemented and the protection operates during a single phase to earth fault, trapped charge will be present on the healthy phases and the circuit breaker will close onto trapped charge. The worst-case scenario would be where three-phase auto reclosing is implemented and the protection operates as per a fault signal, but the fault is not actually present. The circuit breakers open, all three-phases will contain trapped charge and when the reclose operation is activated, all three-phases are switched onto the network with trapped charge. Depending on what the peak source voltage is at the instant of breaker closure, the voltage difference between the trapped charge and source can reach (with neutral displacement of phases) more than 2 p.u.

Regarding over-voltage magnitudes, the CIGRE working group 13.02 published per unit values for the expected over-voltages [19]. These per unit values are based on the 2% over-voltages recorded in the statistical cumulative distribution. The following variables were included within the field tests:

- Energisation scenario.

The impact of a transmission line cold energisation or three-phase reclosing (includes trapped charge) is evaluated to determine the sensitivity on the over-voltage magnitudes.

- Closing resistors.

The inclusion or exclusion of closing resistors when the circuit breaker is switched is expected to have a significant impact on the over-voltage magnitudes.

- Feeding network.

Inductive or complex feeding networks refer to the contribution of additional power system components from the feeding network end. The worst case would be where the feeding network is only inductive and does not comprise additional cables, transformers and transmission lines.

- Shunt compensation.

The contributing effect of the level of shunt reactive power compensation (both capacitive and inductive) included for voltage support is evaluated.

The results obtained in the report lists the over-voltage factors as a function of the above-mentioned variables.

The worst-case over-voltage factors recorded for cold energisation are in combination with no use of single step closing resistors, the feeding network is inductive and the shunt compensation is less than 50 %. For such a scenario over-voltages are below 3 p.u.

During reclosing, much higher over-voltages were recorded. None of these scenarios included the use of single-step closing resistors. The three worst-case scenarios are listed as follows [19]:

1. Feeding network complex, shunt compensation less than 50 %, over-voltage factor of 3.5 p.u.
2. Feeding network inductive, shunt compensation greater than 50 %, over-voltage factor of 3.55 p.u.
3. Feeding network inductive, shunt compensation less than 50 %, over-voltage factor of 3.6 p.u.

The DC trapped charge on a line can persist for several seconds after the line is disconnected. The following table describes the decaying times of trapped charge in different conditions.

Table 2-3: DC Trapped charge decay after 3 seconds [19]

Condition and environment of line	Value of DC charge (p.u) after 3 seconds
Dry	0.98
Sprinkle over part of line	0.85
Damp, dew, mist, fog, snow	0.6
Rain	0.28
Rain-Sleet	0.2

It has been confirmed that the combination of a few factors contributes to the overall wave shape and maximum over-voltage peaks. The transmission line parameters are a function of the tower configuration, conductor parameters and line length. The earthing philosophy and average soil resistivity are also contributing factors. The circuit breaker closing and opening times are also very important when the electromagnetic coupling between phases is evaluated. The impact of electromagnetic induction between the phases has a significant impact on the waveforms. Capacitive and inductive coupling together with travelling waves contribute significantly via superposition. Maximum peak over-voltages are usually encountered where the combination of all factors contribute to a rare instance or point in time to produce the worst-case peak value. Unlike capacitor banks and cables, overhead transmission line switching over-voltage waveforms are severely impacted by the inter-phase electromagnetic coupling. During switching operations, the inductive and capacitive

coupling between phases contributes significantly to distort and manipulate the transient over-voltage.

When a 400 kV single circuit transmission line (length 200 km) is energised, the uncharged transmission line behaves in a similar manner as a capacitor bank in terms of inrush current and over-voltage initiation. But when a capacitor bank and transmission line are compared in terms of switching over-voltage, transmission lines are much more complex. The travelling wave phenomenon is now included in the transmission line transient propagation. When a transient is generated at the sending end of a line, or a lightning flash terminates on a phase conductor, voltage and current waves travel on the conductors and when a point of discontinuity is reached, reflection and refraction of waves are encountered. Waves that are "reflected" travel back to their origin, and waves that are "refracted" are transmitted onwards.

To demonstrate the basic theory of the travelling wave phenomenon, the following section provides some background. Travelling waves shown in Figure 2-8 usually possess a voltage *e* and current *i.* The surge impedance is then $Z = e/i$ [10].

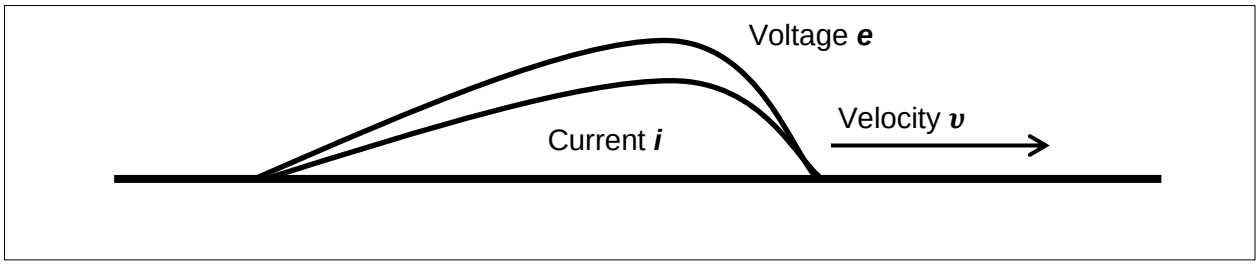


Figure 2-8: Travelling wave [10]

The surge impedance in Figure 2-9 is measured in ohms. Only distributed parameter circuits such as transmission lines, cables or SF_6 busses theoretically possess surge impedance. When the travelling wave reaches a point of discontinuity, the wave is reflected and refracted.

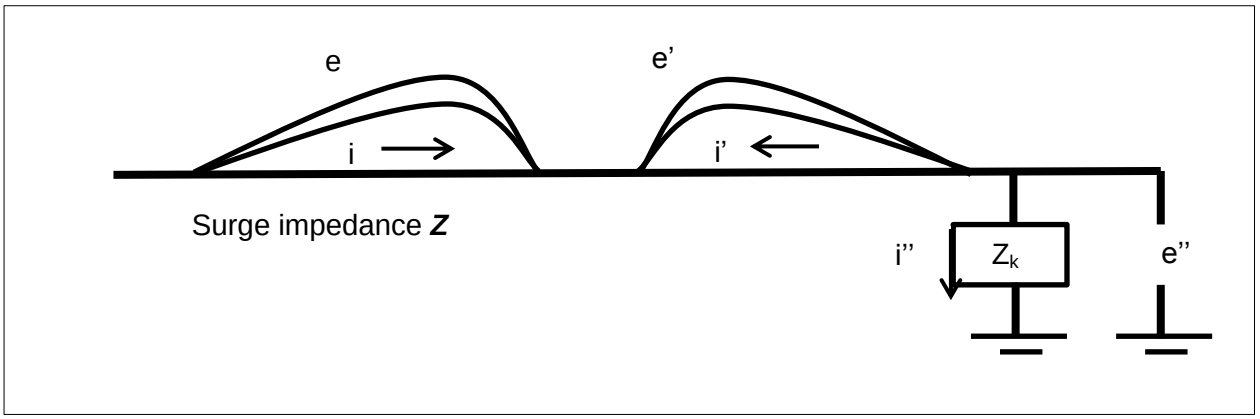


Figure 2-9: Travelling wave behaviour at a point of discontinuity [10]

To demonstrate the behaviour of waves at the point of discontinuity equations are derived to express the travelling waves as a function of their voltage and current. The equations are as follows [10]:

$$e = iZ \tag{2.24}$$

$$e' = i'Z \tag{2.25}$$

$$e'' = iZ_k \tag{2.26}$$

$$i'' = i - i' \tag{2.27}$$

$$e'' = e + e' \tag{2.28}$$

To find *e"* in terms of *e*

$$e'' = e + e' = e + i'Z = e + (i - i'')Z \tag{2.29}$$

Therefore

$$e'' = \frac{2Z_k}{Z + Z_k} e \tag{2.30}$$

A major impedance discontinuity is then when Z_k is open circuit the value approaches infinity. This leads to the reflected wave being up to twice the magnitude of the incoming wave.

$$e'' = 2e \tag{2.31}$$

The voltage doubling effect at the end of an open transmission line is a phenomenon to evaluate very carefully and with regards to the transients entering a substation it is important to evaluate the worst case scenarios and the energy required to be dissipated by the line entrance surge arresters. In this case, corona attenuation is ignored.

The velocity of propagation is then as follows.

$$v = 1/\sqrt{L\,C} \tag{2.32}$$

For overhead lines having a single conductor with radius r, located at a height h above ground and assuming an earth resistivity of zero, the inductance and capacitance are [20]:

$$C = \frac{10^{-3}}{18 \ln\left(\frac{2h}{r}\right)}\ \mu F/m \tag{2.33}$$

$$L = 0.2 \ln\left(\frac{2h}{r}\right) \mu H/m \tag{2.34}$$

And therefore

$$Z = 60 \ln\left(\frac{2h}{r}\right) \Omega \tag{2.35}$$

The surge impedance of a single conductor [10] transmission line usually varies between the value of 250 Ω to 500 Ω and the velocity of propagation between 290 $m/\mu s$ to 300 $m/\mu s$.

For illustration purposes, a 200 km transmission line is reclosed onto trapped charge. The circuit breaker closes at 0.065 s and the difference in time between the initiated transient and receiving end transient is indicated as 680 µs as shown in Figure 2-10.

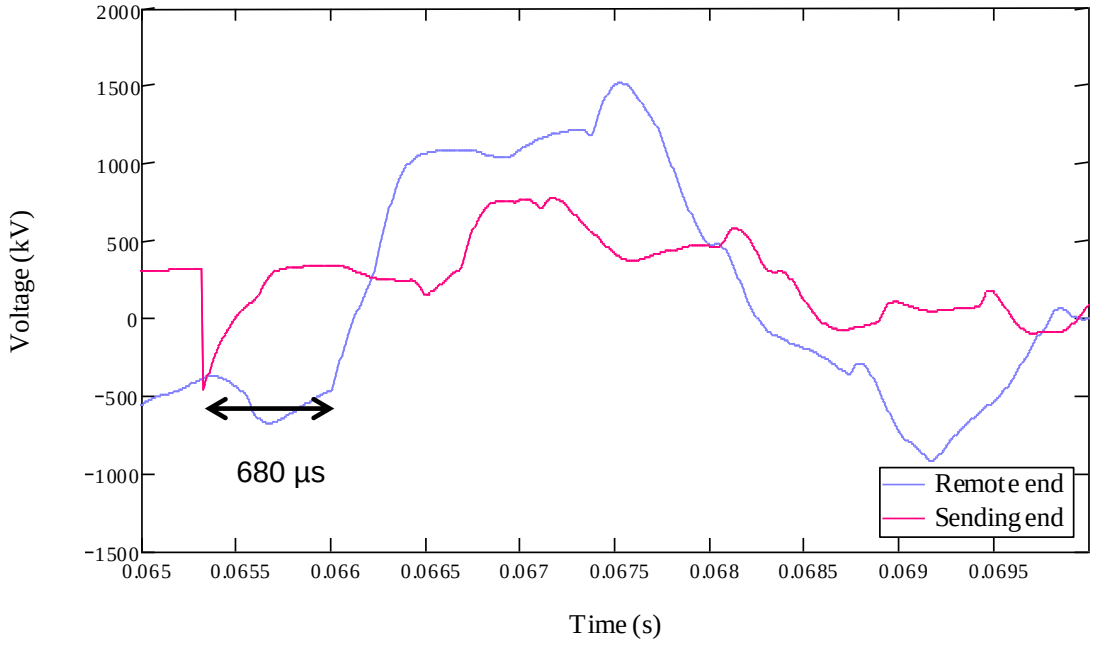


Figure 2-10: Sending and receiving end transient showing the travel time

The travelling wave is initiated by the sudden charging of the transmission line capacitance. The source voltage dips, followed by a rapid increase and overshoot. The transient propagates along the line and reaches the point of discontinuity where the line is open circuited at the remote substation. After a time of 680 µs the receiving end voltage increases dramatically to the peak over-voltage. The sending end over-voltage is 2.2 p.u and the receiving end 4.37 p.u. This is almost double the magnitude of the initial over-voltage. The traveling time is 200 km/680 µs = 294 m/µs which is close to the speed of light. The transmission line is not lossless, and the small deviation from the speed of light can be attributed to this.

Considering circuit breaker times for worst-case scenarios, it is necessary to evaluate the system statistically. With a statistical simulation, numerous simulations can be executed and from the statistical distribution, the worst case can be extracted. For this 200 km

transmission line the following circuit breaker closing times were extracted from the statistical data and tabulated in Table 2-4.

Table 2-4: Closing and reclosing circuit breaker times and over-voltage values

	Circuit breaker closing times (s)			Actual peak over-voltage (kV)			Max (p.u)
	RΦ	WΦ	BΦ	RΦ	WΦ	BΦ	
Closing	0.06216	0.065318	0.062867	-871.9	1005.77	-713.43	2.93
Reclosing	0.06923	0.067959	0.068668	1660.49	1262.86	-950.82	4.84

The exact breaker times produces the worst-case over-voltages for the two separate switching scenarios, closing and reclosing. The results for the two scenarios are shown in Figure 2-11.

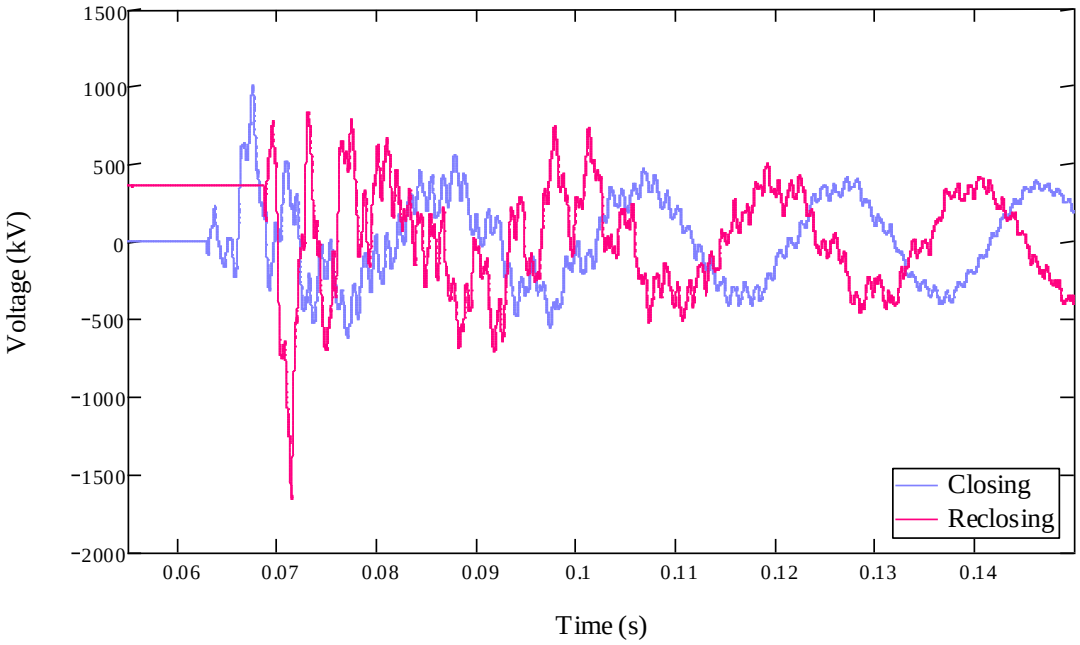


Figure 2-11: Comparison of transient over-voltage during closing and reclosing

2.2.4 Outrush transients

To simulate a fault condition, a circuit breaker closes and the capacitor that is currently operating in steady state, discharges through an impedance R_F and L_F. The transient is a function of the fault impedance and the capacitor capacitance. The magnitudes of the outrush currents depend largely on the fault impedance. If the fault is close to the capacitor the inductance L_F is expected to be relatively small (in the order of tens of micro-Henries). This in turn, could potentially lead to very large outrush currents as shown in Figure 2-12.

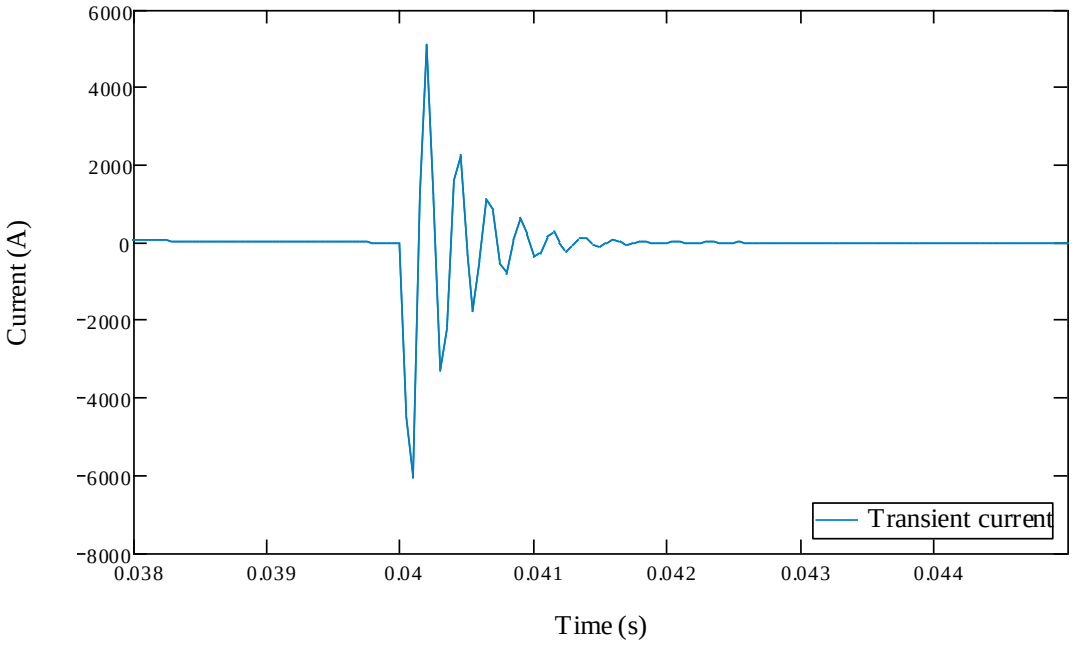


Figure 2-12: Capacitor bank outrush current

The outrush current dissipates through the fault impedance at the moment of the fault. The fault happens at 0.04 s and a maximum peak current of 6000 A flows to earth. The frequency of the oscillation is 5 kHz and is damped out very quickly. No over-voltage issues are expected due to the voltage collapsing to earth potential.

2.2.5 Switching of single core coaxial cables

A single core coaxial cable usually consists of a core, sheath and an armour conductor. A single core coaxial cable in its simplest form can be represented by a capacitor. A coaxial cable in its simplest form consists of one conductor pair (core and sheath). To calculate the equivalent capacitance the following equation is applied [20]:

$$C = \frac{2\pi\varepsilon_0\varepsilon_r}{\ln(\frac{r_1}{r_{out}})} \quad \text{(Per unit length)} \tag{2.36}$$

$$Z = \frac{60}{\sqrt{\varepsilon_r}}\ln(\frac{r_{out}}{r_{cond}}) \quad \text{(ohm)} \tag{2.37}$$

$$v \approx \frac{300}{\sqrt{\varepsilon_r}}\ m/\mu s \tag{2.38}$$

Where

ε_0 = 8.854 x 10^{-12} F/m

ε_r = Relative permeability of the insulating material (usually 2.4 for XLPE)

r_{cond} = Conductor radii, in mm.

r_{out} = Outer radii of first insulating material, in mm.

With a cable length of 2 km, the equivalent capacitance is 0.26 uF/km. The transient current reaches a peak value of 755 A. The frequency of the current is in the range of 1.34 kHz and decays over a time of 0.1 s. The steady state charging current is 28 A. The results are shown in Figure 2-13. The voltage transient is shown in Figure 2-14.

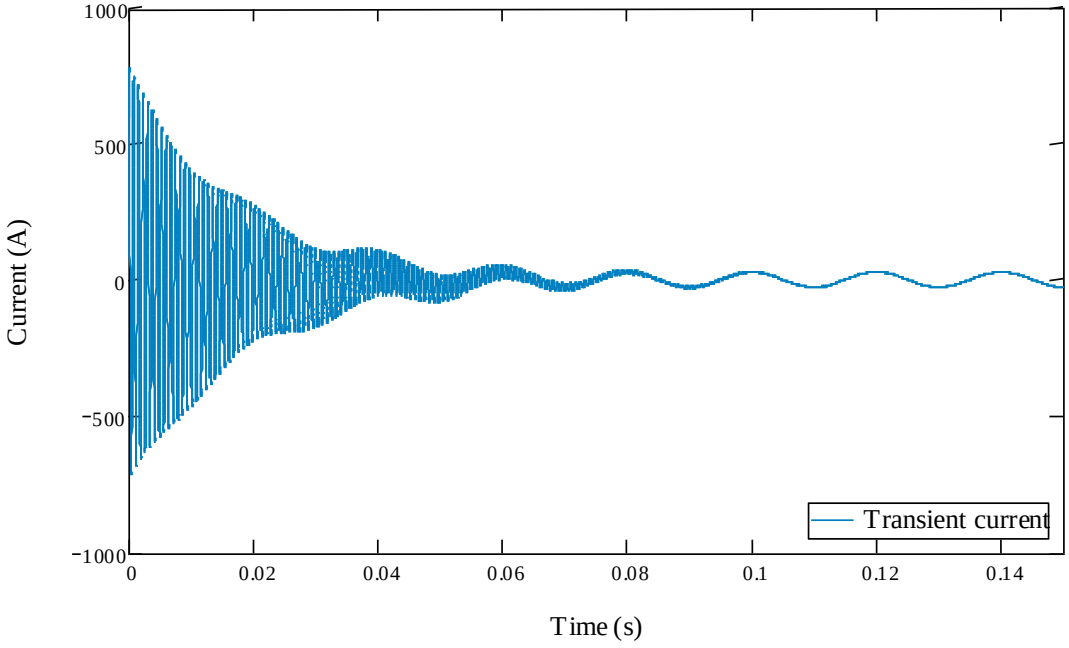


Figure 2-13: Transient inrush current when capacitor is energised

When the source voltage is at its maximum at t = 0, the switch is closed and the transient is initiated. The source voltage is approximated by a cosine function having a frequency of 50 Hz. Superimposed on the 50 Hz voltage is the 1.3 kHz oscillating transient over-voltage.

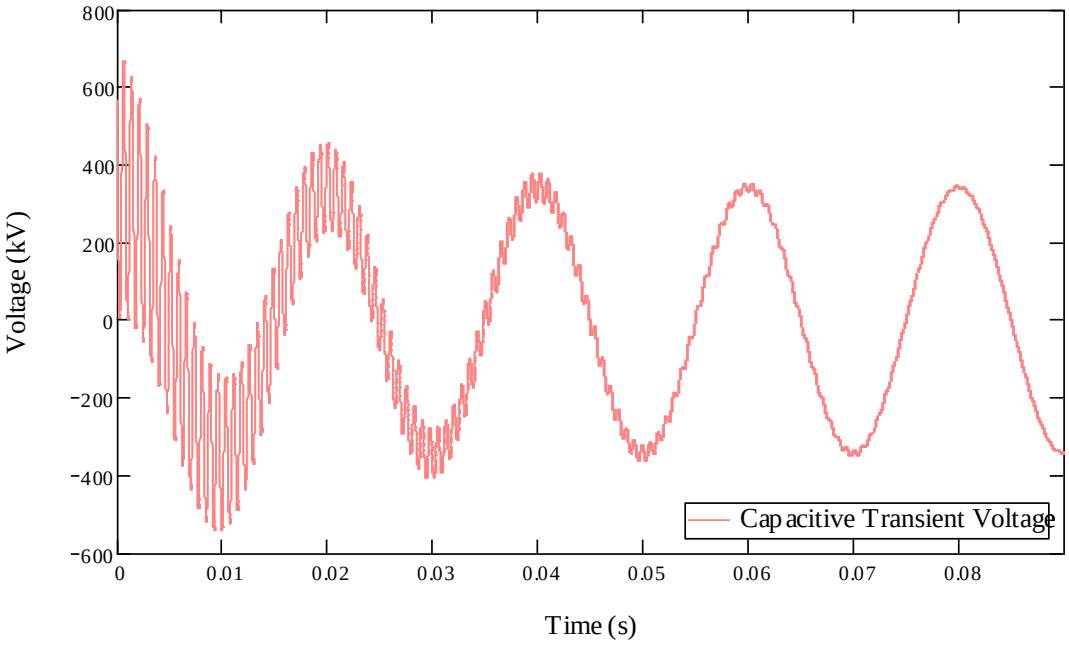


Figure 2-14: Transient over-voltage of capacitor

The high di/dt values through the inductor produce the peak over-voltage of 1.95 p.u (668.5 kV). It should be noted that no surge arrester is included in the model.

2.3 Voltage stress classification

2.3.1 Main over-voltage classes

When it comes to insulation coordination, it is very important to consider and evaluate possible stresses that the insulation will be exposed to. External events such as lightning form part of the Fast-front Over-voltage (FFO) group. Internal events such as faults, switching of circuit breakers and disconnect switches form part of the Switching Slow-front Over-voltage (SFO) phenomenon. Certain internal events such as load rejection and ferro-resonance could lead to Temporary Over-Voltages (TOVs). Very fast-front over-voltages are usually a result of switching or disconnecting operations within a GIS and cable connected motors [17]. The critical over-voltages to take note of are tabulated in Table 2-5.

All over-voltages are classified according to the class, frequency or transient nature. These wave shapes are also specified according to their duration, time to crest, time to half value, etc. For substation voltage uprating or compact design it is expected that the stresses will approach the critical flashover values. Steady state and transient over-voltages should be within the allowable limits specified within a thorough insulation coordination study.

Table 2-5: Critical over-voltages [17]

	Temporary over-voltages (TOV)	**Slow-front over-voltages (SFO)**	**Fast-front over-voltages (FFO)**	**Very-Fast-front over-voltages (VFFO)**
Load Rejection	x			
Transformer Energisation	x	x		
Parallel line resonance	x			
Uneven breaker poles	x			
Back feeding	x			
Line fault	x	x		
Fault clearing	x	x		
Line energisation	x	x		
Line re-energisation	x	x		
Line dropping	x	x		
AIS Busbar switching			x	**
Switching of inductive and capacitive current	x	x	x	
Back-flashover			x	
Direct lightning stroke			x	
Switching inside GIS substation				x
SF_6 Circuit Breaker inductive and capacitive current switching	x	x	x	**
Flashover in GIS Substation				x
Vacuum circuit-breaker switching			x	x
** Low damping and short busbars could allow possible occurrence of VFFO.				

Fast-front transient over-voltages are usually caused by lightning activity and are more relevant for nominal voltages of 245 kV and below. Slow-front transient over-voltges are usually caused by the opening and closing of switchgear and are more relevant for nominal voltages of 245 kV up into the ultra-high voltage (UHV) voltage range. Temporary over-voltages of longer duration require additional consideration of the environmental conditions such as pollution. The following table summarizes the origin of both temporary and transient over-voltages experienced in an interconnected power system.

2.3.2 Fast-front over-voltages

Substation lightning performance is largely a function of the incoming surge waveform and the design of the substation and transmission line earthing system. The transmission line earthing system close to the substation is very important.

Scenarios that could result in high lightning over-voltages include primarily:

1. Direct lightning strikes to substation equipment.

These scenarios are very rare and the probability is highly unlikely but the consequences could be severe. To mitigate against such scenario, overhead earth wires are installed at the substation to intercept all incoming lightning strikes.

2. Lightning strikes to transmission lines.

Due to the increased exposure to lightning over hundreds of kilometres, the probability of lightning striking a transmission line is high. This scenario is the cause for the majority of the phase-to-earth faults in the transmission network. The expected frequency of events is correlated to the line configuration and earthing system. Shielding failures and back-flashovers are the two important events considered when transmission substation lightning performance is evaluated. Induced voltages are not of major concern for higher voltages [21].

For this research, the primary focus will be on the impact of a back-flashover on the substation clearance and insulation design. After a back-flashover, fast-front over-voltages propagate along the phase conductors and enter the substation. The severity of such transients is a function to the following [21]:

- Surge Magnitude (kV or MV).

The magnitude of the surge could very easily be above the withstand levels of the equipment. Counter-measures such as MOV surge arresters and protective gaps are usually installed as a standard counter-measure.

- Surge Steepness (kV/µs).

Very steep wave fronts introduce higher frequency over-voltage oscillations and the non-linear voltage distributions could lead to excessive voltage stress concentrations on non-recoverable insulation. The surge arrester protective distance is a function of the surge steepness and the higher the steepness the less distance it operates successfully to limit the over-voltage to its residual voltage [8], [15].

The magnitude and steepness of the lightning surge is primarily a function of the lightning source current wave shape, and the distance between the struck point and the substation. Significant attenuation is caused by the effect of corona as the surge propagates along the line. Due to skin effect, additional attenuation distorts and limits the steepness of the transient. When lightning performance studies are conducted for substations, the assumption is that the struck point is close to the substation, usually a few spans away.

The substation earth electrode is usually a large copper mesh configuration, which introduces additional capacitance and contributes to a lower surge impedance. It is good engineering practice to earth the terminal towers to the substation earth electrode. The capacitance of the earth electrode improves the ability of the earthing system at the substation to attenuate the fast-fronted transients and to ensure effective dissipation of high frequency fast-front transients. It also improves the tower footing resistance to minimise tower voltage rise during direct strikes to towers or earth wire. The aim should be to minimise structure-footing resistances especially for the first few spans close to the substation. The tower footing resistance is directly proportional to the probability of a back flashover occurring. Back-flashovers may result in very steep lightning over-voltages that may damage equipment [22].

Back-flashovers are the primary root cause of momentary transmission line outages. According to the description of the first negative downward flash mechanism, the termination of the lightning onto the tower or earth wire takes place. When the lightning flash terminates on the earth wire, which is connected to the supporting towers, the tower potential rises to very high values in relation to the phase voltages. Streamers can form between the tower structure and the phase conductors and when the voltage gradients allow for the successful bridging by the leader, an arc forms between the structure and the phase conductors. The voltage on the phase conductors at this instant also contributes to the propagation of the leader [22].

The ac voltage on the phase conductors can sustain the arc. It effectively becomes a single phase-to-earth fault and needs to be cleared by the transmission line protection. Auto reclose operations operate very effectively once the arc channel has cooled and the fault removed.

The voltage across the insulator between the tower and phase conductor is highly sensitive to the earth resistance. Eskom has standardised on footing resistances for the different nominal voltages, but the resistance can vary between 10 and 100 Ω. For 132 kV towers the standardised maximum allowable value is 20 Ω. According to Chisholm and Janischewskyj in 1989, the initial surge impedance of transmission line towers can be estimated as a simple inductance at first and is usually in the range of 0.6 – 0.9 µH/m [23].

With a median peak current of 31 kA and a median steepness of 25 kA/µs at the peak of the negative impulse waveform, the potential rise at the base of the tower is in the range of 700 to 3500 kV. The withstand strength of airgaps during a lightning impulse is in the range of 530 kV per meter. Higher nominal voltages have larger phase-to-earth clearances and the dielectric strength of airgaps increases as a function of clearance. The dielectric strength of airgaps during fast-fronted impulses is also non-linear as a function of time, but decreases when subjected to longer tail times. Although very large clearances exist at extra high voltage range transmission lines, there is still a probability of a back-flashover to occur. The

insulator voltage is highly sensitive to the tower footing resistances and tower surge impedances. To evaluate a worst-case scenario for the impinging surge in a substation, a back-flashover is then considered a few spans away from the substation. The location of lightning stroke to the tower does not allow significant corona attenuation and limits the possibility for the majority of current to dissipate. The tower footing resistance and impedance is relatively high and not connected to the substation earth electrode where lower values for the earth plane surge impedance are expected.

As mentioned before, the tower top voltage after lightning termination is very sensitive to the frequency dependant tower surge impedance, and the resistive tower footing resistance. The total tower top voltage is then the sum of the following two components:

- RI is the current flowing down to earth at the tower multiplied by the tower footing resistance.
- $L\frac{dI}{dt}$ is the rate-of-rise of current multiplied by the inductance of the tower.

The peak voltage stress as a function of the change in current of the lightning surge is then given by [22]:

$$V_{Tower\ top} = R_{Footing\ resistance}I + L_{Tower}\frac{dI}{dt} \tag{2.39}$$

When the overhead shield wire is included in the tower top voltage calculation, the voltage stress on the insulation is reduced in the following two ways:

- The overhead earth wire surge impedance Z_{gw} ranges between 120 – 140 Ω and appears in parallel with the footing resistance and for a ramp current function with a rise time of t_f reduces the tower top voltage to the following equation [22]:

$$V_{Tower\ top} = I\frac{\left[(R_{Footing\ resistance} + \frac{L_{Tower}}{t_f})Z_{gw}\right]}{\left[R_{Footing\ resistance} + \frac{L_{Tower}}{t_f} + Z_{gw}\right]} \tag{2.40}$$

- The second more sensitive contribution includes the mutual coupling between the earth wire and the phase conductors. The coupling coefficient C_n defines the coupling between the shield wires and the phase conductors. This value is usually in the range of 15 – 35 % for typical geometries. This coefficient relates to the magnitude of the induced voltages on the phase conductors, delayed in time, but following the tower top voltage wave shape.

$$Z_{11} = 60ln\frac{2H_1}{r_1} \tag{2.41}$$

Where H_1 is the height of the tower and r_1 is the radii of the tower base.

$$Z_{12} = 60ln\frac{D_{12}}{d_{12}} \quad (2.42)$$

Where D_{12} is the distance of the earth wire to the image in the earth and d_{12} is the direct distance to the phase conductors.

$$C_n = \frac{Z_{12}}{Z_{11}} \quad (2.43)$$

The insulator voltage is then the voltage difference between the tower top voltage and the phase conductor voltage. The insulator voltage becomes:

$$V_{insulator}(t) = V_{Tower\ top}(t) - C_n V_{Tower\ top}(t - 2H/c) \quad (2.44)$$

Where the term $2H/c$ is twice the travel time between the shield wire and its image in the earth representing the time delay of the coupled phase conductor voltages.

When the tower earth wire is struck by lightning, the current divides and spreads out in both directions. The current forms a ladder network, splitting at the point of termination and at the points of where the towers are located. The current dissipates to earth and the effectiveness of the dissipation to earth is a function of the combination of footing resistances and tower earth plane impedances where the latter is frequency dependant.

Generally speaking, when a back-flashover occurs the crest value of the over-voltage transient reaches 1 to 1.2 p.u of the positive polarity CFO of the line insulation. The steepness of the wave front depends largely on the distance between where the back flash occurs and the substation entrance. The steepness decreases along the distance (inverse function of the distance d) and ranges between 700/d kV/µs (single conductor) to 1700/d kV/µs for conductor bundles of 3 to 4. The steepness of the wave usually ranges between 500 kV/µs to 2000 kV/µs. Referring to the tail of the wave, the time to half value ranges between 10 µs to 20 µs [22].

The surge over-voltage produced by lightning is a function of the following variables within the power system [24]:

- Magnitude of lightning current,
- Polarity,
- Wave shape,
- Transmission line tower and line surge impedance,
- Tower footing resistance, and
- Critical Flashover Voltage (CFO) of the transmission line insulation.

2.3.2.1 Lightning Parameters

In 1972 Popolansky [25] [26], embarked on a comprehensive review of all previous direct measured lightning data. The study proved that some errors existed in the previous assumptions and a new correlation was drawn. Based on 624 measurements from different countries he approximated the lightning peak current by a log-normal distribution. At the 1978 CIGRE working group 33.01 [26] (Lightning) meeting it was concluded that a modified summarising curve would be developed which comprised only of the confirmed negative

downward flash measurements. The negative current distributions were for structures having heights less than 60 m. From the work of Eriksson, it was concluded that the incidence of upward positive polarity flashes for these structures (up to 60 m), were less than 10 % [25]. Although positive downward lightning discharges are observed to occur only 10 % of the time, certain weather conditions could increase the probability of occurrence. It has been established that for positive polarity flashes the peak current magnitudes could be significantly higher (up to 300 kA and higher). The largest charge transfers are also associated with positive polarity downward flashes. Examples of weather conditions such as winter storms appear to increase the probability of occurrence. There is however, a lack of direct measured samples to draw statistical correlations for the positive polarity downward flashes.

From direct measurements in Switzerland, Italy, South Africa and Japan, it was concluded that for negative downward first strokes the median return-stroke peak current is about 30 kA [25]. Additional measurements were taken into account and the recommended wave shape parameters established that Berger's peak current distribution consisting of about 100 negative polarity first strokes is still the most accurate representation. However, it was found that for the peak current and minimum currents the distribution did not accurately represent the actual observations. For lightning protection standards, the need to increase the population of observations is imperative. The data of Berger is supplemented by other direct current measurements obtained in South Africa and other non-direct less accurate data. The two primary standards adopted for lightning protection are the IEEE Std 1410-2010 and IEC 62305-1; IEEE Std 1243-1997 and the CIGRE distribution from Anderson and Eriksson [26].

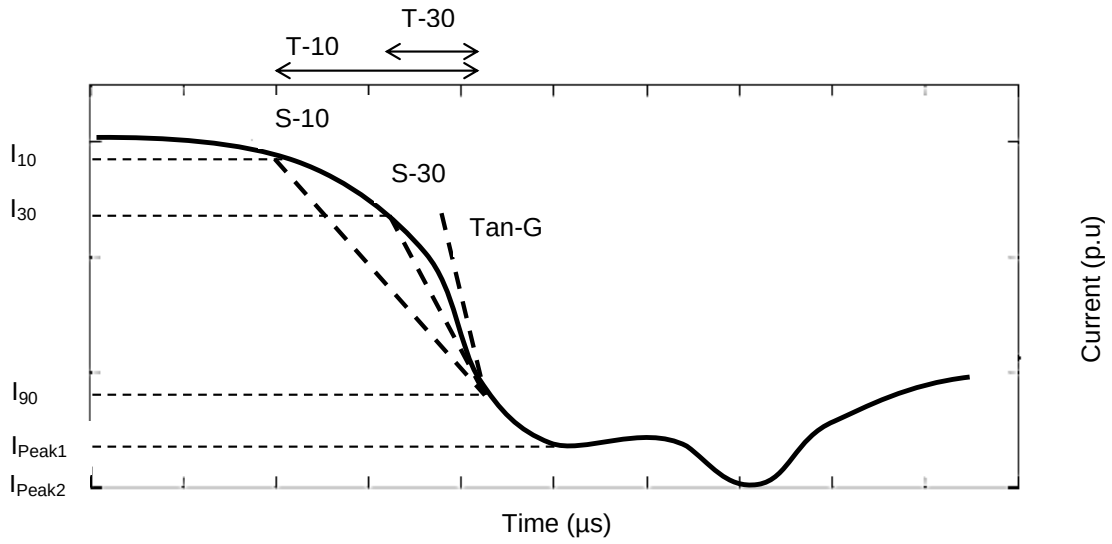


Figure 2-15: Negative downward impulse front definitions [25]

The CIGRE negative downward lightning waveform in Figure 2-15 was then developed with reference to all data obtained to illustrate the impulse front parameters. These parameters represent the idealised form of the negative stroke [25].

These are defined as follows:

T-10: Front duration expressed as time interval between the 10 % and 90 % current magnitude intercepts.

S-10: Average current steepness in kA/µs between the 10 % and 90 % intercepts.

T-30: Front duration expressed as time interval between the 30 % and 90 % current magnitude intercepts.

S-30: Average current steepness in kA/µs between the 30 % and 90 % intercepts.

TAN-10: Rate-of-rise of current on the front at the 10 % peak current intercept.

TAN-G: The maximum rate-of-rise of current on the front of the first Peak.

S-30: The average current steepness in kA/µs between the 30 % and 90 % intercepts.

The statistical analysis has been carried out and the relationship between the peak currents in the log-normal distribution is correlated with the maximum steepness. For the first stroke parameters the following steepness is calculated as ‘n function of the current:

$$S_m = TAN\ G = 3.9I^{0.55} \tag{2.45}$$

And for the 30 % intercept,

$$S_{30} = 3.2I^{0.25} \tag{2.46}$$

With reference to the second peak, it is expected that the peak current is higher but the steepness is a lower value when compared to the maximum values for the first peak. For this study, only the first peak with maximum steepness is considered.

Very strong correlations were found between waveform parameters. The probability of the negative first stroke peak magnitude is given by:

$$P = \frac{1}{1 + \left(\frac{Ipeak}{31}\right)^{2.6}} \tag{2.47}$$

The observation is made that there is a very good fit with the probability distribution function established by Anderson and Eriksson for negative downward flashes to objects with height up to 60 m. The approximations only differ from the log-normal distribution at the extremes, where a shortage of actual data is available. The probability of peak currents is given in Figure 2-16.

The rate of current rise or steepness is also approximated for the first negative stroke. The probability of occurrence of maximum steepness also referred to as TAN-G or S_m is given by:

$$P = \frac{1}{1 + \left(\frac{S_m}{24}\right)^{4}} \tag{2.48}$$

Where S_m is expressed in kA/µs.

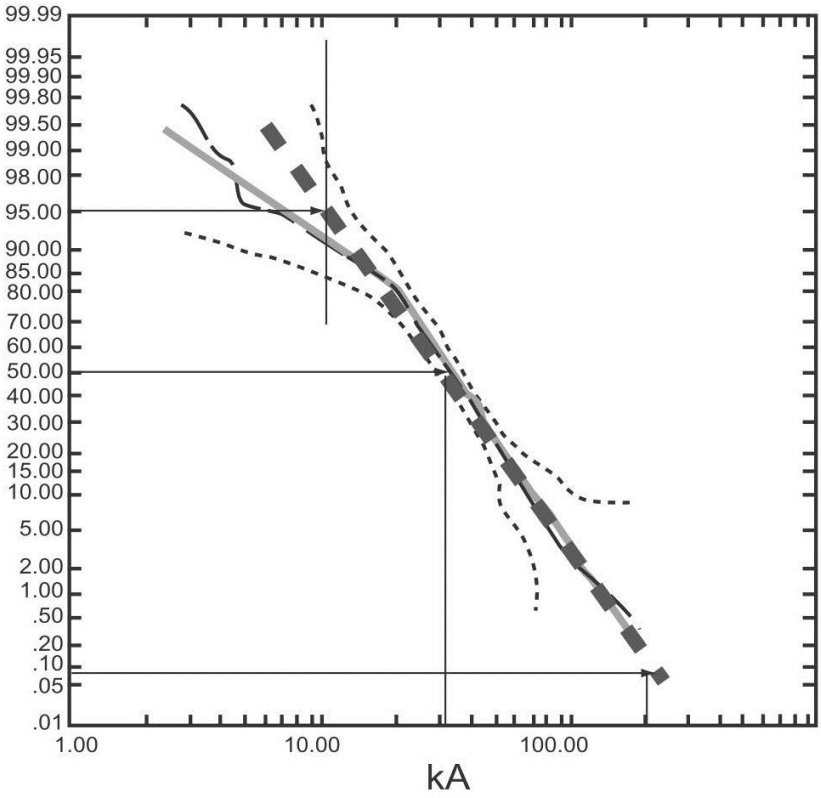


Figure 2-16: Probability of peak lightning currents [22],[25]

It is also important to take note of the ground flash density. With reference to lightning protection, the statistical probability of a flash occurring and the probabilities of waveform parameters to have extreme values all contribute to the total risk. The risk of causing harm to human life, or damage to equipment should be statistically evaluated to optimise all aspects involved.

2.3.2.2 Transmission tower surge impedance

It has been established by Hileman and Wagner that the transmission tower can be represented as a simple short transmission line. The tower surge impedance theoretical values obtained in their work is in between the range of 200 to 280 Ω. Lower values have also been calculated and it was found that the propagation of the surge was 10 % to 30 % slower than that of the speed of light. Tower surge impedance can be expressed as a tower inductance and greatly simplifies the calculations. For a delta vertical tower arrangement with a base radii of r and a height h the following equation expresses the surge impedance of the tower [22]:

$$Z_T = 30ln\left[\frac{2(h^2 + r^2)}{r^2}\right] \tag{2.49}$$

The inductance is then calculated by:

$$L = Z_T\tau \tag{2.50}$$

Where τ is the propagation time.

2.3.2.3 Substation related lightning events

The lightning performance of overhead transmission lines depends on the following important factors [23]:

- Ground flash density,
- Overhead line height,
- Conductor configuration,
- Shield wire configuration,
- Tower footing earthing,
- Insulation strength.

For substations, fast-front transients will stress all of the substation bus conductors and equipment. The stress experienced by the equipment will largely depend on the protective distance and capability of the surge arrester. Among other factors, is the protective distance a function of the steepness of the incoming surge. A back-flashover could potentially produce a surge steepness in the order of 2000 kV/us. The travelling behaviour of the transient will also be a determining factor. The configuration of the substation at the instant where the surge enters the substation will contribute to the reflection, refraction and travelling time behaviour of the surge. It is well known that the steepness of the impinging fast-front over-voltage is reduced by the corona damping effects on an overhead line. Usually when a fast-fronted surge travels great distances on the overhead conductor, the steepness is reduced dramatically. In Eskom it is also advised to strategically locate the capacitive voltage transformers very close to line entry surge arrester. This contributes additional capacitance to improve the surge impedance at the substation termination point.

2.3.3 Slow-front switching over-voltages

Circuit breaker operation as a result of a fault clearing event or line/transformer energisation creates switching over-voltages. Generally these over-voltages are experienced on almost all systems according to the IEEE committee reports [24].

Slow-front over-voltages are a significant determining factor when air clearances is specified. The importance of slow-front transients is usually limited to transmission lines of higher system voltages (132 kV and above). Swinging conductors are usually taken into account due to the risk of phase-to-phase faults occurring as a result of mechanical forces during fault conditions.

Due to the random nature of switching surge over-voltages, and the lack of available theory and application at the time, the deterministic design approach dominated prior to the 1970's. It was only in the late 1970's that the probabilistic method was welcomed as an alternative in transmission line design [19]. The initial drive towards an alternative approach was the question regarding the feasibility of uprating existing transmission lines.

Right of way for servitudes was becoming more challenging and the idea of uprating became ever more attractive. The deterministic approach only considered lightning over-voltages, and the shift in design approach was challenging to the old way of thinking. The probabilistic method included the consideration of switching surge over-voltages, and was mandatory to prove the feasibility of voltage uprating. Today, virtually all EHV transmission lines are

designed based on the probabilistic method. Switching surge over-voltages are not considered to be a design problem for voltage class 1 (nominal voltages of 242 kV and below), and hence no SIWL values are usually specified for this voltage class.

Major sources of slow-front over-voltages are fault initiation and fault clearing scenarios. The earth fault factor essentially determines the expected over-voltage on the healthy phases during single phase-to-earth faults. Due to the frequent occurrence of phase-to-earth-faults in the network, representative over-voltage calculations have been published for a conservative approach. The following calculations are relevant for the determination of slow-front over-voltages during fault initiation and fault clearing [27].

$$U_{et} = (2\,k - 1)U_s\sqrt{2}\,/\sqrt{3} \text{ (kV peak for fault initiation)} \quad (2.51)$$

$$U_{et} = 2U_s\sqrt{2}\,/\sqrt{3} \text{ (kV peak for fault clearing)} \quad (2.52)$$

Where k is the earth fault factor.

2.3.3.1 Stress and strength probabilistic evaluation

The probabilistic approach is essentially the comparison of stress versus strength. The stress is mainly classified as the switching surge over-voltages and can be described by a probability distribution function. The strength is classified as the insulation level and can also be described statistically, more specifically by a Gaussian cumulative distribution [10].

Superimposing these two statistical distributions, the probability of insulation breakdown of flashover can be determined. The risk of failure is quantified in this equation.

It is assumed that the insulation strength characteristic can be approximated as a cumulative Gaussian distribution. The distribution is described by a critical flashover voltage (CFO) and a standard deviation. The CFO is defined as the voltage where 50 % probability exists for a flashover to occur. The coefficient of variation usually ranges between 5% and 7% [10] and the switching impulse withstand level is a statistical function of the CFO.

It is then possible to obtain the actual network arrangement and relevant parameters for the feeding network to initiate the over-voltage determination process. The network should allow for either a worst case scenario where the feeding network is only inductive, or should consider additional and more complex sources to represent the network at a more detailed level. A semi-statistical analysis includes the following [19] [10]:

- Feeding network equivalent source impedance,
- Transmission line modelling,
- Circuit breaker opening and closing times,
- Multiple switching operations (usually between 200 and 500),
- Point of measure identification ,
- Risk of failure analysis (semi-statistical stress and strength comparison).

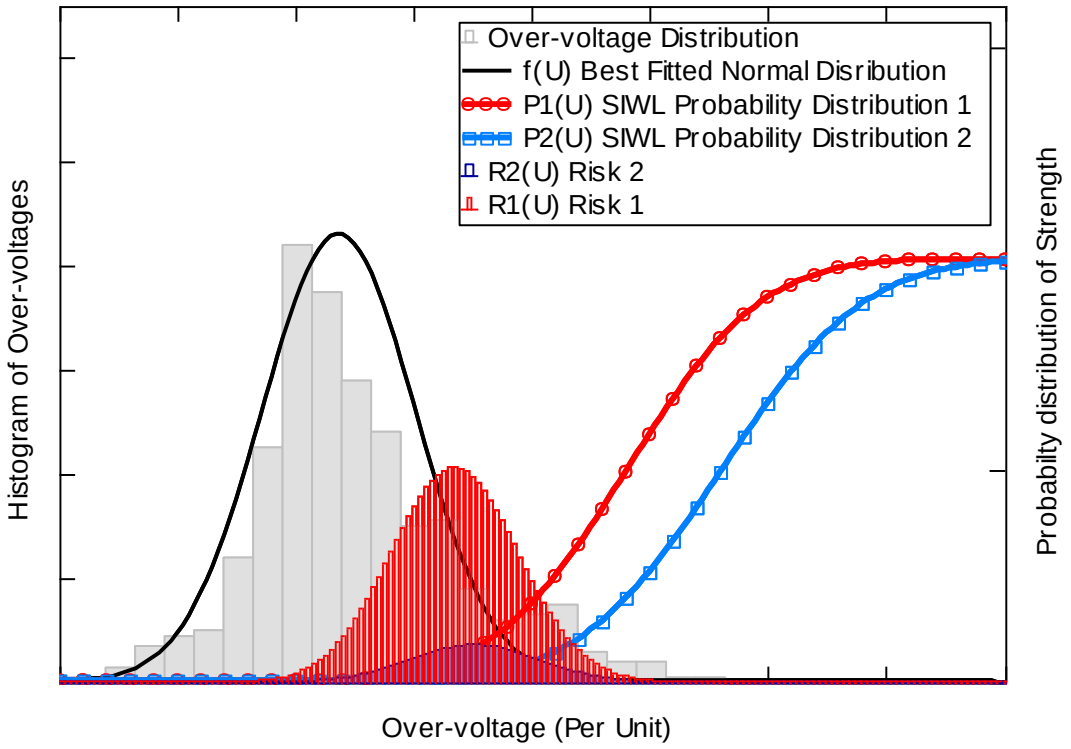


Figure 2-17: Semi-statistical analysis for determining the risk of failure

Figure 2-17 indicates the normal distribution f(U) that represents the over-voltages obtained in the statistical switching study. The strength or withstand distribution is represented by the SIWL probability distributions P1(U) and P2(U). The risk of failures R1(U) and R2(U) are calculated with the following integral [27]:

$$R(U) = \int_{\infty}^{-\infty} f(U).P(U)dU \tag{2.53}$$

For the purposes of evaluating the switching over-voltages relating to substations, it is important to note that the evaluation should include the determination of voltage stress impinging on the substation from the transmission line side, but also the stress introduced from within the substation (capacitor bank switching, transformer energisation etc).

Literature indicates that the switching of transmission lines could potentially produce very high switching over-voltage magnitudes [19]. Slow-front over-voltages enter a substation, but the line entry surge arrester limits their peak to the arrester protective level. This means that even if the surge reaches a magnitude of 4 p.u, the arrester will limit the surge within the range of 1.8 p.u. The slow-front surge travels then into the substation and the travelling wave's reflection and refraction are limited due to the steepness not being so substantial as opposed to fast-fronted surges.

As mentioned before, surges generated inside the substation when capacitive and inductive currents are switched, can produce similar and even more severe over-voltages. The switching of transmission lines is similar to switching a capacitor bank because a transmission line is essentially a capacitor that generates reactive power in steady state. Capacitor bank switching might include back-to-back switching where large inrush currents

flow, but when over-voltages are considered, it is adequate to place the focus of the study on transmission line closing and reclosing [20].

The statistical study for slow-front over-voltages is simplified when the metal-oxide surge arrester is included in the evaluation. The probability distribution of all the over-voltages will be limited to the protective level. To proceed with the risk calculation to obtain a useful value for the risk of failure is then not so relevant anymore. The statistical distribution will produce information on the exact circuit breaker closing and opening times of the worst-case scenarios. This information is very important when evaluating the impact of switching on the arrester energy handling capability.

2.3.3.2 Interruption of magnetising currents

With reference to over-voltage impulses generated inside the substation, switching transformer magnetising currents can produce severe stress on the insulation. In a study conducted to observe the maximum over-voltage magnitudes, 33 different power transformers were included within the field tests. Interruption of magnetising currents were chopped at its peak value and the tests excluded any circuit breaker restrikes. During the tests, only the transformer capacitance was present and not any additional capacitance from bushings, voltage and current transformers, etc.

Table 2-6 is derived from the results obtained within the study to make reference to the standard voltage levels used within Eskom.

Table 2-6: Maximum over-voltage factors during interruption of magnetising currents [19]

Nominal Voltage (kV)	Over voltage factor K (p.u)
88	3.5
132	3.1
220	2.6
275	2.3
400	1.8

The expected values for actual systems in operation will be lower than that of the field test results due to the exclusion of the additional capacitances present during the tests on actual systems in operation.

2.3.4 Temporary over-voltages

Power frequency over-voltages usually consist of damped oscillations lasting for a period of a few hundred milliseconds or longer. Internal events such as single-phase earth faults, load rejection, ferranti effect as a result of long unloaded transmission lines, ferro-resonance, poorly earthed systems could give rise to temporary over-voltages. To evaluate these events the system should be studied to identify the most probable scenarios where TOV might be encountered. Proper application of metal-oxide surge arresters is very important to allow for extended duty cycle energy dissipation. The magnitudes of the TOV could roughly

be estimated by the earth fault factor. The over-voltage experienced by the arrester is also largely related to the earthing philosophy or earthing conditions [27].

Determination of temporary over-voltages caused by earth faults has been simplified and the magnitudes are largely dependent on the system neutral earthing configuration and the fault location. Abnormal earthing configurations should be evaluated as a special case and detailed studies might be required.

2.3.5 Determination of voltage stress

Insulation coordination is essentially a process focused around limiting the probability of insulation breakdown to an acceptable level. The balancing act between reliability and cost determines this probability. The art lies in finding the optimal balance to allow for a safe and reliable, but cost effective coordinated system to operate within the envisioned boundaries set by the engineer. The process includes an extensive determination procedure of the stresses involved, and the justified selection of optimal withstand levels. Methods and devices available to address the stress are applied where needed [10].

The following steps are included in the process:

1. Determination of representative over-voltages,
2. Determination of coordination withstand levels,
3. Determination of the required withstand levels,
4. Selection of standard withstand levels.

2.4 Limiting voltage stress

Limiting transient over-voltages forms part of the requirement to ensure that the stress experienced by the internal and external insulation is within the limits at all times. With a surge arrester installed as the primary over-voltage protection device, other means to assist with protection is also installed where needed. During the switching of capacitive loads, inrush current magnitudes and inrush current frequencies should be limited to ensure that the circuit breaker operates within its design characteristics.

- MOV Surge Arresters

It is standard practice within Eskom to include surge arresters in the substation to protect non-recoverable insulation against transient over-voltages. EHV and HV surge arresters protect power transformers. Capacitor bank surge arresters limit the transients in the substations due to capacitor bank switching and line entrance arresters limit impinging surges entering from the line side.

Regarding the impinging switching surges entering the substation from the line side, It has been proved that the inclusion of MOV surge arresters at the mid-point of the line is a feasible alternative to pre-insertion closing resistors [28] [29]. The small and cost effective solution as opposed to closing resistors offers great economic and maintenance benefits. When over-voltages are controlled on the transmission line, the impinging surges entering the substation are also better controlled and the stress experienced on the substation equipment is expected to be much less.

The concluding remarks state that MOV arresters installed at the sending, receiving and mid-point of the line can limit over-voltages to acceptable values for lines up to 600 km. It is also known that in reality network damping and actual system parameters are not as

conservative as specified in worst-case simulations. Less severe over-voltages are expected in reality and thus the scope to include line MOV surge arresters becomes even more attractive [28].

The following means are utilised within the power system to assist with limiting over-voltages [22]:

- Current limiting reactors.

During back-to-back capacitor/cable switching, high magnitude/frequency inrush current flows and causes over-voltages. Additional inductance in the current path reduces these current transients. The inclusion of inductance in the circuit could add to the inductive current switching strain on the circuit breaker and could possibly include a surge capacitor to control the transient recovery voltage across the circuit breaker terminals.

- Pre-insertion resistors.

A basic solution used is to include a resistor in the circuit prior to capacitive load energisation. The resistor value is matched with the load surge impedance to avoid reflections and to drain the high frequency inrush currents. This method is very effective.

- Controlled switching.

The magnitude of over-voltage during switching is dependent on the point of wave where the circuit breaker makes or breaks the current. Controlled switching employs a very precise switching controller to ensure that the circuit breakers interrupt at specific zero crossings. Ideally, the circuit breaker should not close on trapped charge while the source voltage is at the opposite polarity.

2.5 Dielectric strength of external insulation

External insulation is insulation exposed to atmospheric air with all its contaminants. The dielectric strength refers to the withstand capability of an open airgap between electrodes, and also includes configurations where solid insulation (post insulators, glass discs, etc) are employed to separate electrodes. The dielectric strength of airgaps is influenced by external conditions such as pollution, humidity, etc. It is then important to consider the performance of external insulation when subjected to different transient over-voltages. CIGRE has published a guideline [30] for the evaluation of the dielectric strength and includes experimental data for open airgaps and solid gaps at standard atmospheric conditions. The experiments were done with positive, negative polarity transients in wet and dry conditions.

2.5.1 Breakdown mechanisms of recoverable insulation

Various factors contribute to the behaviour of the airgap during over-voltage stress. These factors include:

- Transient voltage waveform,
    - Rise and tail times.
    - Polarity.
- Electric field distribution,
- Gap distance,
- Gas conditions.

When insulators are present the following should also be considered:

- Insulator string length,
- Insulator type,
- Swing angles,
- Contamination.

Transmission substations operate mainly in the High and Extra High Voltage range. Long transmission lines are exposed to lightning and excessive switching operations. It is then necessary to include both fast and slow-front transients into the calculation when considering adequate clearances within a substation. It is also important to note that both fast and slow-front transient over-voltages can be either positive or negative and this has a significant impact on the insulation strength. With different electrode configurations within a substation, multiple airgap electrode scenarios are included. The electric field distribution becomes very important and has a great influence on the behaviour of the breakdown mechanisms that causes a flashover. The breakdown mechanism is described by three stages and is briefly reviewed [30].

First Corona is the first stage in the development of the discharge. The first corona is an ionization phenomenon and occurs when the electric field reaches an intensity high enough to produce free electrons through collisional processes. The inception voltage is dependent on the gas conditions.

To form an avalanche effect of a certain length, the minimum inception voltage should be exceeded over the total length. When this length reaches a critical length, self-sustained secondary avalanches are generated. These avalanches develop along the pre-existing field strength lines initiated by the first corona. The development is also known as the streamer, a filamentary discharge related to an important corona mode initiated during switching and lightning surges.

Leader propagation is significant during switching impulse and alternating current. For positive leaders the advancement is almost constant at a velocity of 1.5 – 2 cm/µs. The path of the propagation may be either straight or tortuous. The leader channel is sometimes referred to as a conductive channel with an average gradient from 0.5 – 2 kV/cm depending on the length of the leader. When referring to a positive switching impulse with critical time to crest, the leader propagation is continuous. In the case where the time to crest is shorter than the critical time, the propagation of the leader to its full length is prohibited by the premature decay of applied voltage. Due to lightning impulse durations being too short to allow for significant leader propagation, breakdown is dominated by the streamer phase and not the leader phase.

The final stage of the discharge is known as the final jump. This stage is mainly the formation of a self-sustaining discharge due to the gap being bridged. When streamers propagating ahead of the leader tip reach the opposite electrode, the final jump occurs. At this instant electrons are received from this electrode, the leader velocity increases almost exponentially and the channel becomes completely ionized. At this instant the voltage collapses. The leader progression model describes the volt/time characteristic of a specific external insulation gap or insulator. The insulator voltage is a function of time and is a source term for the differential equation that describes the growth of the leader across the

external air or insulator gap. From extensive experimental results, the growth rate and coupling terms have been established and tested to be very accurate. It is important to model non-standard transients. By solving the differential equation, a more realistic breakdown strength as a function of magnitude and time could be obtained. The two important time values relevant during the breakdown mechanism is the time it takes for streamers to develop across the gap between the electrodes. The second important time is the time it takes for the leader to propagate across the gap. It has been established that the streamer development time is a function of the average over-voltage stress in the gap ,compared to the CFO voltage [22]. The CFO is plotted against time to flashover in Figure 2-18. The following expression defines the streamer development time (μs) for impulse voltages of positive and negative polarity.

$$t_{sreamer} = 1/[1.25(V/CFO) - 0.95] \tag{2.54}$$

And the CFO voltage is given by:

$$CFO = \left[400 + \frac{710}{t^{0.75}}\right].L \tag{2.55}$$

Where:

CFO = the median flashover voltage (kV)

t = the time to flashover (μs)

L = the length of the insulator (m)

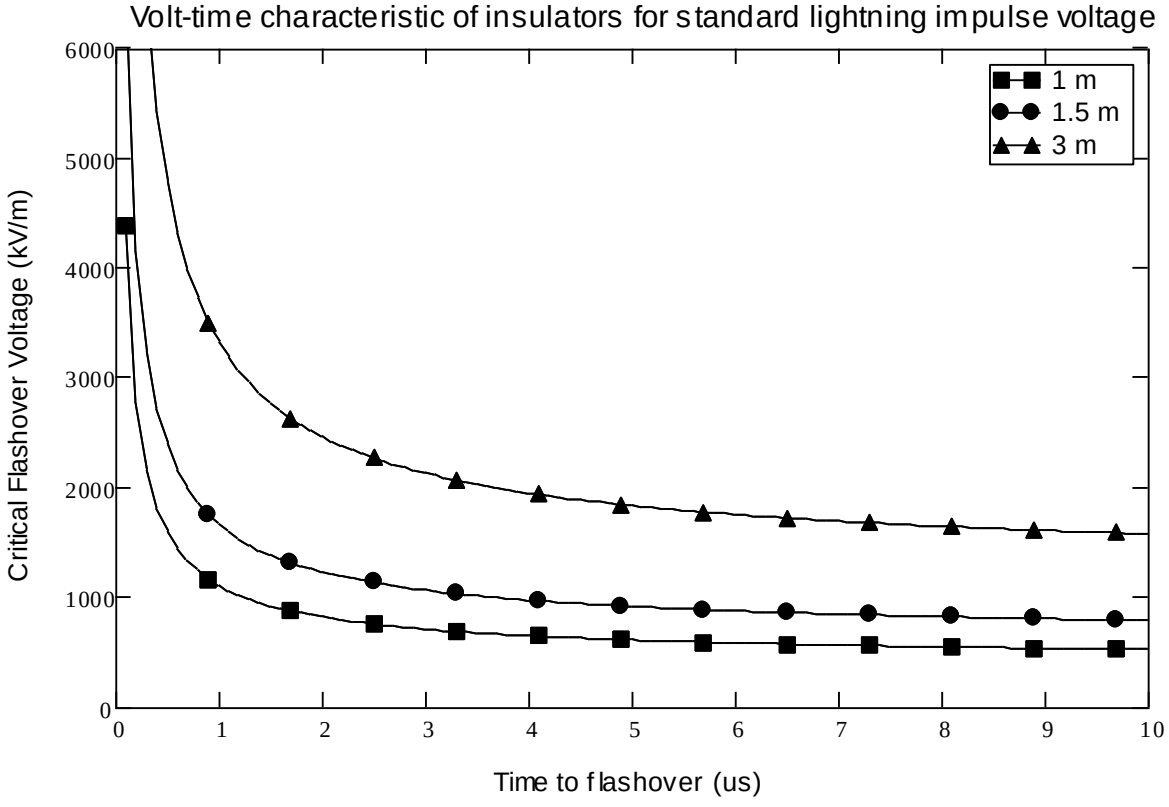


Figure 2-18 : Volt-Time characteristic of insulators for the standard lightning impulse

The second important time is the leader progression time. The combination of the two equations in (2.54) and (2.55) gives the expression for the leader progression time with a CFO of 560 kV/m [22]:

$$t_{leader} = \left(\frac{710}{E-400}\right)^{1.333} - \left(\frac{448}{E-426}\right) \quad (2.56)$$

Where

E = the peak breakdown voltage per meter of insulation (kV/m) and

t_{leader} = time for the leader to propagate across the gap (µs)

The leader propagation velocity is then the change in distance across the gap over time which is simply the gap length divided by the leader propagation time.

Due to the breakdown process of self-restoring insulation being statistical of nature, the breakdown voltage and withstand voltages are always described statistically. It is then important to classify strength in terms of the probability to withstand the stress that is applied to the insulation. As mentioned before, the CFO is the voltage where a 50 % probability exists for the insulation to break down. The Switching Impulse Withstand Level (SIWL) or Basic Switching impulse Level (SIWL) refers to a voltage where a probability of 90 % exists for the insulation to successfully withstand. The same approach is taken when lightning over-voltage is considered.

- Air density.

A reduction in air density relates to the reduction in breakdown voltage of the airgap. This is mainly due to the ionization process that initiates quicker due to the additional increase in the mean free path of electrons. The reduction of air density is directly related to the reduction of corona inception voltage and due to this relationship, the initial phase of breakdown initiates at a lower voltage.

Substations and transmission lines being operated at altitude (1500 – 1800 m) should be carefully considered due to the breakdown voltage being lower. Altitude correction is generally considered in these situations. However, the argument should be considered where the weakest link in the substation should rather be the external insulation, and not the non-recoverable internal insulation. Careful consideration should then be applied on the decision whether or not the air clearances should be corrected for altitude or not. A generally accepted correction factor for air density where k_d is multiplied by the CFO value is given in the following equation.

$$k_d = 0.289\frac{p}{273+t} \quad (2.57)$$

With p = pressure in mbar and t = temperature in ºC

- Humidity.

The development of discharge is greatly hindered when the humidity of the gas increases. The attachment phenomena contribute significantly to an increase of breakdown voltage. It

has been noted in literature that the influence of the humidity of the gas is independent on the gap spacing.

- Rain.

The effect of rain on the CFO of pure airgaps on is normally negligible. There is some instances where the gap configuration in combination with rain, could lower the corona inception voltage. It is possible for rain to have a significant impact on contaminated insulators, but this refers to contamination-discharge effect and not the impact of rain on the CFO in isolation.

2.5.2 Airgap strength when subjected to power frequency voltages

A rod – plane gap produces the lowest CFO voltage when subjected to power frequency voltages. The CFO voltage when subjected to power frequency voltages is about 25 % higher when compared to that of the CFO voltage when subjected to positive switching impulse. The CFO voltage with the gap factor integrated may be approximated by the following equation [17]:

$$U_{50RP} = \left[750\sqrt{2}\ln(1 + 0.55\ d^{1.2})\right].\left(1.35K_g - 0.35K_g^2\right) \tag{2.58}$$

The power frequency withstand level may be taken as 90 % of that of the CFO voltage. A standard deviation of 3 % of the CFO voltage is assumed.

The influence of the gap factor in Figure 2-19 has a notable influence on the withstand capability of the airgap. Figure 2-19 shows that the critical flashover voltage decreases as the gap factor decreases.

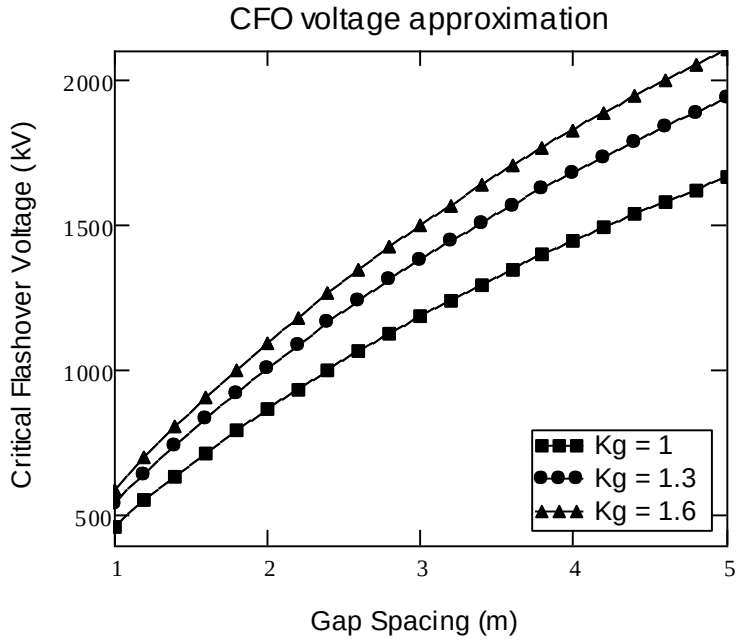


Figure 2-19: Power frequency CFO voltage and the impact of the gap factor

It should be noted that in the presence of insulators, the CFO voltage might decrease substantially, especially in adverse environmental conditions where pollution and humidity might influence the withstand capability.

The worst case includes a scenario where fog or light rain in combination with polluted insulators are subjected to long temporary over-voltages. These conditions might dictate the insulation and clearance design. More detail regarding the impact of pollution on the withstand performance of insulators is given in section 2.5.5.

2.5.3 Airgap strength when subjected to slow-front switching over-voltages

For slow-front switching over-voltages, the impulse front time dominates the breakdown mechanisms. The tail time of the impulse usually has a large impact on the strength when contamination of insulators is present. When subjecting different gaps to slow-front impulses, the critical-time-to-crest of the specific impulse relates to the breakdown voltage of that specific gap.

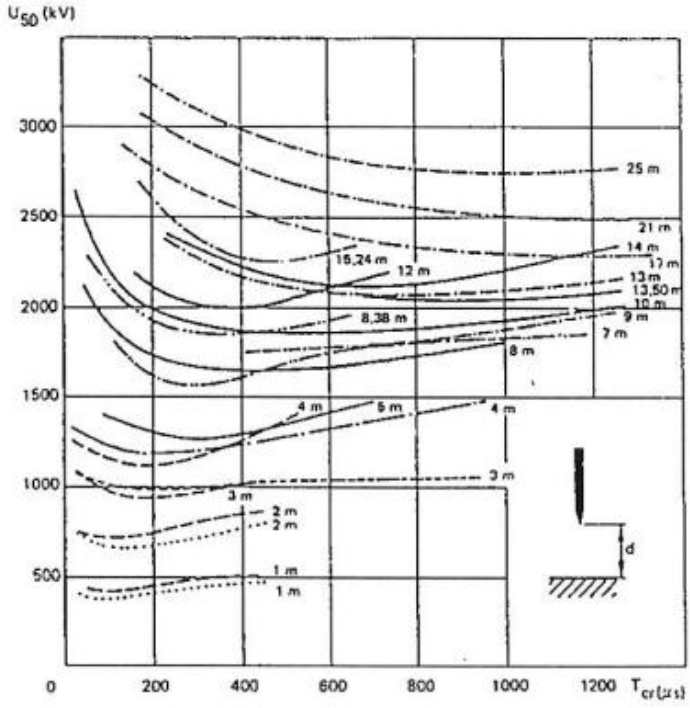


Figure 2-20: U - Curves for rod - plane gaps for slow-front over-voltages [30]

For large gaps, it is clear from Figure 2-20 that the critical-time-to-crest value is in the range of 250 – 300 µs. This means that when considering switching impulse stress where the shape is the standard 250/2500 µs, the breakdown voltage will be at its minimum. It is then a conservative approach due to the gap being exposed to front times much longer than that of the standard waveform. The insulation design for slow-front over-voltage will inherently be benefitting through this conservative approach.

It has been established that for rod – plane gaps of length up to 25 m, the breakdown strength CFO voltage can be approximated by [31]:

$$U_{50RP} = CFO\ A = 1080 \ln(0.46\, d + 1) \quad \text{(kV crest, m)} \qquad (2.59)$$

And for a better approximation during standard 250/2500 µs impulse:

$$U_{50RP} = CFO\ B = 500\ d^{0.6} \quad \text{(kV crest, m)} \tag{2.60}$$

Both the equations above are applicable to standard atmospheric conditions. The result of the difference between the two approximations is plotted in Figure 2-21 and listed in Table 2-7.

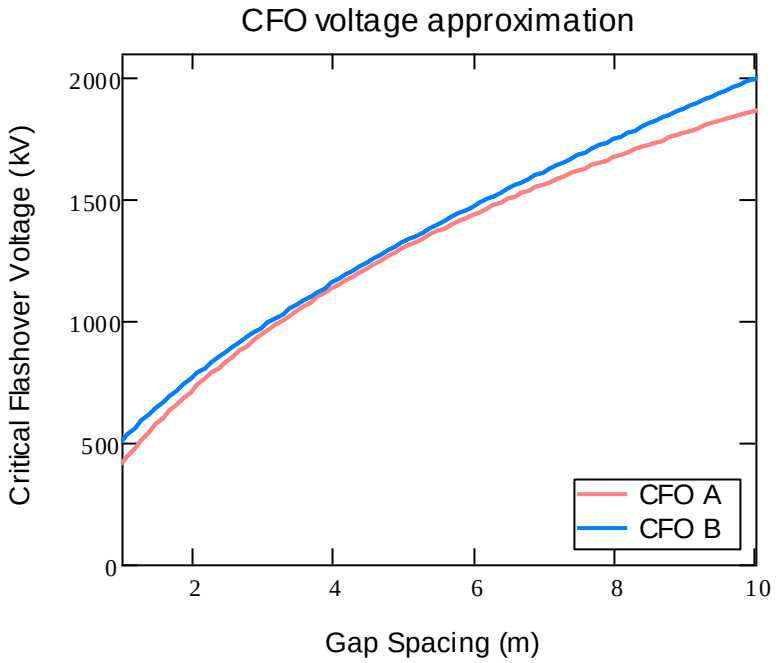


Figure 2-21: External Insulation CFO voltage approximation

For gaps of length up to 10 m, the two approximate equations yield very similar values. The following table lists the standard Eskom clearance gaps and the approximated CFO values. The deviation ratio reduces as the voltage increases from 88 kV to 400 kV. For gaps within 5 m, the results obtained from equation (2.60) yields higher values for the CFO voltage but are considered more accurate during the standard switching impulse stress.

Table 2-7: Standard Eskom clearances CFO voltage approximations

Nominal Voltage (kV)	Phase-to-earth (m)	CFO A (kV)	CFO B (kV)	Deviation Ratio
88	1	408.7	500.0	1.223
132	1.2	474.7	557.8	1.175
220	1.85	665.0	723.2	1.088
275	2.35	791.5	834.9	1.055
400	3.2	977.4	1004.8	1.028

According to Figure 2-20, all of the Eskom phase-to-earth clearances within the range 88 kV to 400 kV (gap distance between 1 m and 5 m) will have an expected CFO voltage level around the impulse rise time of 250 – 300 µs.

2.5.4 Airgap strength when subjected to fast-front lightning over-voltages

Literature indicates [31] that the behaviour of airgap breakdown during fast-front impulses is significantly different from that of slow-front impulse stress. For the standard lightning impulse of 1.2/50 µs, the experimental results show that there exists a linear relationship between the positive impulse and the gap distance. The breakdown voltage is lower when compared to that of the negative polarity impulse voltage, and non-linear. When considering the V/m against the gap spacing for positive polarity impulse, the CFO (V/m) is constant.

The breakdown strength is dramatically reduced when insulators are introduced. The impact of a shielding ring can also be observed, and thereby concluded that even though the gap factors determined for the use during slow-front impulse stress are not applicable during fast-front impulse stress, there exist a relationship.

Hileman has found that for transmission line insulators the recommended voltage gradient for positive polarity CFO+ is 560 kV/m and 605 kV/m for negative polarity. But this recommendation is based on the standard lightning impulse wave shape. When the waveshape differs from the standard 1.2/50 µs, the approximation of the critical flashover voltage becomes very sensitive to the rise and tail times of the impulse. For more detailed approximations, the leader progression model provides a more accurate estimation for the volt-time characteristic of the insulation.

For standard lightning impulse wave shapes of positive polarity experimental data have been approximated to give the relationship [17]:

$$U_{50RP} = 530\, d \qquad \text{(kV crest, m)} \tag{2.61}$$

This relationship is applicable to rod – plane gaps ranging between 1 m and 10 m.

The experimental data obtained reveals that the gap factors for lightning impulse stress can be approximated as a function of the switching impulse gap factor.

$$K_{ff+} = 0.74 + 0.26\, K \tag{2.62}$$

Regarding the CFO of surges that might enter into the substation, the overhead line insulator string arrangements are considered and can be approximated by [17]:

$$U_{50RP} = 700\, d \qquad \text{(kV crest, m)} \tag{2.63}$$

All of the above equations relating to the CFO should be corrected for altitude. For larger gaps, particular voltage ranges II, the CFO could be significantly influenced by the insulator type used and the inherently capacitive contributions to the breakdown process. The negative impact that cap and pin insulators have on the breakdown strength could potentially be addressed by including grading or shielding rings. Using polymeric insulators rather that

cap and pin glass disc insulators could also assist with improving the withstand capability of the gap.

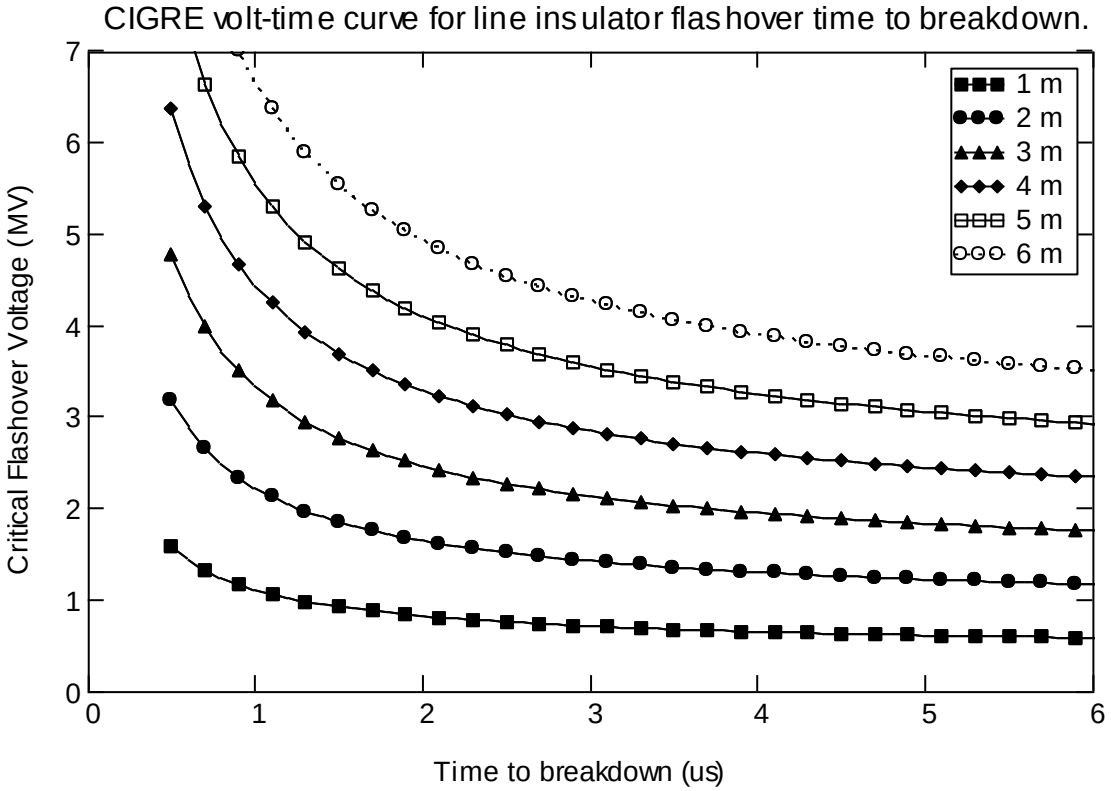


Figure 2-22: CIGRE volt-time curve for line insulator flashover [30]

It is well known that the magnitude of fast-front impulses has a significant impact on the duration of the time to breakdown. The higher the magnitude, the shorter the time to breakdown. For impulses close to the CFO, the flashover occurs usually on the tail of the impulse. In Figure 2-22 the flashover as a function of the time to breakdown is plotted.

2.5.5 Contamination

In the previous sections, the breakdown strength of air is discussed with regards to the slow and fast-front over-voltage stresses. When pollution is taken into consideration, the design could very easily be dominated by the withstand performance of insulators subjected to high levels of pollution [8].

The breakdown mechanism associated with high levels of pollution on insulators is unique in terms of the required combination of factors to allow for flashovers to occur.

With reference to ceramic insulators, it is well known that the combination of two events is required for a flashover to occur. First, a sufficient degree of contamination is required to be deposited on the insulator. The contamination includes a type of soluble salt and is deposited on the surface of the insulator. Secondly, light rain or fog without creating a washing effect is necessary to create a conductive film layer. The combination of the contaminant and the moisture produces the ideal conditions for a flashover due to high pollution levels. The mixture creates conductive paths for leakage current to flow, some of the paths are dried and dry bands are created along the insulator. It is now possible for the

total phase-to-earth voltage to appear across these dry bands and arcs gradually grow outward. When the arcs meet, the flashover occurs [32].

Pollution types could be classified according to the following [33]:

1. Ordinary salt pollution; This type of salt accumulates slowly over time due to exposure to calm wind.
2. Rapid salt pollution; Coastal areas consist of high concentration salts in the wind and this pollution type is deposited rapidly with stronger winds.
3. Industrial pollution; Soot and smoke from nearby factories and industries are deposited on the insulators.

The critical flashover-voltages of insulators have been tested and it is clear that there is significant differences between the withstand capability of I-strings compared to V-string insulator assemblies.

The following information is adopted from [32] and describes the withstand capability of the insulator strings as a function of the pollution (salt) per square centimetre.

The critical flashover voltage (CFO) in Figure 2-23 is measured per unit length of insulator string. I-strings perform the worst in contaminated environments and have a CFO in the range of 75 kV/m when a high SSD is considered.

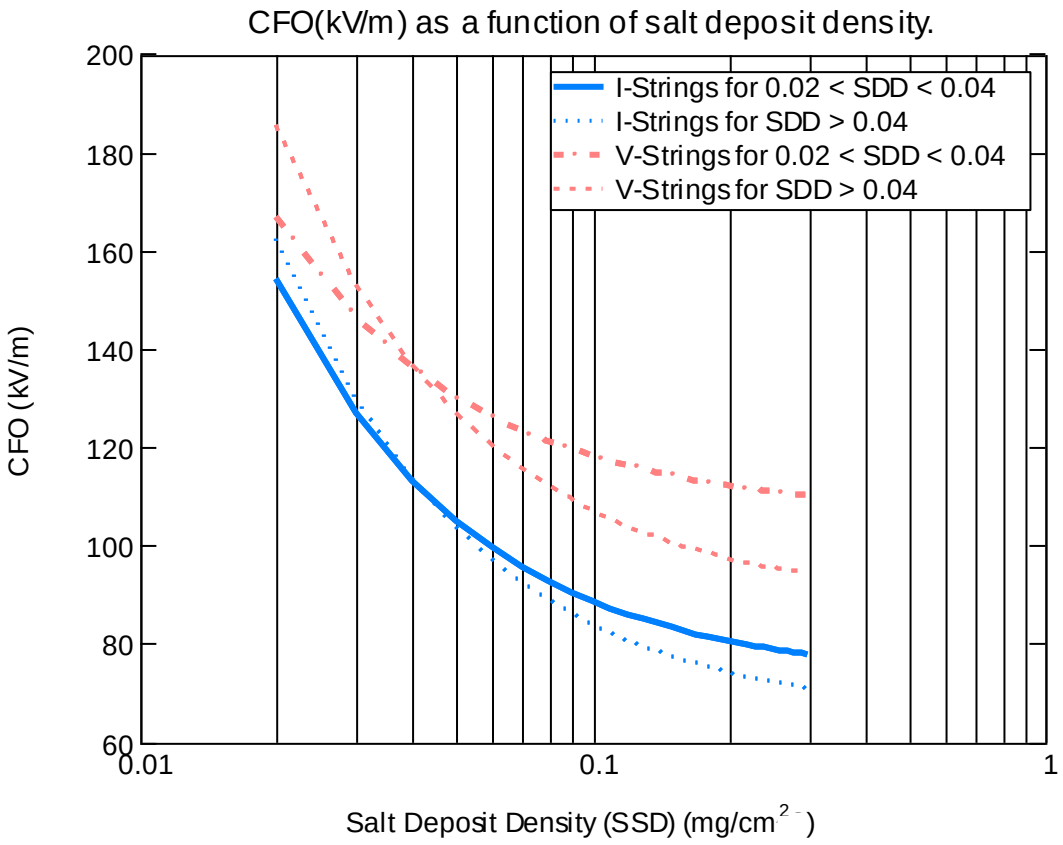


Figure 2-23: Insulator string CFO as a function of SSD [32]

With regards to the difference between the withstand strength of ceramic insulators and silicon rubber (SiR) insulators the following has been established by the authors of [34].

From the test executed, it was recorded that the withstand voltages of SiR insulators are in the range of 50 % to 60 % greater when compared to ceramic or porcelain insulators. SiR and Ethylene Propylene Diene Monomer (EPDM) are two of the primary non-ceramic materials used for polymeric insulators. The performance of EPDM is good in terms of withstand levels when compared to the porcelain insulators and it was recorded to be 20 % to 25 % greater [33].

1. For porcelain and ceramic insulators, creepage or leakage distance is the single most important parameter and should improve the performance if extended distances are employed.
2. Non-ceramic insulators perform better in terms of critical flashover voltage in contaminated environments. SiR insulators perform best when compared to ceramic insulators. In non-contaminated environments, there are other benefits such as weight saving and ease of maintenance.
3. Room temperature vulcanization (RTV) coatings can be applied to ceramic or porcelain insulators to improve performance. The performance could be increased and the same performance as SiR can be achieved.
4. Insulator configuration has a significant impact on the performance. V-strings outperform I-strings. Where possible, convert I-strings to V-strings. The mechanical advantage also includes the minimisation of conductor swing.
5. Other options include semiconducting glaze insulators, greasing and washing. But all of these solutions are overshadowed by better solutions mentioned earlier.

The benefits of non-ceramic insulators include the following: Improved performance in contaminated environments, is lighter in weight, highly flexible, requires less maintenance and reduces radio noise.

Non-ceramic insulators are not 100 % arc resistant and are affected by ultraviolet radiation. Corona should be reduced to mitigate against the negative impact it has on the non-ceramic insulator material.

When the performance of uprated substations in contaminated environments was evaluated by a series of tests [8], the primary conclusion was to include a thorough pollution severity study within the design review. There is very little information regarding the flashover mechanism regarding uprated substations. Mitigations to increase the withstand capability of insulators in uprated substations should be carefully evaluated.

2.6 Design clearances

The AIEE Substations Committee published a guide [11] for minimum electrical clearances for substations. The guide was published in 1954 and presented clearances based mainly on phase-to-earth clearances and lightning over-voltage flashover (1.3 m rod gap [10]) at selected Basic Lightning Impulse withstand levels. The clearance values did however account for altitude correction and, before any safety margin adjustment, reflected a breakdown gradient for air of 600-850 kV/m.

The IEEE Substations Committee published the first reports on minimum electrical clearances based on switching surge phenomena [12] . The electrical clearances listed within this document were published with reference to operating voltages exceeding 242 kV.

In 1972 the committee published updated clearances based on switching surge requirements [13].

In 1975 Georges Gallet [14] et al. presented the well-known and generally accepted expression describing the positive switching impulse strength of air insulation. The concept of gap factor, k_g was also introduced during this time and was valid for airgap configurations between 1 m and at least 30 m.

The initial process of determining the insulation levels allows for the next phase of design where the clearances for the substation are selected. The process usually involves extensive insulation coordination studies to allow the engineer to make sensible decisions in the design of the system. System configuration, surge arrester energy handling capability and over-voltage magnitudes are some of the important factors to consider during this process.

In general, electrical clearances are usually standardized and referenced to the nominal operating voltage. In the past, larger clearances were easily accepted and minimum recommended clearances find value within the environment where voltage uprating might be required.

Some considerations that lead to the requirement for a larger clearance include:

- Altitude,
- Contamination,
- Animals able to bridge the gap,
- High fault current resulting in excessive forces on post insulators,
- High lightning ground flash densities,
- Operating and maintenance access requirements,
- Surge protective device location.

2.6.1 Clearances based on lightning impulse

The method used to determine clearance as a function of the LIWL has effectively not changed since the first publication for recommended clearances based on the LIWL and is described in the AIEE report of 1954 [11].

The clearance calculation includes the determination of the negative polarity critical breakdown gradient of air. The gradient is a function of the arrangement and gap factors present. The gradient has been experimentally determined and is in the range between 500 kV/m and 750 kV/m. Typical gradients relevant to a substation arrangement are in the range of 605 kV/m but can be reduced to 500 kV/m depending on how conservative the design is [30],[17].

The relevant equation to calculate the clearance is given by:

$$S = \frac{V_{\text{crest ph-g}}}{CFO_{\text{gradient}}} \tag{2.64}$$

Where

S Metal to metal clearance in meters,

$V_{\text{crest ph-g}}$ the crest voltage of the standard lightning impulse in kV,

CFO_{gradient} is the critical flashover gradient in kV/m.

As

$$\text{LIWL} = \frac{V_{\text{crest ph-g}}}{1.15} \tag{2.65}$$

Combining the two equations:

$$S = \frac{1.15\ \text{LIWL}}{CFO_{\text{gradient}}} \tag{2.66}$$

For phase-to-phase clearances based on the lightning impulse, it is known that during a lightning strike to a single phase of the transmission line, an induced voltage appears on the other two phases. When the phase-to-phase voltage is compared to the phase-to-earth voltage It is much lower. It is very unlikely that the phase-to-phase voltage will exceed that of the phase-to-earth voltage. For this reason the phase-to-phase clearances are calculated based on the phase-to-earth value with an additional safety margin of 10 %.

In Figure 2-24 the clearance is plotted against the CFO gradient. The gradient increases from 500 kV/m to 750 kV/m. The recommended clearances specified by the IEEE [2] are based on a CFO gradient of 605 kV/m with a 10 % safety factor for the phase-phase clearances. The recommended clearances are captured in Table 2-8.

Table 2-8: Standard Eskom voltage levels and clearance based on LIWL [17],[18]

			IEEE**		**IEC*****	
Nominal Voltage (kV)	**Maximum Voltage (kV)**	**Basic Lightning Impulse Withstand Level (kV)**	**Phase-to-earth clearance (m) ****	**Phase-to-phase clearance (m)**	**Rod – structure (m)**	**Conductor structure (m)**
66	72	350	0.67	0.73	0.63	
88	100	380	0.72	0.79	0.9	
132	145	550	1.05	1.15	1.1	
220	245	825	1.57	1.73	1.7	1.6
*275	300	1050	2.00	2.20	2.1	1.9
*400	420	1425	2.71	2.98	2.85	2.6
*500	550	1550	2.95	3.24	3.1	2.9

*Switching surge conditions usually govern in this voltage level

**CFO voltage gradient based on 605 kV/m, Source IEEE

***Rod Structure and conductor structure refers to gap factors used, Source IEC

The standard Eskom voltage levels from 66 kV to 500 kV have phase-to-earth clearances in the range of 67 cm to 3 m. Further considerations mentioned before that might introduce larger gaps should be investigated when gaps are fixed and accepted.

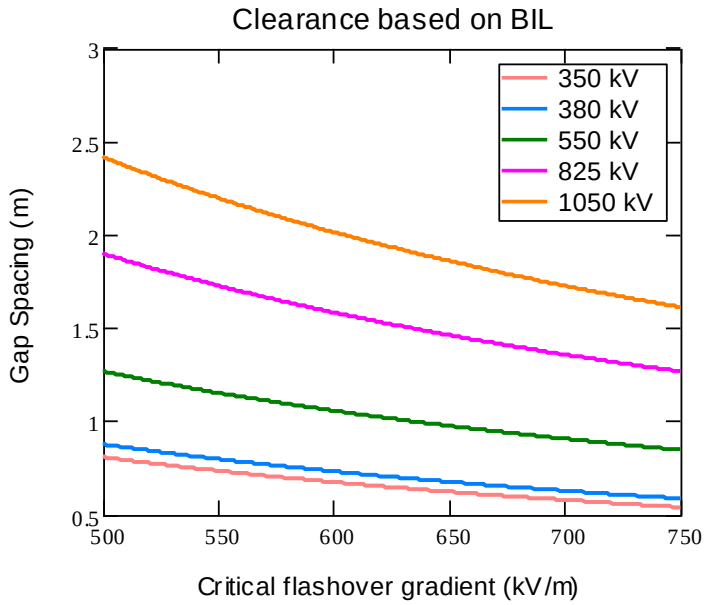


Figure 2-24: Clearance based on LIWL as a function of the CFO gradient [30]

It is clear that when conservativeness is applied, a lower CFO gradient will yield larger gap spacing requirements.

2.6.2 Clearances based on switching impulses

When considering external insulation strength during switching surges the breakdown phenomenon is statistical in nature. The probability of flashover can be described by a curve with the following parameters.

- CFO voltage that is defined as the voltage where the probability of flashover is 50%,
- Coefficient of variation that is essentially the standard deviation σ_f/CFO.

The statistical withstand levels SIWL are then described by the equation:

$$SIWL = CFO(1 - 1.28\frac{\sigma_f}{CFO}) \tag{2.67}$$

For substations the coefficient of variation is usually in the range of 0.07 and the equation becomes [18]:

$$SIWL = 0.9104\, CFO \tag{2.68}$$

$$CFO = \frac{SIWL}{0.9104} \tag{2.69}$$

- Gap configuration and gap factor

The gap factor K_g is defined as the ratio between the actual airgap flashover voltage and the positive rod-plane airgap flashover voltage for the same gap length. Gap factors are determined experimentally where the switching impulse waveforms are kept identical. It is also known that the gap factor slightly increases with the number of sub-conductors according to the following expression [18]:

$$K_{Bundle} = K_{single} + 0.01(N - 2) \quad (2.70)$$

This equation is however only relevant where the number of sub-conductors is between 2 and 8 and the sub-conductor spacing is between 40 cm and 50 cm.

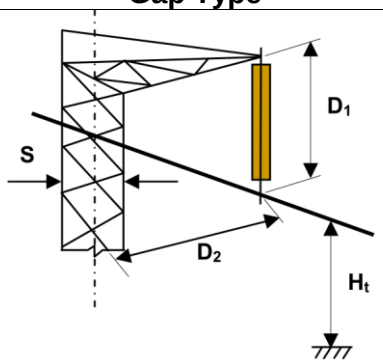
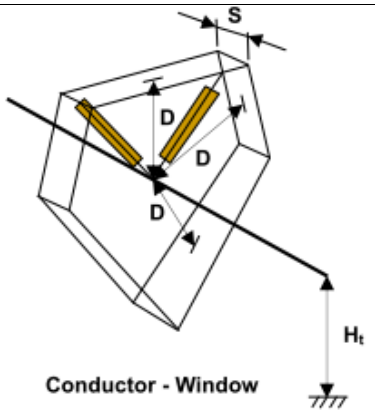
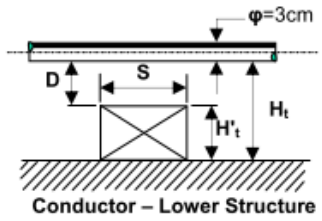
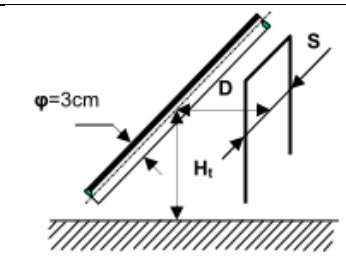
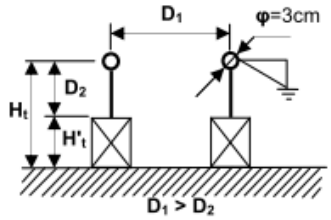
Addressing the field distribution of HV conductor assemblies has a significant impact on the gap factor. Grading rings and hardware designs could potentially increase the gap factor to effectively reduce the required clearance from live apparatus/conductors to the structure.

Recommended gap factors for actual phase-earth configurations are given in Table 2-9, Table 2-10 and Table 2-11.

Table 2-9: Typical phase-earth gap factors recommended by IEC [17]

Configuration	**Typical value**
Conductor – cross arms	1.45
Conductor windows	1.25
Conductor – lower window	1.15 – 1.5 or more
Conductor – lateral structures	1.45
Rod – rod structure	1.3

Table 2-10: IEC recommended gap factors for phase-to-earth switching impulse [17]

Gap Type	Parameters	Typical Range	Reference value	
 Conductor - Structure	K_g	1.36 – 1.58	1.45	
	D_2 / D_1	1 - 2	1.5	
	H_t / D_1	3.34 - 10	6	
	S / D_1	0.167 – 0.2	0.2	
 Conductor - Window	K_g	1.22 – 1.32	1.25	
	H_t / D	8 – 6.7	6	
	S / D	0.4 – 0.1	0.2	
 Conductor – Lower Structure	K_g	1.18 – 1.35	1.15 Conductor-plane	1.47 Conductor - rod
	H'_t / H_t	0.75 – 0.75	0	0.909
	H'_t / D	3 - 3	0	10
	S / D	1.4 – 0.05	-	0
 Conductor – Lateral Structure	K_g	1.28 1.63	1.45	
	H_1 / D	2 – 10	6	
	S / D	1 – 0.1	0.2	
 Longitudinal Rod – Rod structure	K_g	1.03 – 1.66	1.35	
	H'_t / H_t	0.2 – 0.9	0	
	D_1 / H_t	0.1 – 0.8	0.5	

The same approach is adopted to determine the phase-phase switching impulse strength.

Table 2-11: Typical phase-phase gap factors recommended by IEC [17]

Configuration	**α =0.5**	**α =0.33**
Ring-Ring	1.8	1.7
Crossed conductors	1.65	1.53
Rod-rod or conductor-conductor (along the span)	1.62	1.52
Supported busbars (fittings)	1.5	1.4
Asymmetrical geometries	1.45	1.36

This expression describes the CFO for air insulation and it was combined with the concept of gap factor [10].

$$S = \frac{8}{\frac{3400\ K_g\ \delta^m}{CFO} - 1} \tag{2.71}$$

Where

S Metal to metal gap spacing in meters.

K_g Gap factor.

δ^m Altitude correction factor (1.0 at sea level).

CFO Critical flashover voltage (50 % value).

Typical values for the gap factor range between 1 and 1.9 where IEC and IEEE slightly differs in their approach. All gap factors for IEC have been discussed and is summarized in section 2.5.1. The gap factors for phase-to-earth insulations recommended by the IEEE are given in the following table.

Table 2-12: Switching surge parameters for phase-to-earth according to IEEE [18]

Gap configuration	**Gap Factor K_g**	**Coefficient of variation σ_f/CFO**
Rod – plane	1	0.07
Rod – rod (vertical)	1.3	0.07
Rod – rod (horizontal)	1.35	0.07
Conductor- lateral structure	1.3	0.07
Conductor - plane	1.15	0.07

For altitude correction, δ^m is assumed to be 1 for the corresponding insulation at sea level. A recommended gap factor of 1.3 is selected to simplify the Gallet-Leroy equation further. The simplified equation for phase-to-earth clearances presented within the IEEE guideline is [18]:

$$S = \frac{8}{\frac{3400\ K_g\ \delta^m}{CFO} - 1} = \frac{8}{4024/SIWL - 1} \tag{2.72}$$

IEC and IEEE have a different recommendation when it comes to the SIWL phase-to-earth vs SIWL phase-to-phase ratio. IEEE also has recommended switching surge factors for phase-to-phase surges where the coefficient of variation is not fixed at 0.07.

The following table includes the recommended factors relating to IEEE phase-to-phase switching:

Table 2-13: Switching surge factors for phase-to-phase configurations IEEE [18]

Gap configuration	**Gap Factor K_g**	**Coefficient of variation σ_f/CFO**
Conductor – conductor 10 m	1.35	0.035
Rod – rod	1.35	0.05
Conductor – conductor 300 m	1.26	0.02
Crossed conductors	1.34	0.05
Ring – ring or large electrode	1.53	0.05
Asymmetrical gaps rod - conductor	1.21	0.02

$$S = \frac{8}{\frac{3400\ K_g\ \delta^m}{R_{pp}CFO} - 1} \tag{2.73}$$

For the recommended phase-to-phase clearances according to IEEE, a gap factor of 1.35 is selected to represent a 10 m conductor – conductor arrangement as per Table 2-14.

Table 2-14: Basic withstand levels from IEC and IEEE [17], [18]

Nominal Voltage (kV)	**Maximum Voltage (kV)**	**Basic Lightning Impulse Withstand Level (kV)**	**Basic Switching Impulse Withstand Level (kV)**	**R_{pp} IEC**	**R_{pp} IEEE**
66	72	350	-	-	-
88	100	380	-	-	-
132	145	550	-	-	1.35
220	245	825	-	-	1.35
*275	300	1050	850	1.5	1.35
*400	420	1425	1050	1.5	1.37
*500	550	1550	1300	1.5	1.37

The coefficient of variation is 0.035 and δ^m is 1.0 at sea level. The Gallet Leroy equation for the 10 m conductor – conductor phase-to-phase switching arrangement is then reduced to the following equation which results in Table 2-15:

$$S = \frac{8}{\frac{3400\ 1.35\ 1.0}{R_{pp} 1.047\ SIWL} - 1} = \frac{8}{\frac{4384}{R_{pp}\ SIWL} - 1} \tag{2.74}$$

Table 2-15: The recommended minimum clearances according to the IEEE guide [9]

Nominal Voltage (kV)	**Maximum Voltage (kV)**	**Basic Lightning Impulse Withstand Level (kV)**	**Basic Switching Impulse Withstand Level (kV)**	**Minimum phase-to-earth $K_g = 1.35$**	**Minimum phase-to-phase $K_g = 1.35$**
66	72	350	-	-	-
88	100	380	-	-	-
132	145	550	-	-	-
220	245	825	-	-	
*275	300	1050	850	2.065	2.725
*400	420	1425	1050	2.825	3.905
*500	550	1550	1300	3.820	5.475

The differences between the IEC and IEEE recommended clearances based on switching impulses for phase-to-phase configurations (phase-to-earth is similar in the approach) is described in the table below.

Table 2-16: Coefficient of variation comparison

	IEC [17]	**IEEE** [18]
Coefficient of variation	Recommend the value of 0.07 for phase-to-earth and phase-to-phase calculations	Value based on gap configuration. Conductor – conductor 10 m configuration for phase-to-phase and 0.035 for the coefficient of variation
Phase-to-phase Ratio	Ranges between 1.5 and 1.7	Ranges between 1.35 and 1.37 but also recommends IEC ratios.

2.7 Metal-oxide varistor surge arresters

To embark on the selection procedure for the correct arrester a review of durability and capability characteristics is required. The durability and capability tests performed by the IEEE [1,2] and IEC [3,4] standards differ in terms of their approach. However, even though the testing approach differs, the procedure to select the proper arrester rating is identical. The establishment of the arrester protective characteristics was performed with the tests specified in these standards.

In South Africa, the Electrical Engineering Directive (signed in October 1970) [1] specifies the minimum electrical and working clearances for substations. These minimum clearances are based on the silicon-carbide gapped-type arrester. Due to the fact that these standards are employed as a design guideline, the metal-oxide arrester and silicon-carbide (SiC) arresters will both be discussed in this section.

In 1971 the first metal-oxide surge arrester was reported by Matsuoka [5]. The first introduction in North America was in 1977 and was introduced to the power sector by Sakshaug et al.[2] Even though metal-oxide arresters found their way into the South African transmission system quite early, a reconsideration of the standard clearances presented by the EED [1] was never performed. One of the main reasons why the standard clearances were never optimised was the possibility for future live substation work. With live substation work, conservative clearances are encouraged to increase clearances and space for live substation work. This study however does not include the consideration for future live substation work and is purely focused on the optimisation of these clearances for layout minimisation and voltage uprating.

The design of metal-oxide arresters also developed significantly from their inception. Due to the concern for stability and life of the metal-oxide arrester, gaps were integrated to reduce the normal power frequency voltage experienced by the blocks. With improved designs, these gaps were omitted and the gapless metal-oxide arrester emerged [24].

Comparing the metal-oxide arrester with the silicon-carbide gapped-type arrester, the following differences are noted:

Metal-oxide arresters advantages include:

- Simple design, improved quality and decreased risk of moisture ingress.
- Improved protective characteristics, and
- Improved energy absorption capability.

Due to the nominal power frequency voltage being applied to the metal-oxide arrester on a continual basis, a small current is produced that flows to earth. This current is small and is around 1 mA. This current is not detrimental, but when longer than usual TOV occurs, problems could arise. If the TOV is large and long enough, the temperature of the metal-oxide may rise and thermal runaway could occur that will lead to failure.

The conventional “arrester rating” is replaced by the maximum continuous operating voltage. This voltage is the maximum voltage that can be applied to the arrester on a continuous basis.

2.7.1 General Characteristic of the metal-oxide arrester

The metal-oxide surge arrester can be described by the voltage-current (VI) characteristic. The characteristic can be subdivided into three regions namely [24].

Region 1: Maximum Continuous operating voltage region; The current is less than 1 mA and is primarily capacitive. The MCOV is selected according to the rated voltage.

Region 2: Switching surge and temporary over-voltage (TOV) region; The current ranges between 1 mA to 1000/2000 A and is primarily a resistive current.

Region 3: Lightning region; The current ranges between 1 and 100 kA. With very large currents the characteristic approaches a linear relationship with the voltage and becomes pure resistive.

It should be noted that the thermal efficiency of the heat dissipation within the metal-oxide should be optimised. When the temperature increases the resistive component of the current increases and in turn leads to more power dissipation and heat. To prevent thermal runaway, adequate heat transfer between the arrester and the atmosphere is needed. Voltages that exceed the MCOV rating of the arrester will lead to increased temperatures. And so the continuous voltage across the arrester should be maintained well within the MCOV rating. TOV should also be within the allowable time limit of the characteristic.

2.7.2 Arrester Classes

Arresters can be classified into three classes described by their durability and capabilities [24].

- Station class arrester: Usually utilised in HV and EHV systems,
- Intermediate class arrester: Between distribution and station class arrester,
- Distribution class arrester: Used in Distribution systems but can be further divided into heavy duty, normal and light duty arresters.

2.7.3 Energy Handling and discharge characteristics

When the arrester is exposed to excessive energy absorption, the arrester can be driven into a state of thermal runaway. The situation where heat generated within the arrester exceeds the heat dissipated into the atmosphere can further increase the valve element temperature. The failure of the arrester because of excessive heat usually causes damage to the valve element material, and ultimately the failure of the arrester.

Non-uniform energy dissipation or an imbalance of energy density within the arrester could also lead to localised high temperature gradients. This could lead to arrester failure in the form of cracking or puncture of the material.

The energy handling capability of an arrester is described in terms of kilojoules per kilovolt of the arrester MCOV. Alternatively, the capability is described by kilojoules per duty-cycle rating.

The energy handling capability of an arrester is a function of the following arrester discharge current characteristics:

- Magnitude ,
- Shape of waveform,

- Duration.

Over-voltage transients and temporary over-voltages can be classified according to their source current characteristics [24].

2.7.4 Protective Margin

There are a number of standards that specify the protective characteristics. These characteristics are defined by a specified discharge current magnitude and shape, at a given voltage across the arrester.

The margin of protection is the difference between the equipment withstand level (LIWL or full-wave withstand) and the protection characteristics (discharge voltage) of the surge arrester. The protective margin is described by the relationship between insulation level and the arrester protective level. The margin of protection can be expressed as follows [24]:

$$Protective\ margin = \left[\frac{Insulation\ withstand\ level}{Arrester\ protective\ level} - 1\right].100 \quad (2.75)$$

2.7.5 8/20 µs and 30/60 µs Discharge Voltage

Also referred to as the minimum residual voltage of a surge arrester is the voltage that appears across the arrester during the conduction of a surge current. More specifically the voltage is expressed as the crest voltage experienced when conducting currenta surge current of a specified wave shape. These wave shapes are classified for both lightning surge and switching surges. For lightning surge the 8/20 µs wave shape is considered and for switching 30/60 µs. Referring to the protective margin, the crest value of the discharge voltage for these standard current waveforms should be less than that of the LIWL of the protected equipment. Eskom specifies a protective margin of 30% for HV and EHV systems. The protective margins may be increased when high levels of lightning ground flash density are anticipated [24].

2.7.6 Arrester Protective Distance

The ability of the surge arrester to protect against over-voltages is not only dependent on the volt/current characteristic of the metal-oxide arrester. Due to the distance effect, the distances of stringer conductors between the arrester terminals and the protected equipment becomes very important. Transient front time or steepness (kV/µs) is a variable with significant importance.

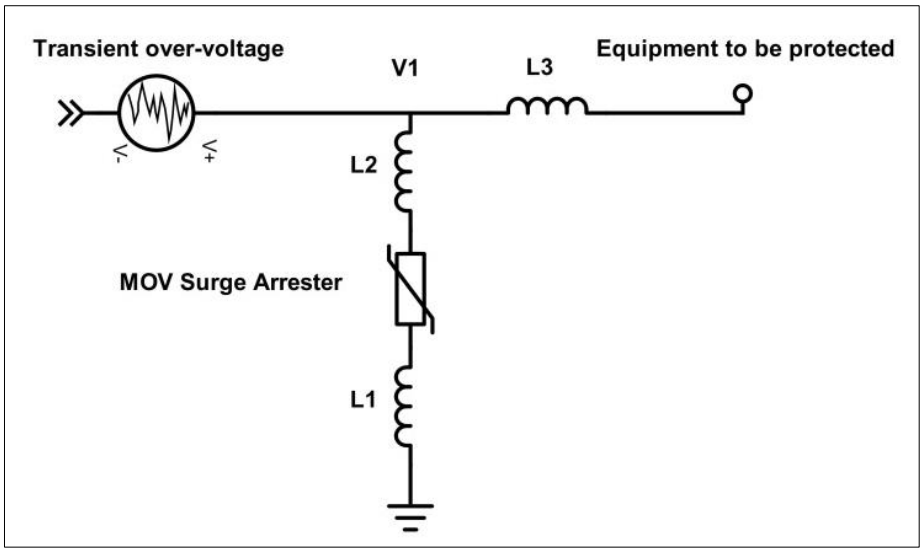


Figure 2-25: Arrester protective distance

A surge arrester is usually mounted on a steel support structure with a certain height. Copper earth conductors are connected from the base of the arrester to the substation earth electrode. The length of conductor is important because of its inductance. In Figure 2-25 the arrester is placed next to the equipment to be protected. The conductors have inductance where L1 represents the structure height between the arrester base plate and true earth. L2 and L3 represents the stringer conductors that connect the arrester to the equipment node. There will be a significant difference between the terminal voltage of the arrester and the connection point of the equipment during fast-front transients. During slower front transients, this effect could be significantly smaller.

The following equation describes the protective distance of the arrester [15]:

$$L_{max} = v.\frac{\left[\frac{BIL}{(1+M_p)} - U_{res}\right]}{2s} - (H_{SA} + H_{struct}) \tag{2.76}$$

Where

L_{max} is the maximum allowable separation distance (m).

H_{SA} is the surge arrester height (the actual arrester length and distance L2 in m).

H_{struct} is the structure height representing L1 in m.

v is the propagation velocity which is approximately 300 m/µs.

LIWL is the basic insulation level of the equipment (kV).

M_p is the protective margin required (suggested value of 25% to 30%).

U_{res} is the arrester protective level (kV).

s is the steepness of the incoming surge in kV/µs.

3 CALCULATIONS AND SIMULATIONS

In order to determine the stresses relevant for switching HV and EHV circuits, slow-front transient studies yield valuable information. With the breakdown strength of large airgaps being lower for slow-front impulse stress, thorough switching-voltage analysis is very important when considering voltage uprating. For the voltages of concern in the HV range (88 kV and 132 kV), lightning could pose a higher risk of insulation breakdown. The following studies are considered:

1. 275 kV uprating to 400 kV

Slow-front switching over-voltages are of greater concern at EHV voltage levels due to several aspects mentioned earlier. Switching performance evaluation provides valuable information to evaluate the risk of failure within the substation. In this study, 275 kV transmission line tower arrangements were modelled. Detailed substation modelling is excluded, but the bay elevations are evaluated in terms of available electrical and working clearances. Equipment that will be exposed to the over-voltage will be identified. The switching studies included scenarios where trapped charge, pre-insertion resistors and surge arresters were included.

2. 88 kV uprating to 132 kV

The HV transmission line and substation electrical clearances are smaller and considering the increased exposure to lightning due to the number of lines in the network, lightning should be considered as the primary transient over-voltage concern. Switching over-voltage distributions are expected to be much lower due to the absence of residual voltages and reclosing operations. Distribution lines are also relatively short when compared to the transmission lines of voltage range 2. The relevant scenarios where lightning causes over-voltages that are of concern for the substation are back-flashovers close to the substation and shielding failures. The substation bay configuration and equipment positions are evaluated. Electrical clearance calculations based on the switching impulse withstand level are calculated to allow for a complete evaluation.

3.1 Methodology for slow-front over-voltage studies

As mentioned before, a slow-front transient analysis includes a semi-statistical approach to determine the relevant over-voltages. A probability distribution function describing the potential over-voltages of a specific circuit or network configuration is required as an input into the insulation coordination process. Representative over-voltages, combined with the selected withstand capability of the internal or external insulation allows informed decisions to be made based on the calculated risk of failure.

The methodology of analysing slow-front switching over-voltages includes the following:

- Modelling of representative interconnected networks,
- Modelling of representative switched components such as transmission lines, capacitor banks, transformers, cables, etc.
- Configuration of circuit breaker switching times and number of simulations,
- Capturing the stress distribution,
- Addressing the stress when over-voltage limiting devices are present,
- Selection of the withstand levels and evaluating the risk of failure.

The modelling of a representative interconnected power system requires special attention when accurate results are expected. The required data for a thorough transient analysis is as follows:

- Configuration and operation procedures,

The number of transmission lines in service and the operating procedures such as reclosing philosophy, must be modelled accurately. It is necessary to evaluate the probability of the possible configurations for a realistic representation. To represent a worst-case scenario, the model is limited to one or two substations away from the line being energised. Additional transmission lines and source impedances might represent a more realistic scenario, but will add additional damping to the transients.

- Fault location,

The location of the fault and type of fault to be modelled is important and will have a significant impact on the expected over-voltage.

- Number of operations per year

To calculate the expected failure rate, the number of circuit breaker operations for a certain time frame is required.

- Circuit breaker probabilistic data,

To model the system accurately the circuit breaker probabilistic data is included in a statistical switch.

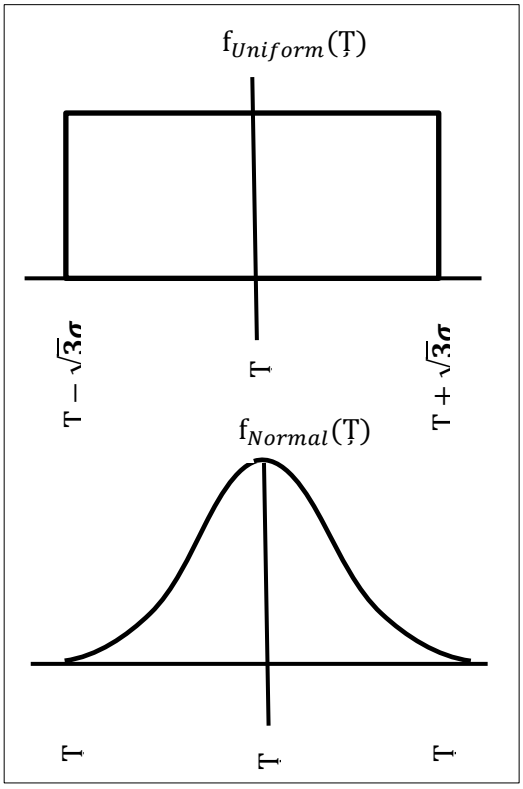


Figure 3-1: Statistical switch distributions

The statistical switch that represents the circuit breaker includes the following important information:

- Mean time of closing,
- Standard deviation of the closing time,
- Type of distribution (normal or uniform) for the closing time frame.

$f_{Uniform}(T)$ in **Error! Reference source not found.** represents the closing distribution of the master statistical switch. The circuit breaker operating time covers the 50 Hz 20 ms cycle in order to represent a random switching scenario. The slave switches (remaining two phases) follows the master switching time with a normal distribution. The slave switching times represents the delay between the breaker mechanisms and is usually in the order of 4 ms.

3.2 Methodology for fast-front over-voltage studies

The methodology usually employed to consider the random nature of lightning usually consist of an analytical calculation based on a number of assumptions, or a semi-statistical approach. The lightning wave shape has been statistically defined as a log normal distribution and the source lightning currents are represented as such [25].

The method mainly includes the following:

- Determination of protective distance

As mentioned before, the arrester protective distance during fast-fronted over-voltages is significantly dependant on the rate-of-rise of the transients. In addition, with longer distances between the struck point and the equipment/air-gap of concern, the steepness is attenuated by corona and the capacitance of the transmission lines. The fast-fronted surge transforms into a slow-fronted surge and in turn is not so sensitive to the protective distance of the arresters.

- Lightning stroke scenarios

In this study, a worst-case scenario is represented by a back-flashover that occurs a few spans away from the substation with wave parameters correlated to the statistical data obtained in the work of CIGRE study committee C4 [26] .

- Over-voltage evaluation

The over-voltages within the substation are evaluated in terms of the withstand capability of the equipment. The external and internal insulation withstand capabilities are selected based on the equipment specification and air clearance calculations.

The required data for the study includes the following:

- Substation layout (positions of instrument transformers, disconnectors, circuit breakers etc.),
- Withstand levels (BIL and SIWL) of equipment,
- Surge arrester current/voltage characteristic,
- Transmission line geometry,
- Conductor details,
- Shield wire details,

- Tower footing arrangement and impedances,
- Ground flash density,
- Position of surge arresters.

3.2.1 Withstand levels and protective margin

As a starting point, all protective margins are calculated based on the metal-oxide surge arrester maximum residual voltages. All standard Eskom nominal voltages are referenced in terms of the protective margins at the arrester terminals. It is known that due to the inductance of conductors, the changing voltage of the arrester is high during current surges. Further simulations are thus necessary to consider the reflections of travelling waves in the substation and to include the arrester protective distance into the process of stress versus strength evaluation.

3.3 Uprating 88 kV to 132 kV

For the substation bay configuration, two voltage levels are considered. The 88 kV feeder bay is reviewed in terms of existing dimensions as shown in Table 3-1. Key dimensions include busbar height, busbar phase clearance, and main steelwork support structure positions. In the past, 132 kV equipment has already been installed in 88 kV high voltage yards in Eskom's transmission substations.

Table 3-1: 88 kV bay layout dimensions

Dimension	**Length/Height (mm)**
Earth wire attachment height	11440
Stringer and Beam height	9284
Busbar height	6706
Busbar phase-to-phase	2438
Bay stringing phase-to-phase	2400
Bay width	8534

For the substation layout, a typical Eskom 88 kV feeder bay layout represents the 88 kV substation to be uprated. The distances between the high voltage equipment and electrical clearances between the live electrodes are captured. For the fast-front study, distributed line models are used together with small simulation time steps. The busbar parameters are listed in Table 3-2 and the bay layout shown in Figure 3-2.

Table 3-2: 88 kV Busbar parameters

Positive sequence transmission line parameters	**Value**
Resistance	0.0171 Ω/km
Inductive Reactance	0.2389 Ω/km
Inductance	0.76 mH/km
Capacitive Susceptance	0.4806 x 10^{-5} S/km
Capacitance	15.3 nF/km
Surge Impedance	222 Ω
Zero sequence transmission line parameters	**Value**
Resistance	0.164 Ω/km
Inductive Reactance	1.48 Ω/km
Inductance	4.73 mH/km
Capacitive Susceptance	0.23 x 10^{-5} S/km
Capacitance	7.35 nF/km
Surge Impedance	802 Ω

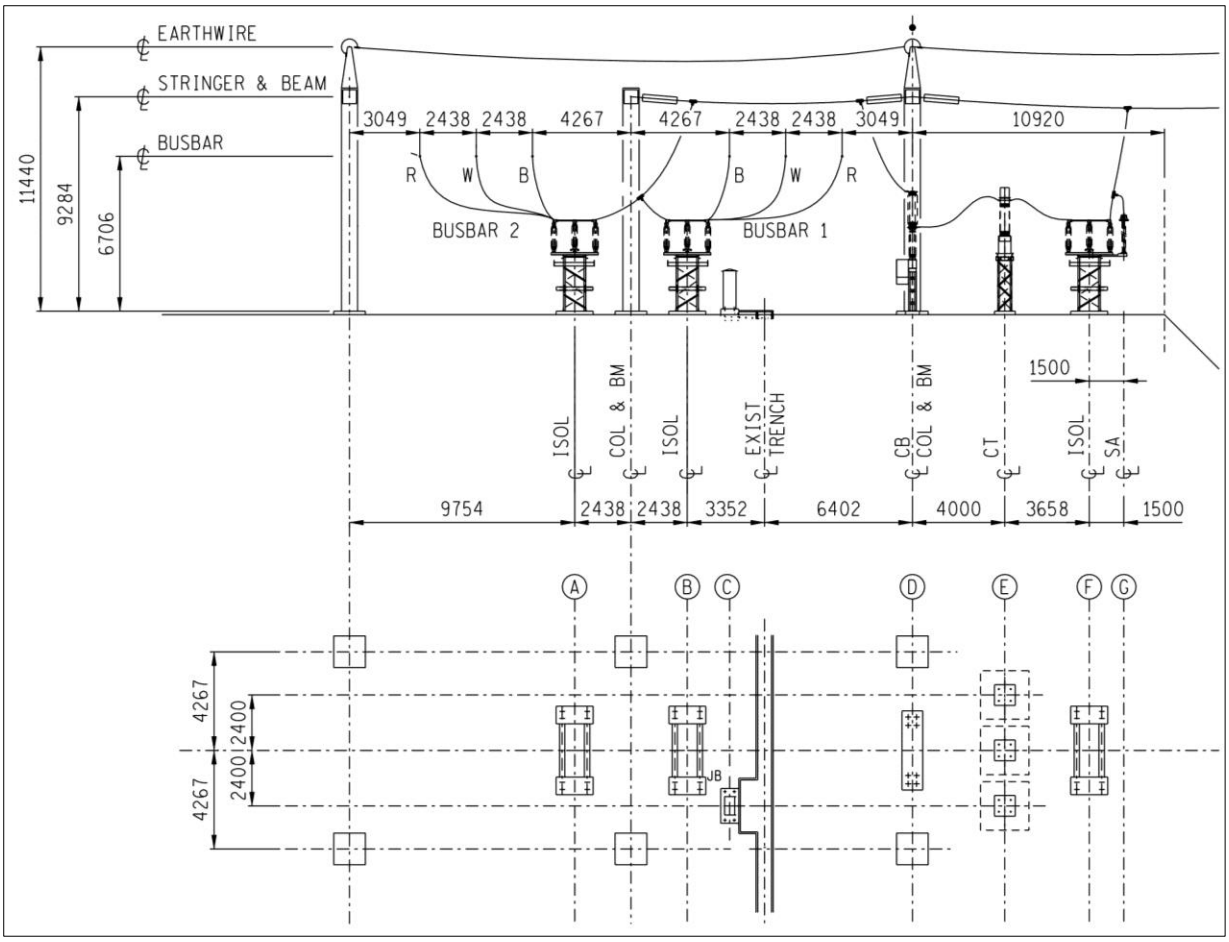


Figure 3-2: 88 kV Feeder bay layout

Where

A and B are the busbar disconnectors (isolators),

C is the control plant junction box,

D is the circuit breaker,

E is the current transformer,

F is the line disconnector,

G is the MOV surge arrester.

Table 3-3: 132 kV substation equipment distances

Section	Lumped RLC Pi Model	Length (m)
a - b	1	50
c - d	1	4
D - e	1	50
d - e	1	50
e - f	1	50
a - CBa	2	25
CBa - CTa	2	4

CTa - SAa	2	3.5
SAa - TRFRa	2	4
b - CBb	2	25
CBb - CTb	2	4
CTb - SAb	2	5

For simulation purposes, a double busbar switching arrangement is selected to represent all relevant voltage levels. The substation consists of a two transformer/feeder combination together with a bus coupler and is connected as indicated in Figure 3-3. The distances between the relevant connection points are listed in Table 3-3.

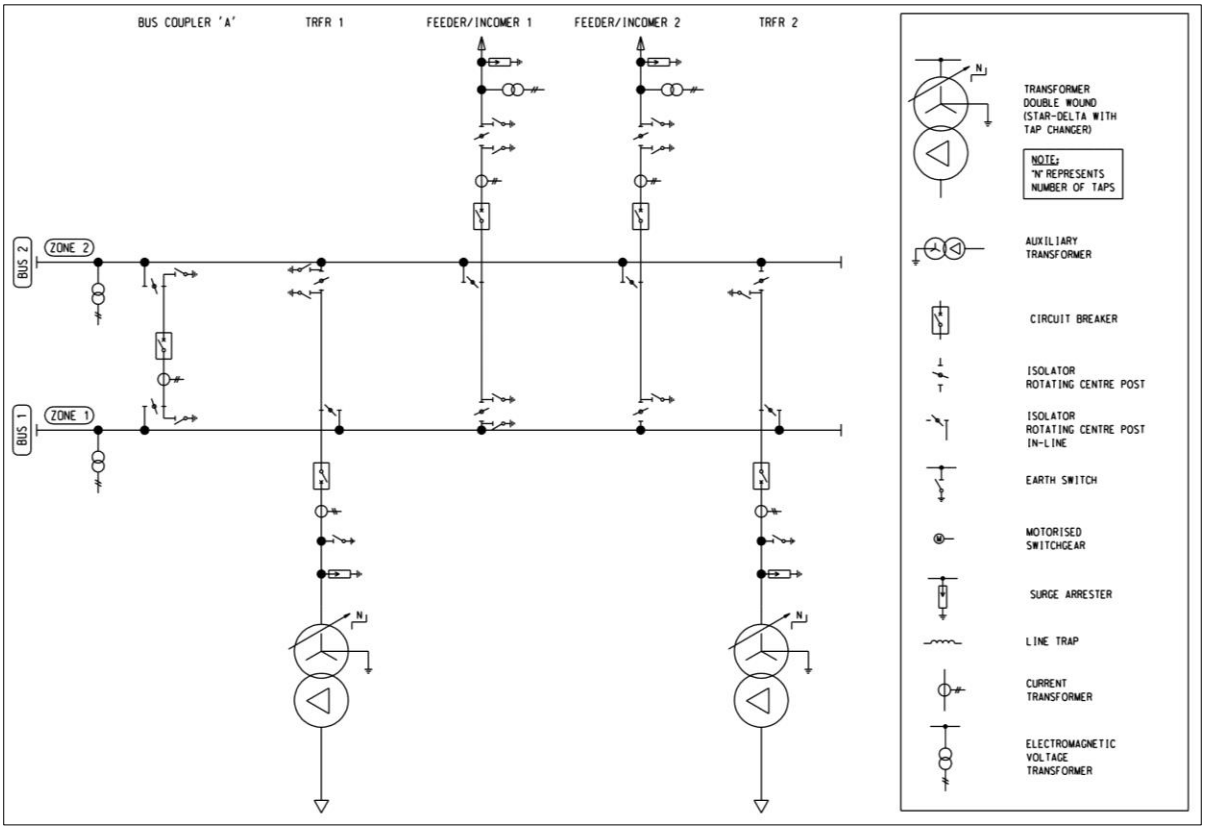


Figure 3-3: Single-line diagram of substation with double busbar switching arrangement

3.3.1 Slow-front transient analysis

When considering the performance of the substation regarding switching over-voltages in this voltage range, it is expected that the over-voltage distributions will not be of significantly high values. 88 kV and 132 kV transmission lines rarely reach lengths greater than 100 km. To demonstrate that the over-voltages are well within limits consider the following switching scenario in Figure 3-4..

3.3.1.1 Network diagram

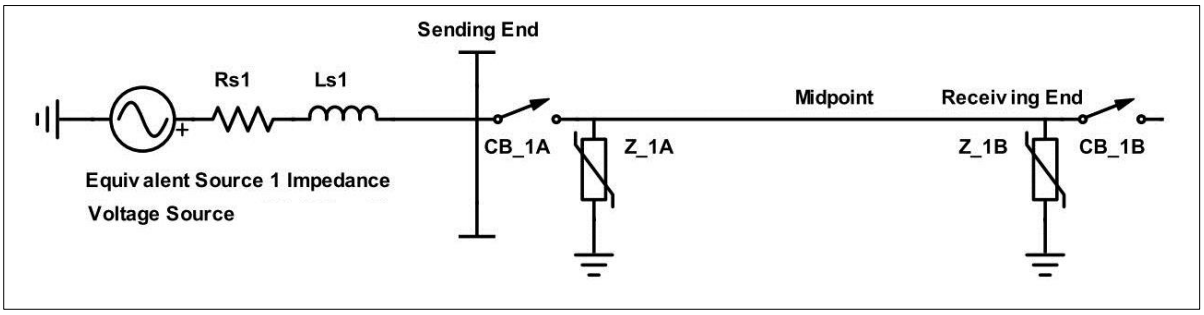


Figure 3-4: 132 kV Interconnected transmission lines and substations

3.3.1.2 Source

The equivalent sources are modelled with two different short-circuit powers. Only the positive sequence values are considered in this case. An assumption is made that the 88 kV transmission line structures will be re-used and operated at 132 kV. For this scenario, the X/R ratio is selected to be 7.

Although it is unlikely for trapped charge to be present at this voltage level, the study includes the scenario where it is possible. Trapped charge is represented as auxiliary voltage sources of 1 p.u (Phase A +1 p.u, Phase B -1 p.u and Phase C +1 p.u).[27] At the initial steady state, the sources are connected to the transmission line and are disconnected at the start of the simulation. Zero current chopping is considered to eliminate the possible unwanted transients prior to the primary switching operation. The source parameters is given in Table 3-4.

Table 3-4: Study 1 Positive sequence source parameters

145 kV (Max L-L Voltage)	3 Phase short-circuit power (GVA)	R (ohm)	L (mH)
Equivalent Source A	1	2.4	66
Equivalent Source B	7	0.35	9.5

3.3.1.3 Surge Arresters

The surge arresters included in the study has a rated voltage of 108 kV and the details are listed in Table 3-5 and Table 3-6. The voltage/current curve is given in Figure 3-5.

Table 3-5: 108 kV Rated voltage surge arrester parameters

Parameter	Value			
Rated Voltage (U_r)	108 kV			
Maximum continuous operating voltage (U_{MCOV})	86 kV			
Nominal discharge current (IEC)	10 kA			
Line discharge class 2 (IEC)	5.1 kJ/kV (U_r) = 551 kJ			
Maximum residual voltage (MRV) for $U_{8/20\ \mu s}$	5 kA	10 kA	20 kA	40 kA
	276 kV	294 kV	323 kV	367 kV

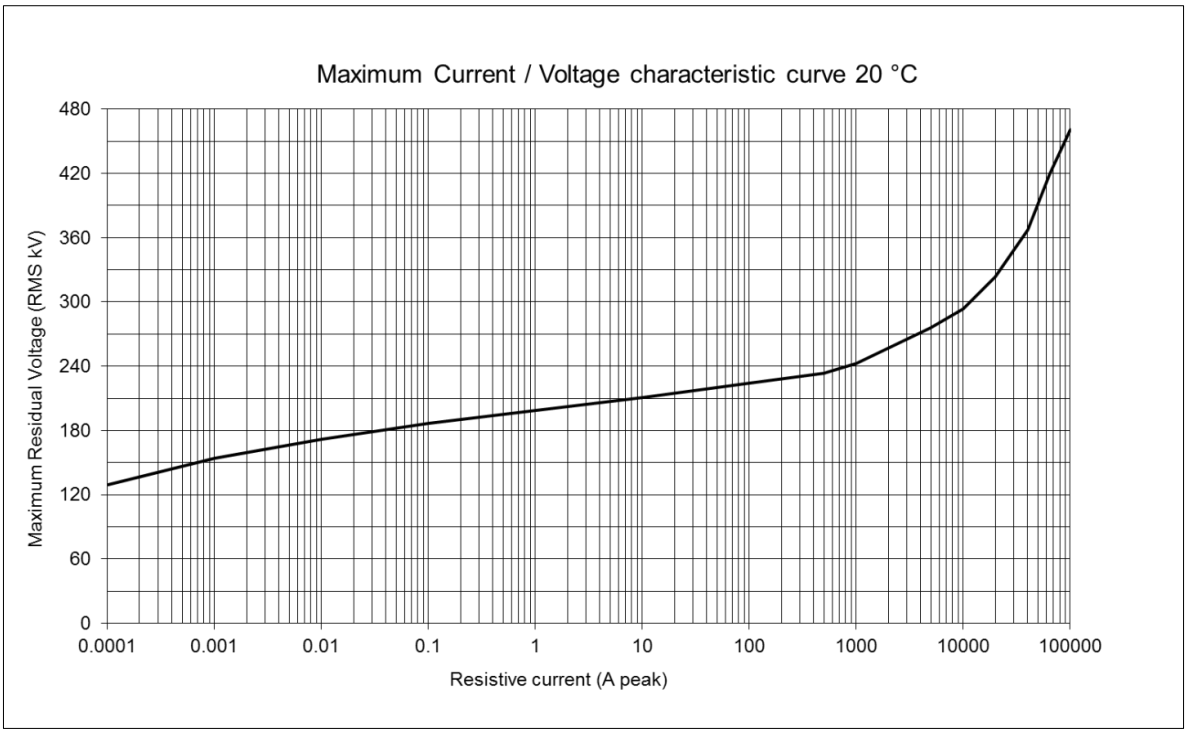


Figure 3-5: 108 kV Rated Voltage Maximum Current / Voltage characteristic curve

Table 3-6: 108 kV Rated arrester voltage/current characteristic

Current (A)	Voltage (kV)
0.0001	129
0.001	154
0.01	172
0.1	186
1	199
10	211
100	224
500	234
1000	242
5000	276
10000	294
20000	323
40000	367
65000	420
100000	461

3.3.1.4 Circuit breaker parameters

For the study, 500 closing operations were executed. In each instance the master circuit breaker pole had an equal probability of closing anywhere in the 50 Hz cycle The remaining two circuit breaker poles were slaves and following the master with a delay having a normal distribution with a 4 ms standard deviation. The details are shown in Figure 3-6.

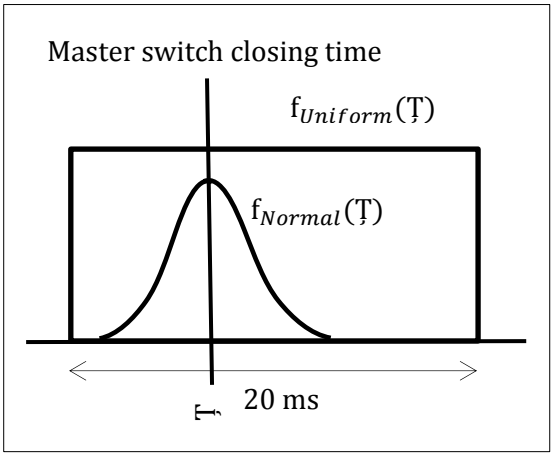


Figure 3-6: Statistical switch parameters

Where

$f_{\mathrm{Uniform}}(T)$ is the master circuit breaker pole with a closing instant having a uniform distribution over a full 20 ms cycle.

$f_{\mathrm{Normal}}(T)$ is two slave circuit breaker poles with a normal distribution and standard deviation of 4 ms.

3.3.1.5 Remote circuit breaker

The remote end circuit breaker refers to the circuit breaker connected on the remote end of the line at the receiving end substation. This circuit breaker is in the open position. All substation equipment from the line entry point up until the line circuit breaker will experience the worst case over-voltages due to the point of discontinuity in impedance at the open end of the transmission line.

3.3.1.6 Transmission lines

For the switching study, a detailed model is used to represent the transmission line accurately. It is not of great importance to include the earth wires for the switching study. For a typical 88 kV suspension transmission line tower configuration, consider the following tower geometry and conductor details in Figure 3-7:

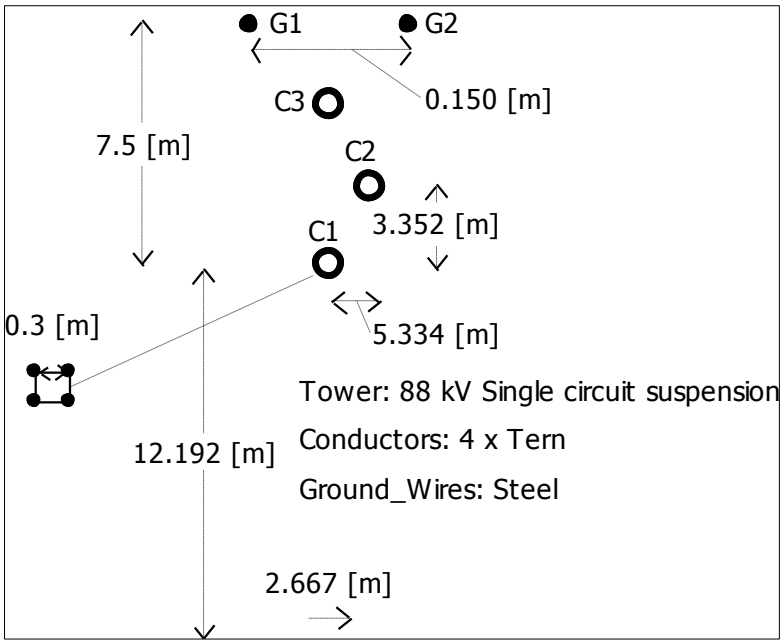


Figure 3-7: 88 kV Transmission line tower configuration

The transmission line parameters are calculated using the EMTP line constants subroutine and is captured in Table 3-7.

Table 3-7: 88 kV Single circuit transmission line parameters

Positive sequence transmission line parameters	**Value**
Resistance	0.0189 Ω/km
Inductance	0.758 mH/km
Capacitance	16.4 nF/km
Propagation velocity	278 x 10^6 m/s
Surge Impedance	214.7 Ω

3.3.1.7 88/132 kV Substation arrangement for the switching study

For the switching study, the detail regarding distances between equipment is not important. The switching arrangement includes a source with a sending end circuit breaker that is randomly closed 500 times for each case. The equivalent transmission line model and the receiving end substation line entrance is included in the simulation. Surge arresters are included at the sending and receiving ends.

3.3.2 Fast-front transient analysis

The need to investigate uprating the 88 kV substations to 132 kV arises from thermal overload constraints combined with the unavailability of new servitudes. The length of transmission lines evaluated within this study ranges from 10 km to 100 km. The scope of this study is focused around fast-front transients because lightning dominates in this voltage range.

3.3.2.1 Substation single-line diagram and equipment arrangement

For fast-front transients it is important to model the substation in more detail. The distances between equipment becomes important since the faster rise times result in decreased

arrester protective distances. Each conductor suspended above ground in the substation has a combination of inductance and capacitance, which contributes surge impedance.

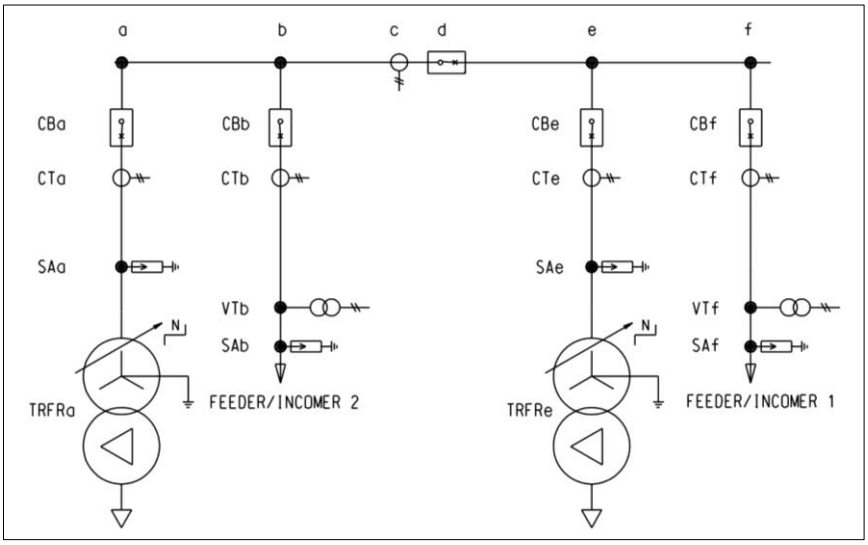


Figure 3-8: 132 kV Substation single-line diagram

The substation is evaluated and the worst-case scenario is selected as shown in Figure 3-8. One such scenario could be where TRFRa is disconnected from the bus and CBa is in the open position. When Feeder 2 is also disconnected from the bus, only two arresters are able to limit over-voltages entering into the substation form Feeder 1. Only SAe and SAf is in service to limit voltages. In this arrangement, the distance between the arresters and the TRFRa circuit breaker open terminals could potentially be significant. This distance is shown in red in Figure 3-9.

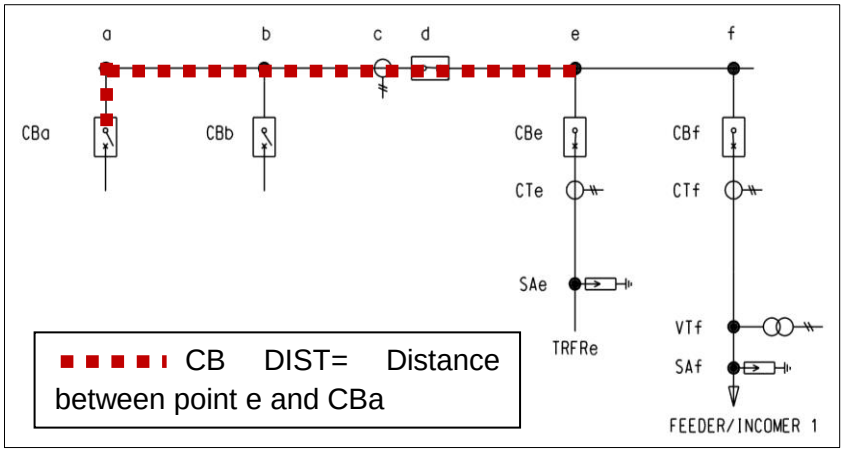


Figure 3-9: 132 kV Substation simplified Scenario 2

3.3.2.2 Lightning current source parameters

The actual measured waveforms of the lightning currents are of concave shape and the changing slope defines the rate-of-rise as a function of time. The steepest points recorded are near the current peaks. When a lightning flash terminates on a shield wire, the tower top voltage rises and is very sensitive for the maximum steepness and maximum current. The double exponential function does not provide adequate steepness close to the current peak and naturally has lower steepness values at the peak. For lightning, it is then better to

model the wave shape with a linear slope adjusted to the TAN-G or S_m steepness values obtained from the approximation of maximum steepness. The values for the rise times are adjusted to obtain specific current magnitudes correlated to the TAN-G steepness values [25],[26],[22]. Initially four different current peaks are selected to represent multiple stroke current sources, the source details are given in Table 3-8 and the ramp type waveforms are plotted in Figure 3-10.

Table 3-8: Lightning current source parameters

Ramp Type Current Source	Current Peak (kA)	Probability of occurrence (%)	TAN-G Steepness (kA/µs)	Front Rise Time (µs)	Time to half value (µs)
Source 1	10	95	13.83	0.72	75
Source 2	30	52	25.32	1.185	75
Source 3	80	7.8	43.42	1.842	75
Source 4	160	1.4	63.58	2.5	75

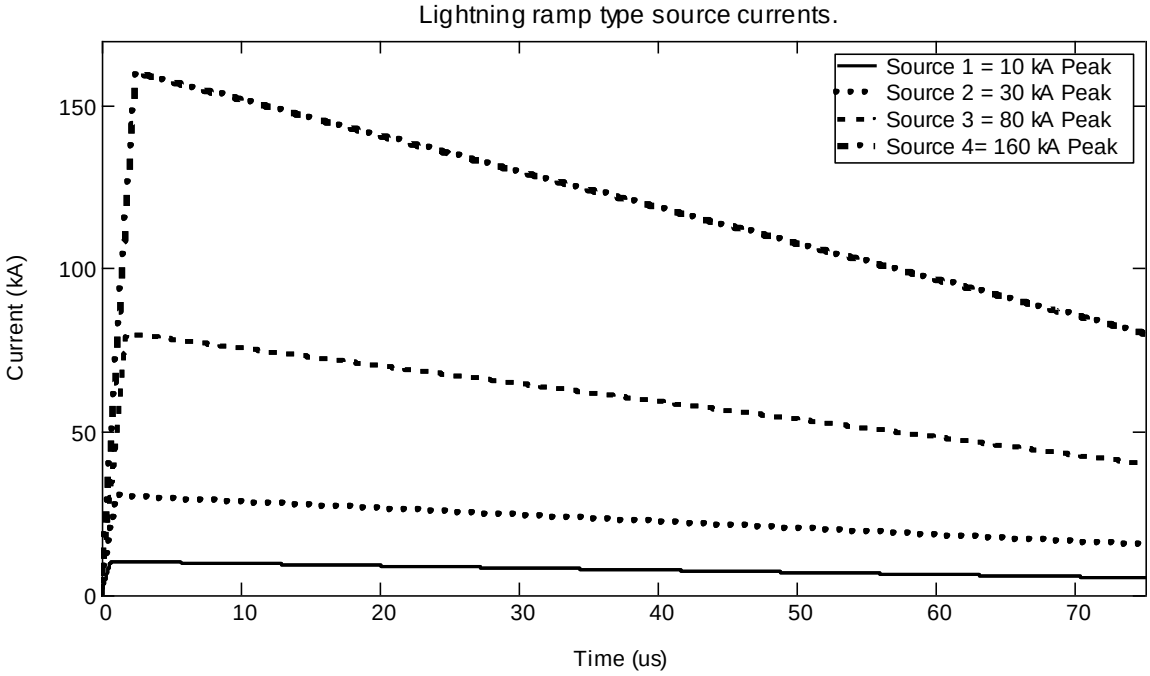


Figure 3-10: Ramp type lightning current sources for simulation

3.3.2.3 Flashover mechanism

When a lightning flash terminates on the transmission line earth wire, the tower top voltage increases. The phase conductor voltages increase as a function of the tower voltage and follow the same profile. When the differential voltage between the phase conductor and the tower top voltage exceeds the threshold voltage gradient, the leader starts propagating across the gap. The mechanism can be complex and it is very important to determine if flashover will occur. With reference to the substation lightning performance, the aim is to evaluate the incoming surges during a back flashover and shielding failure. The reality is that the flashover mechanism greatly determines the details of when the flashover will occur based on the non-linearity of the withstand strength of airgaps and insulator strings when subjected to lightning impulses of different waveshapes. Regarding a 1 m airgap, the logic is simplified for this study in that the flashover occurs simply when the differential voltage between the two electrodes reaches 530 kV. The complexity of streamer development and

leader propagation is excluded in this study. The primary requirement to assess the voltages in the substation is to ensure that the flashover occurs on the transmission line between at least one phase and earth.

3.3.2.4 Transmission line

For the lightning study, a detailed model needs to be used to represent the transmission line accurately. The same geometry is used for the lightning and switching study. The earth wires are included in the lightning study.

To determine the tower surge impedance the following equation is applied with reference to the tower geometry [22]:

$$Z_T = 153\ \Omega \tag{3.1}$$

To calculate the tower inductance, the assumption is that the tower footing resistance is small and then the inductance is calculated as:

$$L = 14.4\ \mu H \tag{3.2}$$

Where τ is the height of the tower divided by 70 % the speed of light. The per meter inductance is 0.73 µH/m and is within the expected range of values.

Transmission line tower footing resistance is specified by Eskom to be 20 Ω for 132 kV. For this application the same value is used, but the sensitivity on the over-voltage is also evaluated based on higher values.

3.3.2.5 Surge Arresters

The surge arresters used for this study have the same parameters and rating as the arresters used in the slow-front transient analysis.

The lead lengths of the surge arresters are important due to the high current steepness values. The conductor leads between the arrester terminals and the bay stringing conductor are modelled with a simple inductance representing a value of 1 µH/m. The length of the lead is 3 m and the supporting steel structure has length 2 m.

3.4 Uprating 275 kV to 400 kV

To evaluate clearances for uprating 275 kV to 400 kV, a 275 kV transformer bay layout is studied. All the voltages sensitive equipment that consists of non-recoverable insulation is assumed to be replaced for uprating purposes.

3.4.1 Slow-front transient analysis

To perform a switching study, the relevant power network needs to be modelled. For this study, a transmission line was connected between substation A and B. The source was modelled with equivalent impedances representing the rest of the network. The short-circuit power and damping of the network at the focus area was very important and had a significant impact on the transient over-voltage magnitudes and waveform shapes.

The over-voltage probability distribution was determined by capturing maximum over-voltage values during each of the 500 individual simulations. For every simulation case, the maximum of the three-phases of the phase-to-earth voltages was recorded and included in

the distribution. Only phase-to-earth voltages were studied. The best-fit normal distribution was used as a representative over-voltage probability distribution. The withstand level was statistically defined and the over-voltage distribution function was correlated with the withstand level to determine the risk of failure. Surge arresters were also included in the simulation to determine the protective margins. Selecting a withstand level based on the acceptable risk of failure and protective margin led to the calculation of the required electrical clearances for the substation.

3.4.1.1 Network diagram

The network diagram consisted of two 400 kV substations (substation A and B) interconnected with a transmission line. The circuit breakers, surge arresters and line parameters were the main components included in the circuit shown in Figure 3-11.

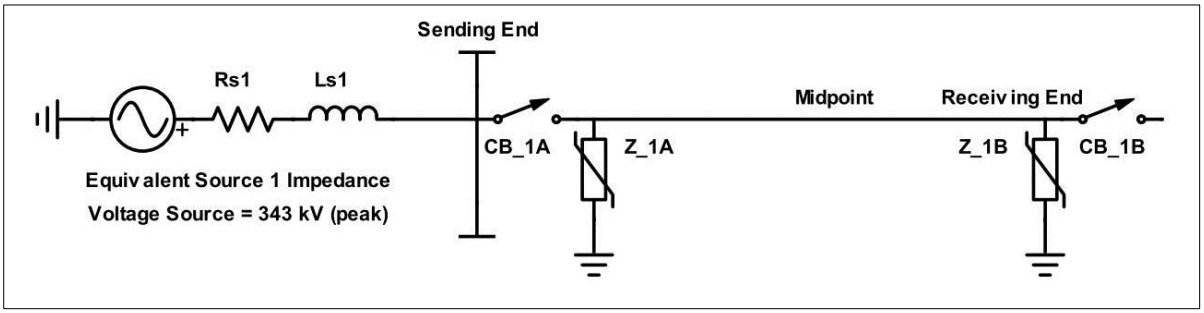


Figure 3-11: 400 kV Interconnected transmission lines and substations

3.4.1.2 Source

The equivalent sources were modelled with three different short-circuit power values and is listed in Table 3-9. Only the positive sequence values were considered in this case. An assumption was made that the 275 kV transmission line structures will be re-used and operated at 400 kV. Large clearances between phases and earth on overhead lines result in large values of inductance. For this scenario, the X/R ratio was selected to be 10.

Trapped charge is represented as auxiliary voltage sources of 1 p.u (Phase A +1 p.u, Phase B -1 p.u and Phase C +1 p.u). At the initial steady state, the sources were connected to the transmission line and was disconnected at the start of the simulation. Zero current chopping is considered to eliminate the possible unwanted transients prior to the primary switching operation.

Table 3-9: Study 1 Positive sequence source parameters

420 kV (Max L-L Voltage)	3 Phase short-circuit power (GVA)	R (ohm)	L (mH)
Equivalent Source 1A	5	3.5	112
Equivalent Source 1B	10	1.75	56
Equivalent Source 1C	15	1.17	37

3.4.1.3 Surge Arresters

The surge arresters included in the study has a rated voltage of 312 kV and the details are listed in Table 3-10 and Table 3-11. The voltage/current curve is given in Figure 3-12.

Table 3-10: 312 kV Rated voltage surge arrester parameters

Parameter	**Value**		
Rated Voltage (U_r)	312 kV		
Maximum continuous operating voltage (U_{MCOV})	249.4 kV		
Nominal discharge current (IEC)	10 kA		
Line discharge class 3 (IEC)	7.8 kJ/kV (U_r) = 2.4 MJ		
Maximum residual voltage (MRV) for $U_{30/60\ \mu s}$	0.5 kA	1 kA	2 kA
	600 kV	618 kV	642 kV

For slow-fronted surges the arrester is modelled for a current range below 3 kA.

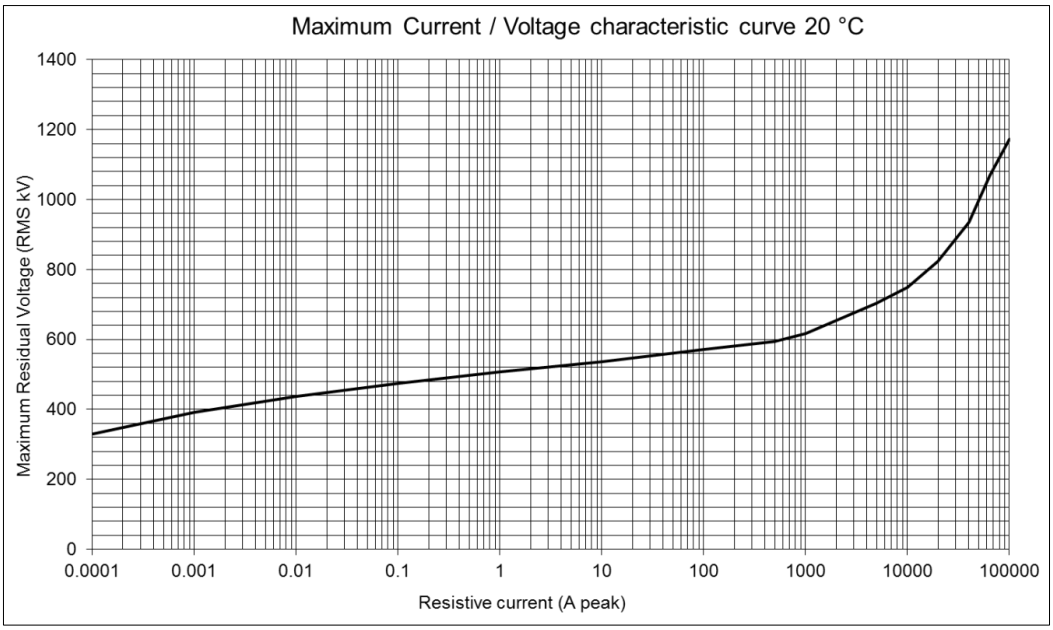


Figure 3-12: 312 kV Rated Voltage Maximum Current / Voltage characteristic curve

The full current/voltage characteristic is described by Figure 3-12 and the residual voltages are given in the following table.

Table 3-11: 312 kV rated arrester characteristic for current impulse $U_{30/60\ \mu s}$

Current (A)	**Voltage (kV)**
0.0001	330
0.001	392
0.01	438
0.1	475
1	506
10	536
100	571
500	595
1000	618
5000	704
10000	749
20000	823
40000	936
65000	1069
100000	1173

3.4.1.4 Circuit breaker parameters

The same statistical parameters were applied for the circuit breaker operations as specified previously. This study consisted of multiple configurations with sub cases where each case was a combination of 500 simulations.

The impact of closing resistors on the switching over-voltage was also considered. The pre-insertion resistors were inserted as a secondary contact prior to the primary contact closing operation. The value of the resistors was selected to match the surge impedance of the transmission line. In this case the value was 237 Ω.

3.4.1.5 Remote end circuit breaker

The remote end circuit breakers were in the open position and represent the first major discontinuity at the remote end substation. The change in impedance at the open end during line energisation causes the doubling effect and the reflected wave was expected to be very high.

3.4.1.6 Transmission lines

The transmission lines were modelled with the distributed parameter EMTP transmission line models. The model was selected to be frequency independent. The geometries of the 275 kV structures as shown in Figure 3-13 were included to calculate the line parameters.

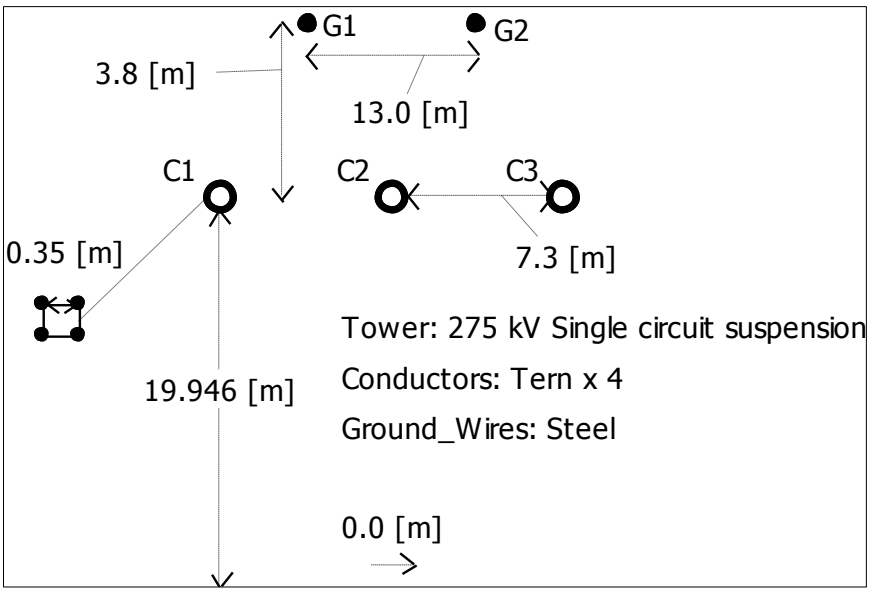


Figure 3-13: 275 kV Single circuit suspension tower

A standard 275 kV transmission line geometry was chosen to be modelled. The conductor bundle consisted of 4 x Tern stranded aluminium conductors which are common in the Eskom transmission system. For 400 kV ground clearances, the minimum height of the conductors should be no less than 8.1 m. The sag of the conductors is correlated with this minimum value. The transmission line parameters are given in Table 3-12.

Table 3-12: 275 kV Single circuit transmission line parameters

Positive sequence transmission line parameters	**Value**
Resistance	0.0189 Ω/km
Inductance	0.81 mH/km
Capacitance	14.4 nF/km
Propagation velocity	287 x 10^6 m/s
Surge Impedance	237 Ω

3.4.1.7 275/400 kV Substation arrangement

The standard 400 kV equipment used in Eskom is rated for a SIWL of 1050 kV and a LIWL of 1425 kV. For substation voltage uprating, the equipment that includes non-recoverable insulation such as the circuit breaker, current transformer, voltage transformer will be replaced with 400 kV rated equipment. Due to the size of some of the equipment, other options such as disconnect circuit breakers and compact switchgear are considered. In the 275 kV feeder bay layout, the conventional circuit breaker is replaced with a disconnecting circuit breaker. The advantages include space savings due to the inclusion of ring type current transformers. Addionally, tubular conductors are installed for a more rigid low profile connection.

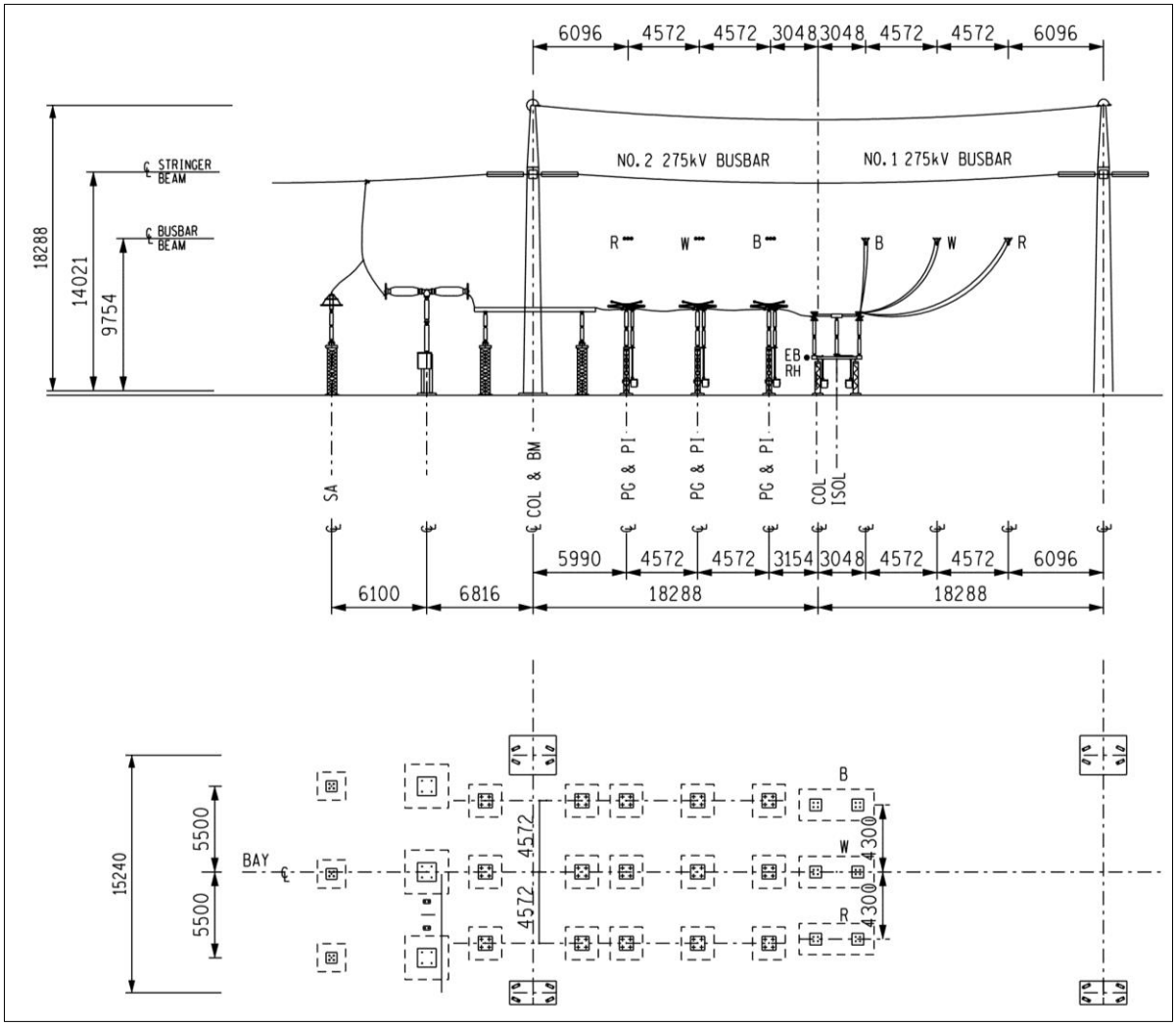


Figure 3-14: 275 kV Feeder bay layout for uprating to 400 kV

Tubular conductors could potentially contribute significantly where small clearances prohibit conductor swing. The distance between phases can be fixed and a more reliable solution during short-circuit events could be achieved.

In both the feeder and transformer bays the disconnecting circuit breaker or compact switchgear contributes to the solution of the space limitations. In both cases, the current transformers and circuit breakers are relocated away from the main support steelwork columns and tubular conductors are included as the new connections. A conceptual bay layout is shown in Figure 3-14 and in Figure 3-15.

The majority of old substations in the transmission grid consist of flexible strung conductors. Larger bay spacing caters for larger clearances, but conductor swing during windy or fault conditions could pose significant limitations to voltage uprating. Refurbishing bus conductors and replacing the strung conductors with tubular conductors with additional “V” suspension insulators could potentially form part of the solution.

Newer substation bus conductors are constructed primarily with tubular conductors. Clearances are smaller (for 400 kV phase-to-phase 5.5 m is used). Conductor swing in the bay stringing is limited by shorter distances between equipment. It is expected that for substations already utilising tubular conductors for the bus arrangement, some benefits could arise for the feasibility of uprating.

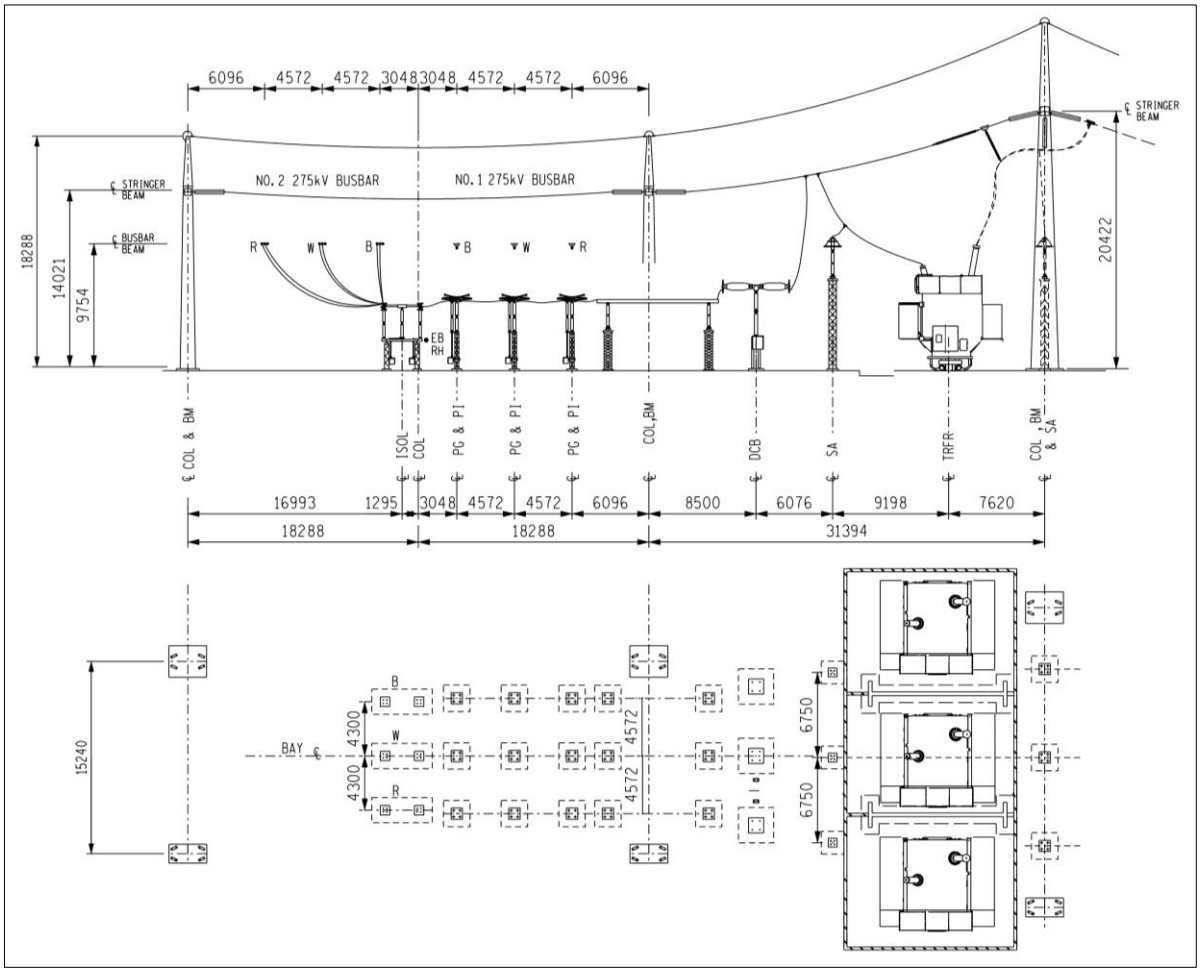


Figure 3-15: 275 kV Transformer bay layout for uprating to 400 kV

Table 3-13: 275 kV bay layout dimensions

Dimension	Length/Height (mm)
Earth wire attachment height	18288
Stringer and Beam height	14021
Busbar height	9754
Busbar phase-to-phase	4572
Bay stringing phase-to-phase	4300
Bay width	15240

3.5 Other considerations

3.5.1 Increased Electromagnetic field strength

It is also very important to consider the impact of voltage uprating on the health of humans. With compact substation design, it is important to ensure that low frequency time-varying electric, magnetic and electromagnetic fields are simulated and evaluated. The International Commission on Non-Ionizing Radiation Protection (ICNIRP) issued a guideline for limiting Electromagnetic Field (EMF) exposure to decrease the risk of known adverse health effects. The Guideline specifies allowable limits of exposure, and it is critical to adhere to these limits within a compact power substation environment [35]. The impact of low frequency time domain electromagnetic interference in the substation is not covered in this research and should be further investigated.

3.5.2 Altitude correction

The Highveld region in Southern Africa is at an altitude of 1500 – 1700 m above sea level, altitude correction should be considered for external insulation. However, when strengthening the external insulation by correcting for altitude, the stress could be moved to the internal insulation of equipment. This is not ideal and the approach should rather be to allow a more conservative margin for the internal or non-recoverable insulation. It is therefore important to ensure that the protective margins are maximised for internal insulation. Substation voltage uprating at higher altitudes will include the operating of substations at higher nominal voltages. This forces the engineer to allow for smaller external air clearances. When correcting for altitude is required, it is good practice to consider higher energy rated MOV surge arresters with lower protective levels. This will improve the limitation of over-voltages where non-recoverable insulation is of concern.

4 RESULTS

4.1 Uprating 88 kV to 132 kV Results

4.1.1 Switching study

4.1.1.1 Switching over-voltage stress simulation

The simulations include two source short-circuit powers of 1 GVA and 7 GVA. The equivalent three-phase-to-earth short-circuit currents were 5.6 kA and 40 kA respectively. Each of the source X/R ratios were fixed at 8.5. The transmission line lengths were varied and simulations were executed for 50 km and 100 km. Other variables such as the inclusion and exclusion of trapped charge, surge protective devices were also considered. Only the expected worst cases were considered for the final evaluation. The worst case for the sending end over-voltage distributions were expected to occur where the source is weak (1 GVA) combined with the shorter line length of 50 km. For the mid-point of the line and the receiving end the strong source of 7 GVA was combined with the longer line of 100 km. For each case the $U_{2\%}$ value is obtained. The $U_{2\%}$ value is the per unit value that includes 98 % of all over-voltages (98 % confidence interval). Only 2 % of all values obtained in the distribution are excluded.

Table 4-1: Switching over-voltage distributions

Source Short-circuit Power	Line length (km)	Trapped charge	Surge arresters	Per unit (118 kV peak voltage) Over-voltage distribution $U_{2\%}$		
				Sending End	Midpoint	Receiving End
1 GVA	50	Present	Present	1.9	2.6	1.9-
7 GVA	100	Absent	Present	1.9	2.8	1.9

With reference to the maximum $U_{2\%}$ values of 1.9 p.u and 2.8 pu, the equivalent over-voltage values were 225 kV (substation sending and receiving ends) and 330 kV (worst case mid-point of the line). The results for the switching study is tabulated in Table 4-1.

4.1.1.2 Switching over-voltage strength of external insulation

Standard clearances for the two voltage levels is given in Table 4-2. The switching impulse withstand levels of standard 88 kV phase-to-earth and phase-to-phase clearances were calculated with the Gallet-Leroy equation and are given in Table 4-3.

Table 4-2: Eskom standard clearances for 88 kV and 132 kV substations

Nominal Voltage (kV)	Phase-to-Earth (mm)	Phase-to-Phase (mm)
88	1000	1350
132	1200	1650

Although protective margins are usually related to the protection of equipment and primarily internal non-recoverable insulation, they were used in this scenario to demonstrate the switching impulse withstand capability of the external insulation. From Figure 4-1 it is clear that an improved gap factor is required to yield the same 25% margin of protection.

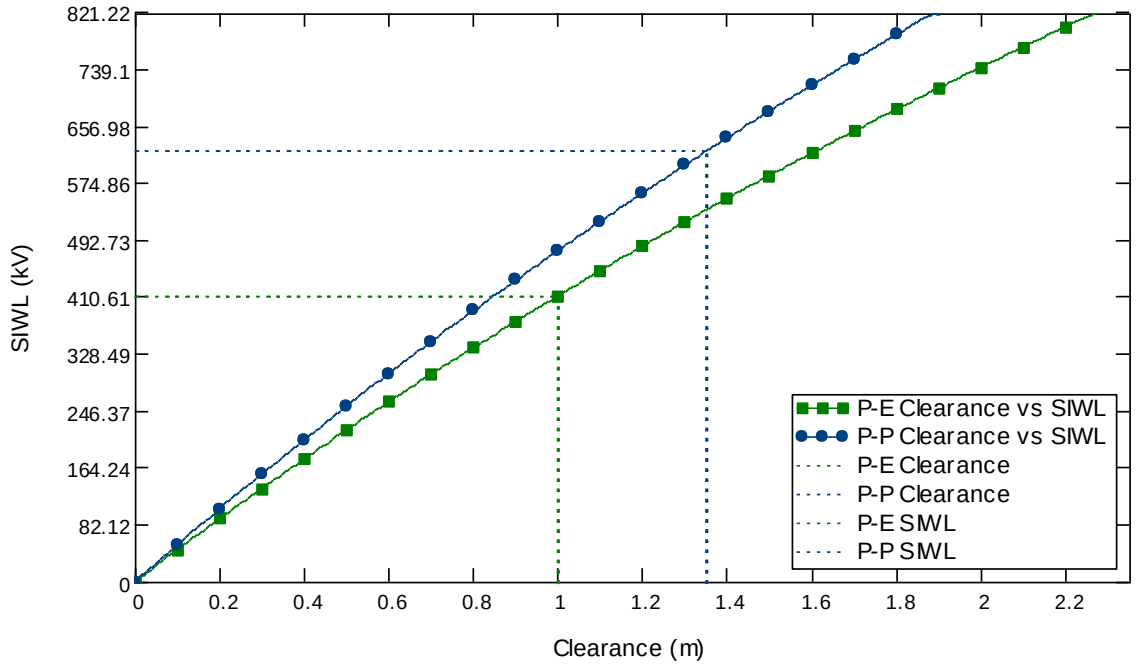


Figure 4-1: 88 kV standard clearance and SIWL for mid-point

To maintain the required 25 % protective margin between the maximum stress of 330 kV and the switching impulse strength of the airgap, the gap factors required for the representative 88 kV clearances were 1.2 phase-to-earth and 1.39 for phase-to-phase. The ratio between phase-to-phase and phase-to-earth withstand levels is 1.5.

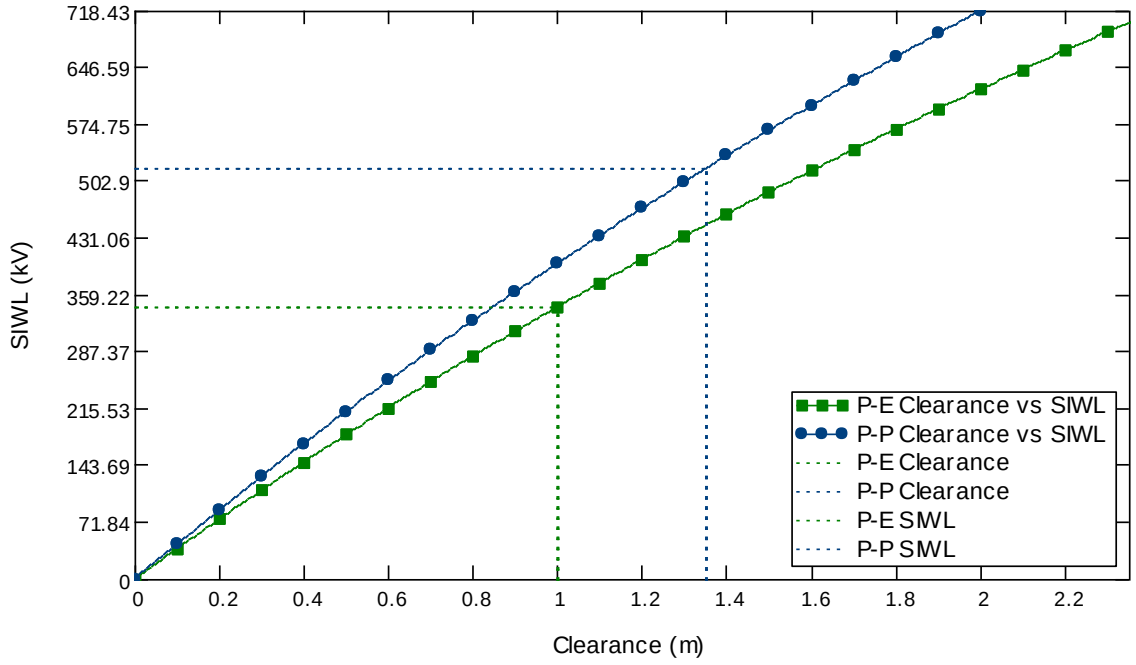


Figure 4-2: 88 kV Standard clearance and SIWL for sending/receiving end

It is clear from Figure 4-2 the gap factor of 1 yields a SIWL of 344 kV, and when compared to the over-voltage stress of 225 kV it can be concluded that the a protective margin of 52 % is acquired. The margin of protection is more than double the required 25 %. This is based on switching over-voltage distributions with maximum values where trapped charge was included in the simulation. The surge arresters limit switching over-voltages to 1.9 p.u at the sending and receiving end substations and it is clear that there is significant margin of protection between the maximum stresses and the surge arrester protective level.

Table 4-3: Required SIWL for 88 kV airgaps when uprating to 132 kV

	Stress (kV)	Clearance (mm)		Gap Factor allowed		SIWL required (kV)	
		Phase-to-earth	Phase-to-Phase	Phase-to-earth	Phase-to-Phase	Phase-to-earth	Phase-to-Phase
Mid-point	330	1000	1350	1.2	1.39	413	621
Sending/Receiving End	225			1	1.16	344	518

4.1.1.3 Results summary

Protecting the equipment with reference to internal non-recoverable insulation, 132 kV equipment rated at 550 kV LIWL will be well protected for switching surges. It is therefore clear that switching transients will not be of significant importance when the aim is to minimise the risk of insulation failure in an uprated substation in this voltage range.

4.1.2 Lightning study

4.1.2.1 Simulation model of the back-flashover

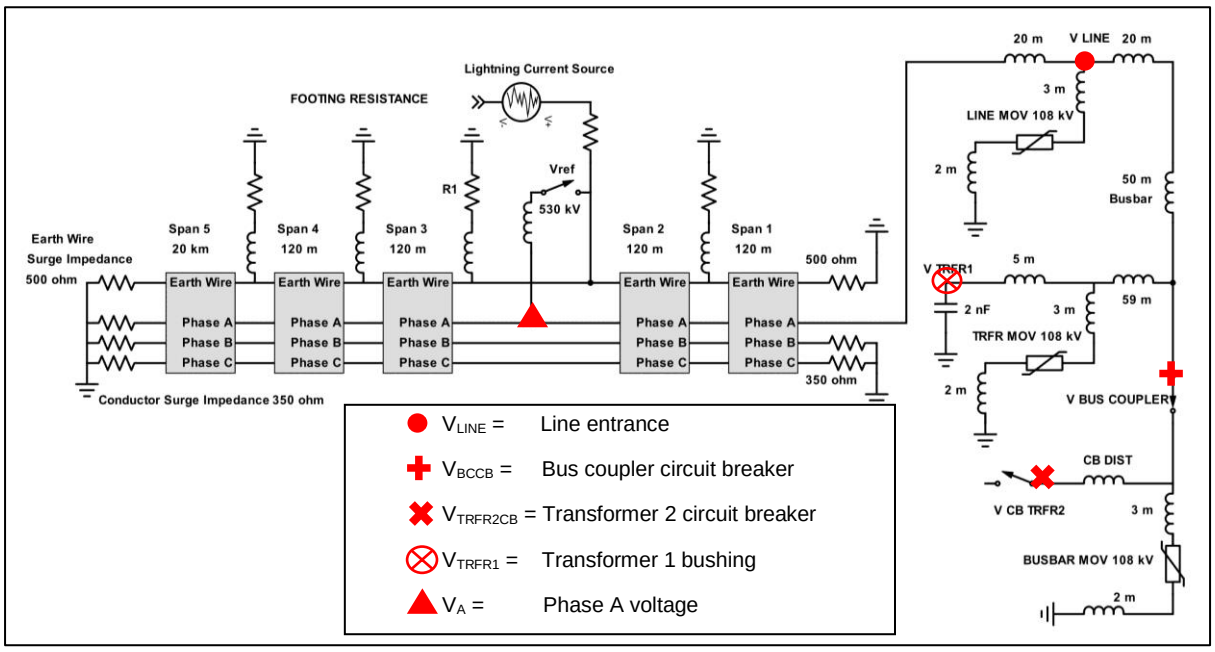


Figure 4-3: 88/132 kV back-flashover simulation model

4.1.2.2 Tower top voltage calculation compared with EMTP simulated results

The back-flashover simulation model includes 5 spans, and incorporates the lightning current source as shown in Figure 4-3. To calculate the tower top voltage as a result of a direct lightning stroke to the tower or earth wire, the following equation was applied for the different source peak first stroke currents and their respective rise times. [22] The combined surge impedance for the earth wire is selected to be $Z_{gw} = 130\ \Omega$ and the footing resistance $R_{Footing\ resistance} = 20\Omega$. The current peaks were $I = 10, 30, 80, 160\ kA$ with their rise times as specified in Table 3-8.

$$V_{Tower\ top} = I\frac{\left[20\Omega + \frac{14.4\mu H}{t_f})130\Omega\right]}{\left[20\Omega + \frac{14.4\mu H}{t_f} + 130\Omega\right]} \tag{4.1}$$

The following table gives the calculated and simulated values:

Table 4-4: Calculated and simulated tower top voltages

Source type	Calculated (MV)	EMTP Simulated (MV)
Source 1	0.306	0.361
Source 2	0.774	0.710
Source 3	1.834	1.706
Source 4	3.436	3.021

4.1.2.3 Insulator voltage

The voltage across the insulator can be calculated as a function of the tower top voltage and induced voltages on the phase conductors. As mentioned before the insulator voltage is highly sensitive to the tower surge impedance and footing resistances. For a rough estimate of the withstand capability of airgaps during a lightning impulse a value of 530 kV per meter is used [30]. In this model, the flashover will occur if the insulator voltage increases above this value. For 88 kV clearances in Eskom a phase-to-earth distance of 1 m is the standard. In this case, when the insulator voltage exceeds V_{ref} 530 kV, the current source and phase A are connected to each other through the closing of an ideal switch.

4.1.2.4 Transmission line footing resistance

The footing resistance limit for 88/132 kV towers is 20 Ω. Although this study does not focus on improving the flashover rate, it is always important to minimise the footing resistance to limit the maximum tower top voltages.

When the voltage across the airgaps between the tower top and the phase conductors exceeds their dielectric strength, flashover occurs. The phase conductor voltage rises to the tower top to produce a voltage transient on the phase conductors. By limiting the tower top voltage, the maximum value of this transient can be limited. By limiting the maximum transient voltage, the energy duty on the arresters will be reduced.

The sensitivity for the tower footing resistance is evaluated in the following figure:

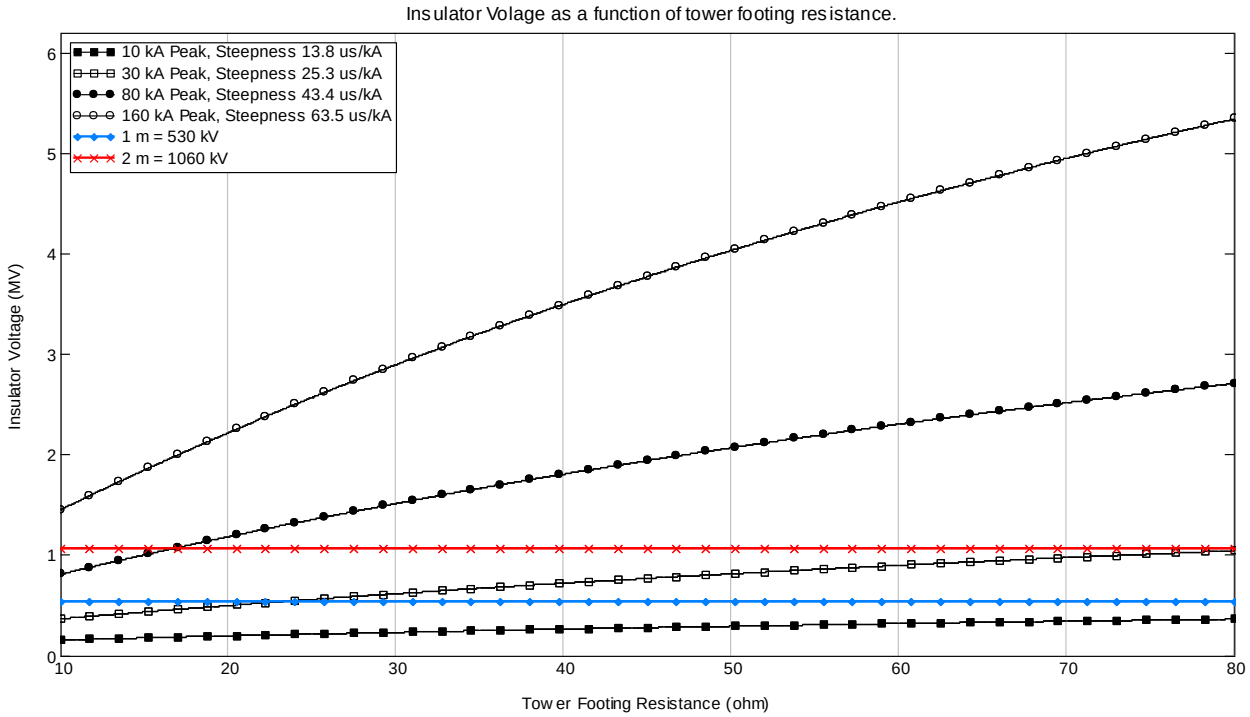


Figure 4-4: Insulator voltage as a function of tower footing resistance

From the footing resistance sensitivity analysis it was apparent that for the high current of 160 kA with steepness of 63.5 kA/µs the flashover for a gap of 2 m will occur even with a low tower footing resistance of 10 Ω. The tower footing resistances of 20 Ω will only prevent flashovers for the lightning source 1 and 2 (10 kA and 30 kA). Only current source 1 produces tower top values low enough to have an insulator voltage below the withstand level of 530 kV/m for the range of resistances between 10 Ω and 80 Ω. The average lightning peak current of 30 kA with a steepness of 25.3 kA/µs will cause a flashover for any footing resistance greater than 15 Ω – 17 Ω. This is the reason for the required footing resistance values to be below 20 Ω for 88 kV where 1 m gaps are present. Although the probability is low (7.8 %) for the peak current to reach 80 kA, the 1 m gap will not be able to withstand the stress and a flashover will occur. It is only the 2 m gap with a tower footing resistance of less than 15 Ω that will prevent a flashover to occur.

4.1.2.5 Over-voltages at the substation

Regarding the transient voltage waveforms propagating within the substation, it is important to evaluate the arrester protective distance, which is highly sensitive for the transient voltage rate-of-rise. To introduce additional attenuation to limit the steepness, transmission towers close to the substation should be connected to the substation earth electrode. This will improve the surge impedance of the tower impedances to terra earth and assist with attenuation of the rate-of-rise. Capacitive voltage transformers at higher voltages also contribute to attenuation with the introduction of lower surge impedance at the line entrance. Surge capacitors will also add to the attenuation and will improve the protective distances of arresters.

With reference to the impact of lightning on the substation clearance, the over-voltages in the substation should be evaluated. Incoming surge magnitudes and steepness are considered as the dominant variables that may cause excessive stresses in the substation. The minimum clearance in the 88 kV uprated to 132 kV substation should not be less than 1 m. This results in the conclusion that the over-voltages should not exceed 530 kV. We also know that the equipment lightning impulse withstand level is selected to be 550 kV. The arresters are rated for 108 kV and limit the lightning over-voltages at their terminals well below the LIWL. The primary function of the arresters is to protect the equipment, but in doing so the airgap is also protected even though it has a similar withstand level of 530 kV per meter.

It is evident from the insulator voltage calculations in Figure 4-4 that a lightning source current with parameters similar to Source 1 (peak of 10 kA), will not produce an insulator voltage large enough for flashover to occur. This has been confirmed in the simulations. Figure 4-5 shows the tower top voltages and phase A voltages for the 30 kA, 80 kA and 160 kA current sources. All of these phase voltages follow a similar pattern.

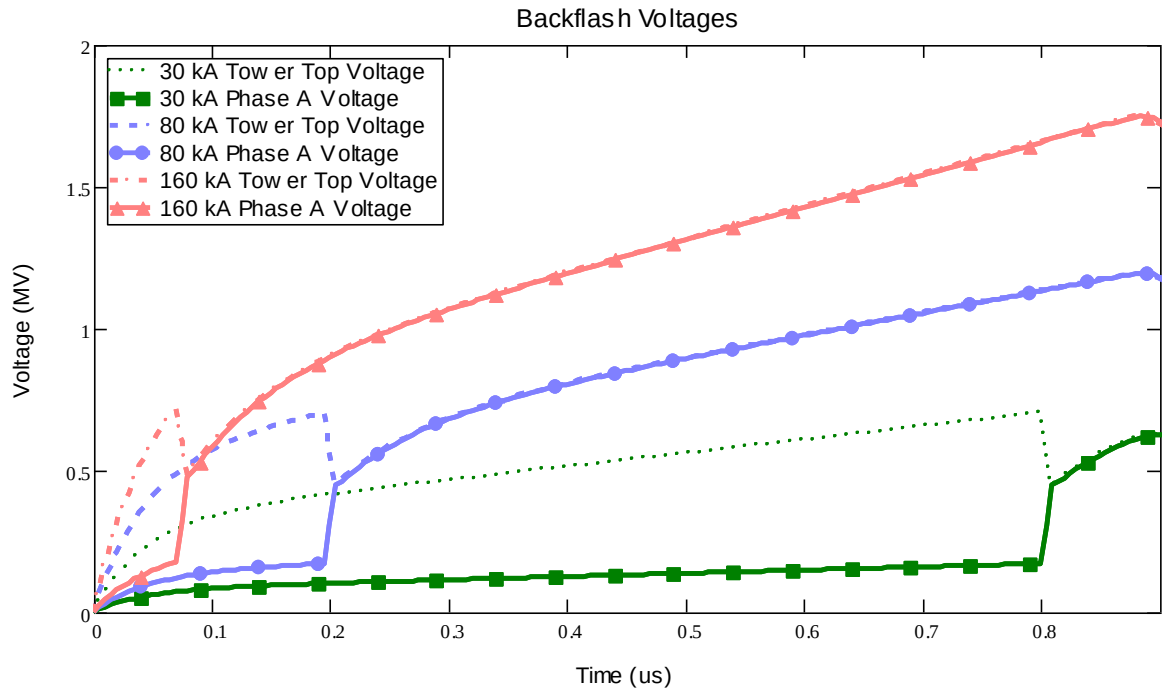


Figure 4-5: Tower top and phase A voltages indicating flashovers

The electromagnetic coupling between the earth wire and the phase conductors causes the phase voltages to rise. The differential voltage (insulator voltage) increases and when the reference potential exceeds 530 kV, the flashover occurs. At this point, the phase voltage assumes the same voltage of the tower top and a voltage transient appears on the phase conductor. The steepness of the transient over-voltages were:

- Source 1 (10 kA): Flashover not occurring, no impinging surge on substation.
- Source 2 (30 kA): Peak of 710 kV with a steepness of 1250 kV/µs.
- Source 3 (80 kA): Peak of 1.706 MV with a steepness of 1076 kV/µs.
- Source 3 (160 kA): Peak of 3.022 MV with a steepness of 1205 kV/µs.

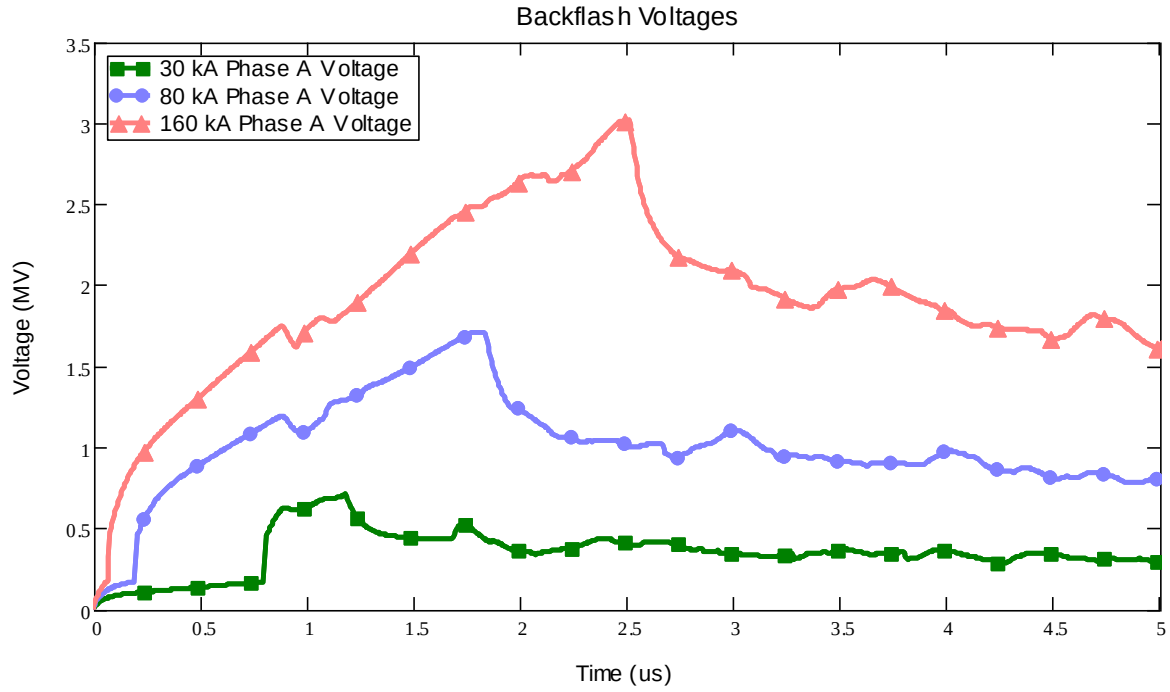


Figure 4-6: Transient voltages propagating towards the substation

The evaluation of the fast-fronted over-voltages in the substation provide important information on to the extent of stress the equipment and external insulation will experience. With reference to Figure 4-3, the important nodes in the substation where voltages were analysed include:

Feeder bay entrance (where surge enters substation) = V_{LINE}

Transformer 1 bushing voltage = V_{TRFR1}

Bus coupler circuit breaker terminal = V_{BCCB}

Transformer 2 Circuit breaker terminal = $V_{TRFR2CB}$

The worst-case over-voltage was expected to appear at the live point of the open Transformer 2 circuit breaker terminal. This position in the substation includes a point of discontinuity (breaker is in open position) and has the largest separation distance from a surge arrester. Initially the substation is evaluated without busbar surge arresters installed. The impact of increasing the separation distance between the transformer 2 circuit breaker and the nearest surge arrester was investigated.

The worst-case over-voltage occurs during the lightning current with a peak value of 160 kA. It produces an over-voltage transient with a peak value of 3.022 MV and steepness 1205 kV/µs. The worst-case over-voltages and arrester energy dissipation will occur for this scenario. All the impinging surges are plotted in Figure 4-6.

The peak over-voltages with the respective protective margin for a LIWL of 550 kV is captured in Table 4-5:

Table 4-5: Substation peak over-voltages in the substation for Source 4

Voltage Node	**Peak voltage (kV)**	**Protective margin for LIWL 550 kV (%)**
V_{LINE}	335	64
V_{TRFR1}	330	66
V_{BCCB}	343	60
$V_{TRFR2CB}$ (CB DIST = 60 m)	392	40
Airgap withstand 530 kV/m	392	33

When the Transformer 2 circuit breaker terminal was moved further away from the arrester positions, the arrester protective distances decreased and the peak voltage increased at the terminals. To evaluate the sensitivity of the protective distance, CB DIST was increased in steps of 20 m to represent larger substations. The results for the varied distance is tabulated in Table 4-6.

Table 4-6: Sensitivity of arrester protective distance on transformer 2 CB

CB DIST (m)	**$V_{TRFR2CB}$ (kV)**	**Protective margin (%)**
60	392	40
80	395	39
100	465	18.2
120	492	11.7
140	550	0

It is clear that for the protective margin to be decreased below 25 % and diminish the available margin of protection the substation configuration would be impractical. Very large distances of 100 m to 140 m between arresters and equipment are highly unlikely in 88/132 kV substations.

The inclusion of busbar arresters had a significant impact on the over-voltages. It is thus recommended to install additional arresters on the busbar where operating configurations allow for large separation distances.

In this case, the 140 m separation distance is divided into the bay distance of 60 m, and busbar separation distance of 80 m. With surge arresters installed at the bus coupler (in the middle of the total length of busbar) the voltage at the Transformer 2 circuit breaker is reduced to a maximum value of 440 kV. The margin of protection is restored to 25 %. When arresters are included at both ends the margin increases to 57 %. This is a significant improvement and proves that the MOV surge arrester could increase the protective margins in substations where separation distances becomes unusually large.

4.1.2.6 Busbar surge arrester energy capability

When a lightning surge similar to source 4 initiates an over-voltage transient, it is possible to overstress the arrester that encounters the incoming surge first. Additional arresters on the busbar will also contribute to dissipate the energy of the transient.

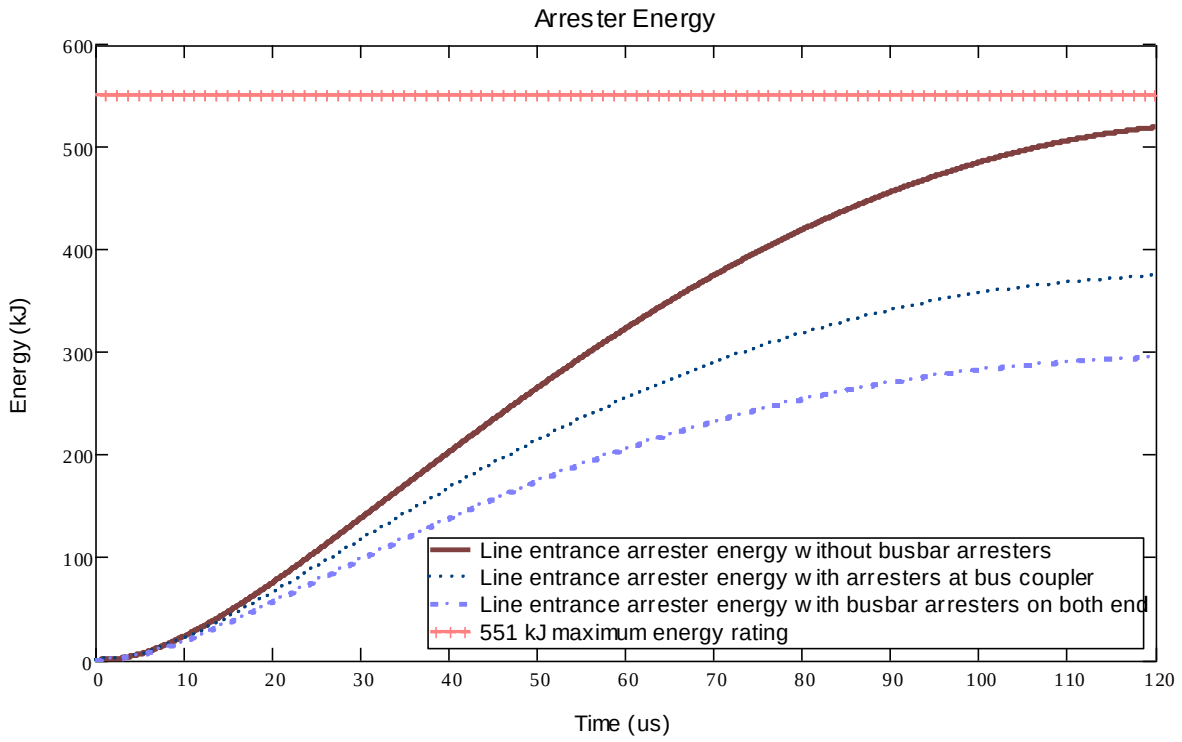


Figure 4-7: Line entrance arrester energy

When source 4 with peak current of 160 kA initiates an over-voltage transient, the incoming line entrance arrester dissipates a significant amount of energy. The maximum allowable energy for this arrester is 551 kJ. Without busbar arresters, the line entrance arrester dissipates 518 kJ and almost reaches its limit as shown in Figure 4-7. With busbar arresters installed at the bus coupler, the line entrance arrester energy is decreased to 373 kJ. With surge arresters installed at both ends of the busbar, the energy is reduced to 297 kJ. This proves that busbar arresters assist with the energy handling capability of the incoming lightning transient and will contribute to the reliability of the substation.

4.1.2.7 Results summary

Regarding the external insulation, a very conservative approach was taken to evaluate the airgap withstand as a linear volt-time function where the CFO is 530 kV/m. It is clear from the simulation that the voltage is limited to below the LIWL of the equipment except where CB DIST was increased to 140 m. This scenario is highly unlikely but the inclusion of busbar arresters significantly improves the protective margins throughout the substation. The inclusion of MOV arresters on the busbars contributes to the improvement of the substation reliability. Due to the high energy content of transients initiated by severe lightning current (such as Source 4), busbar arresters assist the line entrance arrester to dissipate the energy. Protective distances are increased to prevent over-stressing of non-recoverable insulation in substation worst-case configurations. The external insulation volt-time characteristic for its breakdown mechanism is of such nature that the stresses expected will not be of concern. The probability of a flashover occurring in the substation due to a back-flashover is highly unlikely if the arresters are positioned according to the current Eskom standard practice (line entrance and power transformers).

It is therefore clear that to coordinate the insulation for the protection of the non-recoverable insulation, the probability of external insulation failing also decreases. Busbar arresters will assist with the required additional energy dissipation for severe fast transient over-voltages initiated by a back-flashover close to the substation. Busbar arresters will also limit over-voltages to the maximum allowable protective margin of 25 %, where very long conductor distances separate equipment from installed arresters at the line entrances and transformers.

4.2 Uprating 275 kV to 400 kV results

4.2.1 Switching over-voltage stress simulation

For the simulation of switching over-voltages, a few cases are considered to gather an adequate number of over-voltage distributions that represent the maximum expected values.

The simulation included three sources with short-circuit powers of 5, 10 and 20 GVA. Each of the source X/R ratios was fixed at 10. The line lengths were varied and simulations are executed for 50 km, 100 km, 200 km and 400 km. Other variables include the inclusion and exclusion of trapped charge (residual voltages), pre-insertion resistors and surge arresters (sending and receiving ends). There were 36 cases in each configuration. For each case, the over-voltage distribution is obtained by means of a statistical switching operation (500 closing operations). The over-voltage distribution was analysed and for each distribution, the $U_{2\%}$ value was obtained. The $U_{2\%}$ value is the per unit value that includes 98 % of all over-voltages. Only 2 % of all values obtained in the distribution were excluded.

4.2.1.1 Configuration 1

Configuration 1 is similar to a cold energisation of a transmission line. To evaluate the over-voltage distribution without the impact of MOV surge arresters the sending and receiving end substation line entrance arresters was excluded from this simulation. All the results are tabulated in Table 4-7.

- Configuration 1: Excluding all of the following: trapped charge, pre-insertion closing resistors, and surge arresters.

Table 4-7: Configuration 1 over-voltage distributions

Source Short-circuit Power	Line length (km)	Trapped charge	Pre-insertion resistors	Surge arresters	Per unit (343 kV peak voltage) Over-voltage distribution $U_{2\%}$		
					Sending End	Midpoint	Receiving End
5 GVA	50	Absent	Absent	Absent	2.096	2.426	2.686
	100				2.004	2.394	2.650
	200				1.872	2.436	2.887
	400				1.742	2.477	3.149
10 GVA	50	Absent	Absent	Absent	2.002	2.432	2.656
	100				1.887	2.495	2.900
	200				1.721	2.559	3.115
	400				1.639	2.606	3.154
20 GVA	50	Absent	Absent	Absent	1.835	2.478	2.948
	100				1.726	2.563	3.077
	200				1.596	2.609	3.172
	400				1.689	2.627	3.174

The highest over-voltage distributions at the sending end were recorded where the source short-circuit power is 5 GVA combined with the energisation of the shorter lines. This is expected as the equivalent capacitance of the transmission line is small and the source inductance is large.

The highest over-voltage distributions at the receiving end were recorded for the strongest source combined with the longest lines. In this case, the source short-circuit power does not contribute significantly to the sensitivity of the magnitudes. The line length or the equivalent capacitance contributes significantly to the total over-voltage. The line length also allows more time for the superposition of travelling waves and to produce the higher values at the point of discontinuity (receiving end circuit breaker) where reflections of the travelling wave occurs.

4.2.1.2 Configuration 2

For Configuration 2 the same transmission line is energised while residual voltage exists on the line. This scenario is similar to an auto-reclose event when temporary faults are cleared automatically. To evaluate the peak over-voltages for worst-case switching arrangements, and to evaluate the maximum steepness of the over-voltages, the sending and receiving end arresters were excluded from this simulation.

- Configuration 2: Including trapped charge, excluding pre-insertion resistors and excluding surge arresters.

Table 4-8: Configuration 2 over-voltage distributions

Source Short-circuit Power	**Line length (km)**	**Trapped charge**	**Pre-insertion resistors**	**Surge arresters**	**Per unit (343 kV peak voltage) Over-voltage distribution $U_{2\%}$**		
					Sending End	**Midpoint**	**Receiving End**
5 GVA	50	Present	Absent	Absent	3.473	4.169	4.693
	100				3.212	4.035	4.547
	200				2.839	4.138	5.075
	400				2.653	4.327	5.804
10 GVA	50	Present	Absent	Absent	3.159	4.089	4.601
	100				2.924	4.279	5.224
	200				2.547	4.356	5.608
	400				2.411	4.708	6.100
20 GVA	50	Present	Absent	Absent	2.886	4.375	5.384
	100				2.648	4.518	5.652
	200				2.449	4.704	5.877
	400				2.348	4.709	6.326

The presence of trapped charge significantly increases the $U_{2\%}$ values and the same trend is realised for maximum over-voltage distributions. The increased over-voltages can be observed in Table 4-8. Although the results obtained in Configuration 2 are not true reflections of what to expect in reality, the results were a good indication of the maximum expected stresses that the transmission line and substations could experience without surge arresters.

4.2.1.3 Configuration 3

The MOV surge arresters were installed as standard practice at the line bay entrances and at the power transformers. When a switching surge with a relatively small rate-of-rise enters the substation, the surge arrester limits the over-voltage to its protective level. However, due to the front of the switching transient being slow, the protective distance is increased. The protective distances during switching transients are evaluated later.

- Configuration 3: Including trapped charge, excluding pre-insertion resistors and including surge arresters.

Table 4-9: Configuration 3 over-voltage distributions

Source Short-circuit Power	**Line length (km)**	**Trapped charge**	**Pre-insertion resistors**	**Surge arresters**	**Per unit (343 kV peak voltage) Over-voltage distribution $U_{2\%}$**		
					Sending End	**Midpoint**	**Receiving End**
5 GVA	50	Present	Absent	Present	Over-voltage limited to maximum residual voltage (MRV) of 1.8 p.u.	2.365	Over-voltage limited to maximum residual voltage (MRV) of 1.8 p.u.
	100					2.544	
	200					2.610	
	400					2.861	
10 GVA	50	Present	Absent	Present		2.569	
	100					2.632	
	200					2.684	
	400					2.981	
20 GVA	50	Present	Absent	Present		2.614	
	100					2.580	
	200					2.818	
	400					3.068	

The sending and receiving end surge arresters limit all switching over-voltages to 1.8 – 1.9 p.u. It is important to note that the mid-point of the transmission line experience over-voltages between 2.4 p.u and 3 p.u, depending on the line length. All the results are captured in Table 4-9.

4.2.1.4 Configuration 4

The inclusion of closing resistors will have a dramatic impact on the peak over-voltages. Prior to the transient propagation along the transmission line, the energy is dissipated in the resistors. Significantly lower over-voltages are expected throughout the length of the total system. An alternative to closing resistors is the installation of transmission line arresters at the mid-point or controlled closing.

- Configuration 4: Including trapped charge, including pre-insertion resistors and including surge arresters.

Table 4-10: Configuration 4 over-voltage distributions

Source Short-circuit Power	Line length (km)	Trapped charge	Pre-insertion resistors	Surge Arresters	Per unit (343 kV peak voltage) Over-voltage distribution $U_{2\%}$		
					Sending End	Midpoint	Receiving End
5 GVA	50	Present	Present	Present	Over-voltage limited to maximum residual voltage (MRV) of 1.8 p.u.	1.960	Over-voltage limited to maximum residual voltage (MRV) of 1.8 p.u.
	100					1.793	
	200					1.675	
	400					1.915	
10 GVA	50	Present	Present	Present		1.761	
	100					1.715	
	200					1.687	
	400					1.837	
20 GVA	50	Present	Present	Present		1.705	
	100					1.720	
	200					1.707	
	400					1.817	

Pre-insertion resistors limit over-voltages at all points. Sending, receiving and mid-point over-voltages are limited to significantly lower values. For voltage uprating, transmission line arresters or closing resistors could potentially contribute significantly to increasing the feasibility of voltage uprating of the transmission line. All the results are tabulated in Table 4-10.

4.2.1.5 Worst-case results for sending end, mid-point and receiving end.

The worst-case over-voltage for the sending end substation during reclosing was recorded to be 3.324 p.u. The highest sending end over-voltages were observed where the source short-circuit power was at its weakest (5 GVA), and the line length was the shortest (50 km). The shorter line length contributes a smaller capacitance. The magnitude of the over-voltage is indirectly proportional to the capacitance of the line. A larger capacitance or longer line will produce lower over-voltage values at the sending end. A weaker source means that the source inductance is large. The damping is weaker and more superposition could take place to produce higher over-voltages at the sending end. The worst case sending end over-voltage distribution has a $U_{2\%}$ value of 3.473 p.u (from the best fit normal distribution).

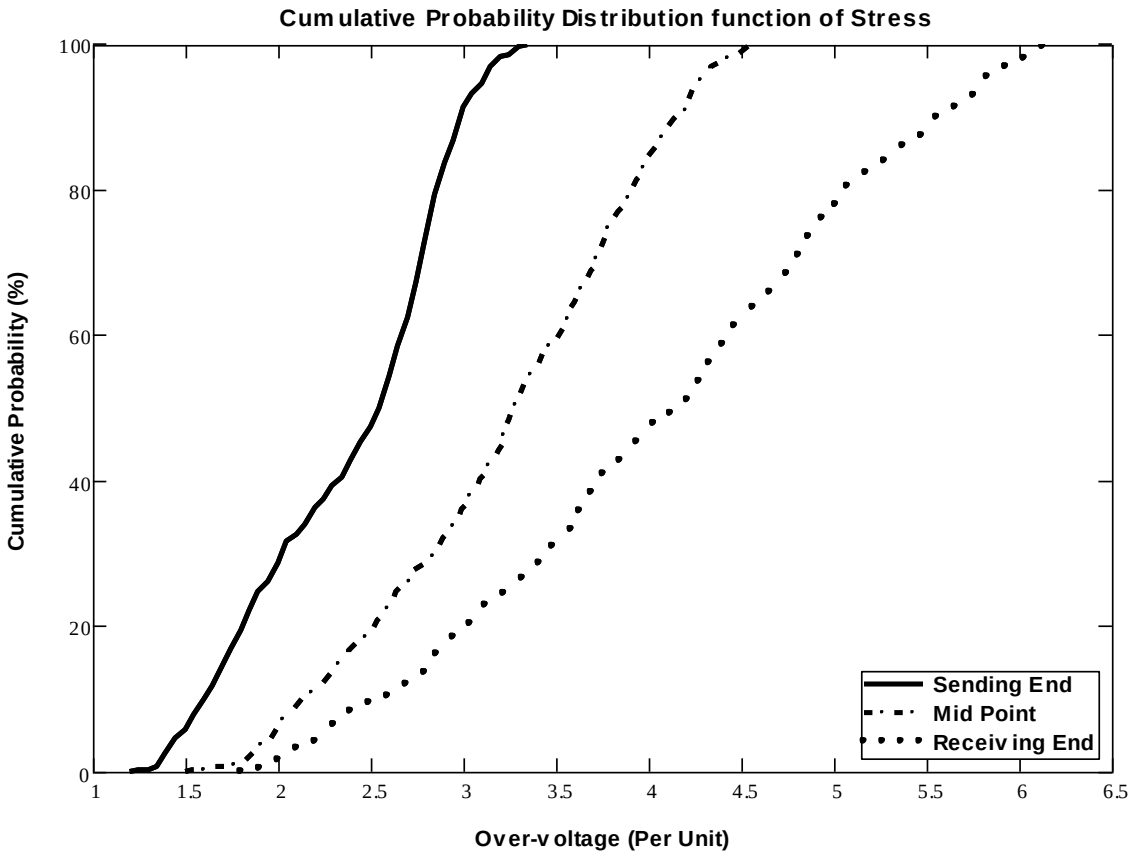


Figure 4-8: Worst-case distributions for sending, mid-point and receiving end

The mid-point of the line experiences its worst-case over-voltage distribution in the case where the transmission line is very long and where the source is at is strongest. This is directly related to the travelling wave theory where the reflected wave at the receiving end is at its largest. The arresters at the sending and receiving ends limit the over-voltages but when the travelling transient propagates away from the point of discontinuity, the transient rises in magnitude again. At the mid-point of the line the voltage distribution has a $U_{2\%}$ value of 4.709 p.u as observed in Figure 4-8.

The receiving end worst case distributions were recorded where the longer transmission line lengths were combined with stronger sources. Although the sending end over-voltage distributions in these cases consisted of the lowest magnitude switching transients, the receiving end over-voltages were significantly higher. Due to longer propagation times, more superposition occurs and maximum doubling effect at the point of discontinuity occurs. It is expected that the surge arrester energy for these cases will be the highest. The following table describes the sending end maximum over-voltage during the 50 km line energisation with source short-circuit power of 5 GVA.

Table 4-11: Sending end worst-case over-voltage scenario

Arrester and circuit breaker details	**RΦ**	**WΦ**	**BΦ**
Arrester Current (A)	300	1015	1152
Arrester Energy (kJ)	66.1	324.1	267.8
Circuit breaker closing times (s)	0.056401	0.054796	0.054575
Actual peak over-voltage (kV)	-759.055	-1140.15	930.242

The peak over-voltage in Figure 4-9 (without arresters) at the sending end of the transmission line is 1140 kV.

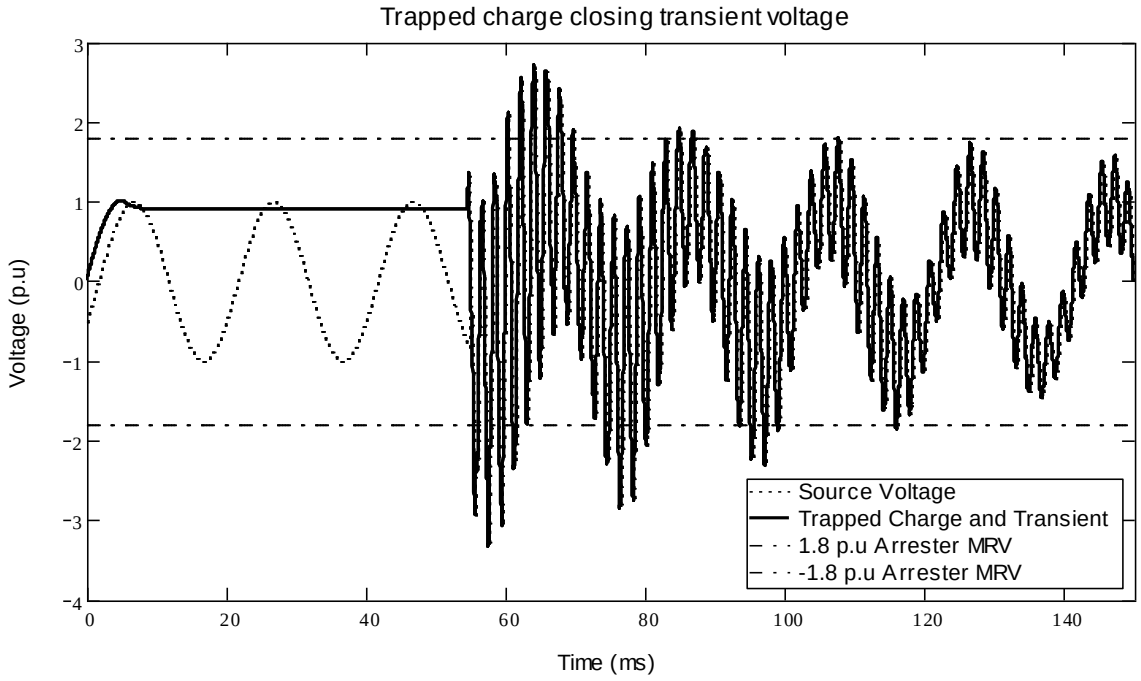


Figure 4-9: Sending end worst case switching over-voltage

With surge arresters included in the simulation, the over-voltage was limited to 1.8 p.u and the damping was increased by the metal-oxide surge arrester.

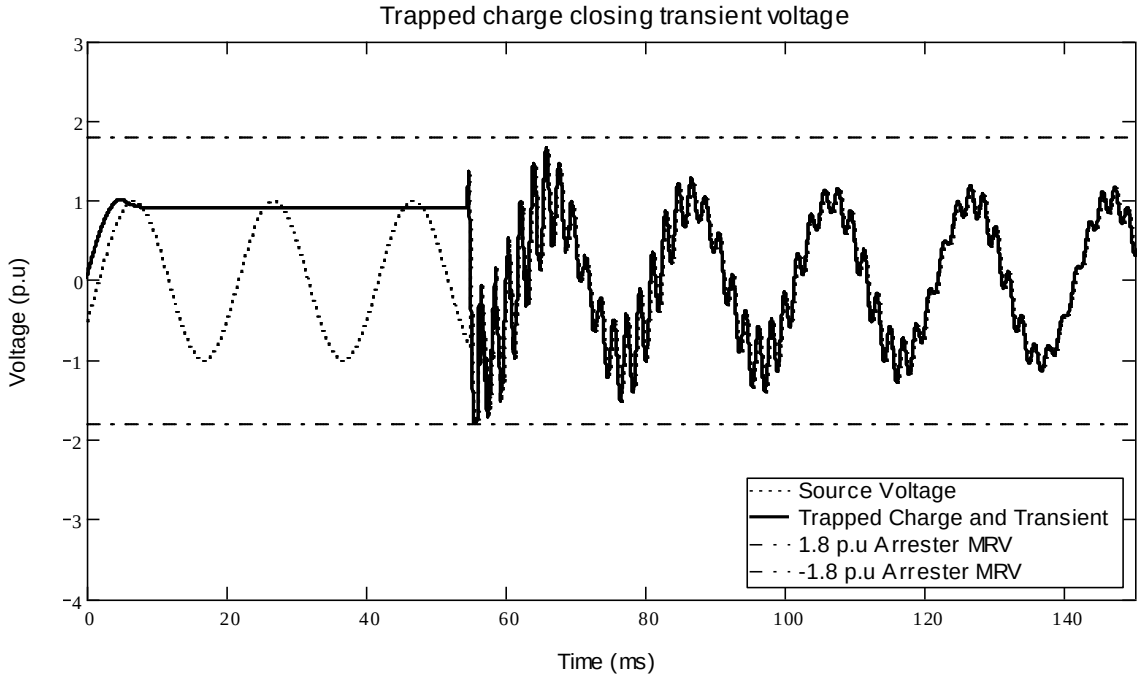


Figure 4-10: Sending end worst case switching over-voltage (with arresters)

4.2.1.6 Maximum surge arrester energy demands

The maximum switching surges at the sending end for each case is evaluated to calculate the maximum expected energy dissipation for the sending end arresters. For each case, the worst case switching scenario is extracted out of the 500 recorded operations. Each worst case is evaluated in the time domain with the exact circuit breaker operating times. The maximum arrester energy dissipation is recorded. The transient steepness is also recorded (without surge arresters). The results are tabulated in Table 4-12.

Table 4-12: Sending end arrester energy analysis

Source, Line length	Circuit breaker closing time (s)			Peak Voltage (kV)			Max Peak (kV)	Max Peak (p.u)	Max Arrester Energy (MJ)	Steepness (kV / µs)
	RΦ	WΦ	BΦ	RΦ	WΦ	BΦ				
5 GVA, 50 km	0.0564	0.0547	0.0545	759	1140	930	1140	3.32	0.127	1.7
5 GVA, 200 km	0.0567	0.0577	0.0529	774	1076	1012	1076	3.14	0.086	1.5
10 GVA, 50 km	0.0564	0.0547	0.0545	845	1076	1011	1076	3.14	0.108	1.88
10 GVA, 200 km	0.0560	0.0550	0.0552	632	742	949	949	2.77	0.091	2.37
20 GVA, 50 km	0.0595	0.0577	0.0590	857	836	1015	1015	2.96	0.052	2.17
20 GVA 200 km	0.0567	0.0577	0.0529	672	909	603	909	2.65	0.108	2.8

From the table it is clear that the sending end arresters were stressed to a maximum of 5%–6% of their energy handling capability. Minimal stress is applied to the sending end arresters during worst case reclosing operation. Maximum over-voltages for the different configurations at the mid-point of the transmission line are obtained during the following scenarios plotted in Figure 4-11 and tabulated in Table 4-13.

Table 4-13: Maximum transmission line mid-point distributions

Configuration		Source (GVA)	Line length (km)	$U_{2\%}$ (p.u)
1	Cold energisation	20	400	2.627
2	Trapped Charge	20	400	4.709
3	Trapped Charge, Arresters	20	400	3.068
4	Trapped Charge, Arresters and Closing resistors	20	400	1.817

The over-voltage distributions for the transmission line mid-point are plotted against each configuration. Mid-point over-voltages reached high values for longer transmission line lengths. Worst-case scenarios include 20 GVA source short-circuit power and 400 km line lengths. Shorter lines such as 100 km also produced high values for the mid-point and were of the order of 2.6 p.u.

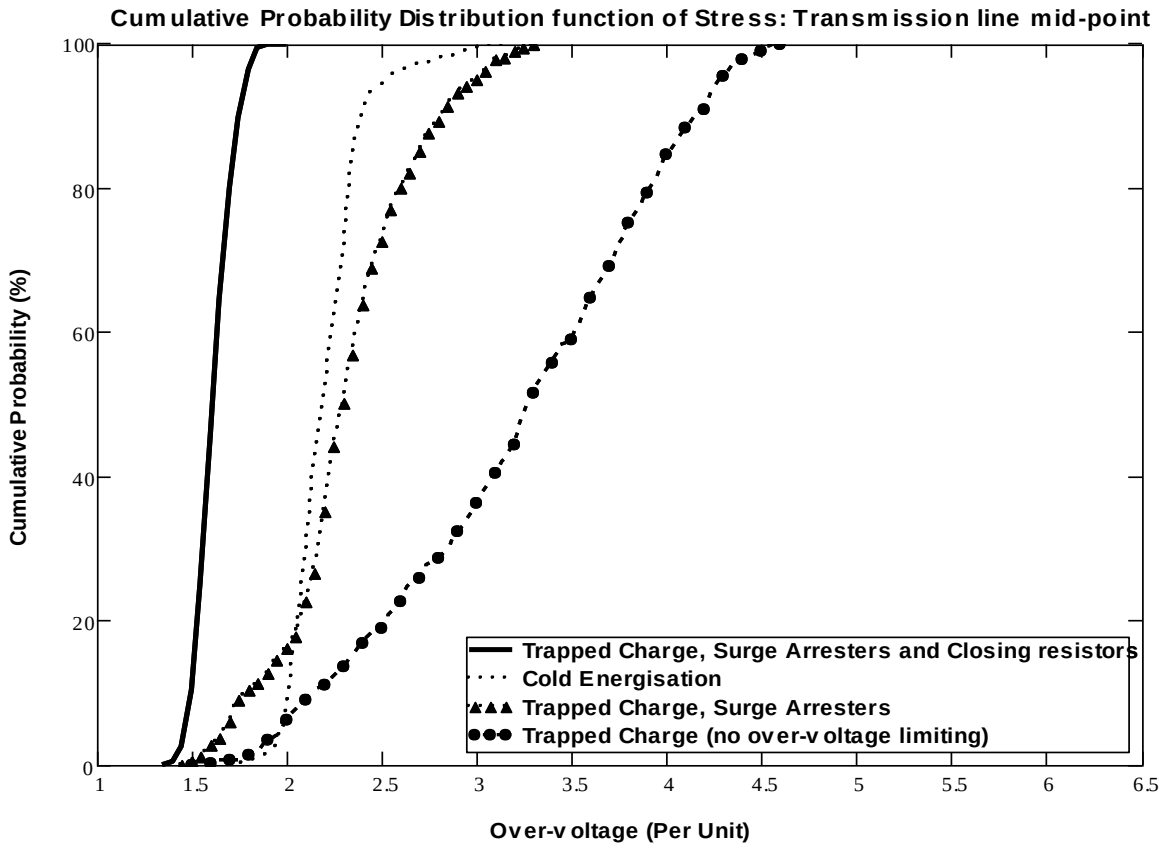


Figure 4-11: Transmission line mid-point over-voltage distributions

The risk of flashover at the mid-point of the transmission line is calculated for each case and is presented. The clearance could be calculated as a function of the Switching Impulse Withstand Level (SIWL) of the actual tower configuration. Three SIWL values were used for the risk calculation and the corresponding risk factor was calculated for each.

Table 4-14: Risk of flashover at transmission line mid-point

Source Short-circuit Power	Line length (km)	Trapped charge	Pre-insertion resistors	Surge arresters (sending and receiving ends)	Per unit (343 kV peak voltage) Over-voltage distribution $U_{2\%}$			
					Midpoint $U_{2\%}$ (p.u)	Risk (%) of flashover based on SIWL		
						850 kV	950 kV	1050 kV
5 GVA	50	Present	Absent	Present	2.365	0.277	0.006148	0.00019
	100				2.544	1.325	0.058	0.00692
	200				2.610	2.143	0.2078	0.0187
	400				2.861	9.20	1.52	0.1652
10 GVA	50	Present	Absent	Present	2.569	1.55	0.1447	0.0124
	100				2.632	2.28	0.2679	0.035
	200				2.684	3.2	0.4038	0.0351
	400				2.981	13.2	2.94	0.445
20 GVA	50	Present	Absent	Present	2.614	2.02	0.23	0.029
	100				2.580	1.68	0.162	0.015
	200				2.818	5.89	1.06	0.135
	400				3.068	16.37	4.33	0.81

It was assumed that the risk of flashover is almost zero when the over-voltage is below the maximum residual voltage of the surge arrester. When pre-insertion resistors were included in the circuit breaker, the mid-point over-voltage distributions did not exceed values of $U_{2\%}$ higher than that of the 1.8 p.u MRV. This leads to the assumption of minimum risk of failure.

The inclusion of pre-insertion resistors has a dramatic influence on the total over-voltage distributions and is observed in the decreasing risk captured in Table 4-14. Assuming the sending and receiving end surge arresters limit any switching over-voltage to 1.8 p.u, the mid-point of the transmission line over-voltages were reduced to acceptable values. The simulation result obtained produced a mid-point $U_{2\%}$ value of 1.817 p.u as shown in Figure 4-12. In this scenario the worst case was where the source short-circuit power was 20 GVA and the transmission line length was 400 km.

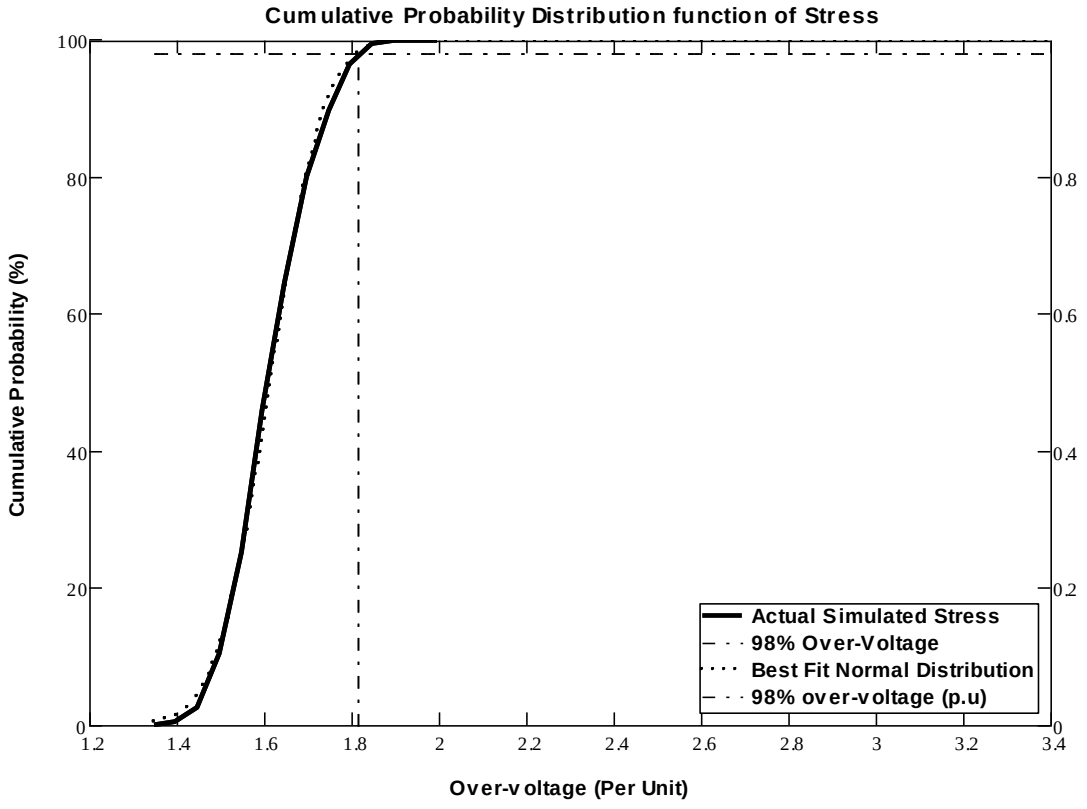


Figure 4-12: Mid-point over-voltage distribution (including pre-insertion resistors)

When comparing the over-voltage distribution to the SIWL of 750 kV, a very small risk of failure of 0.0047 % was obtained. The distribution of over-voltages was captured within the limits of the maximum residual voltage of the sending and receiving end surge arresters, additionally lower values were obtained due to the inclusion of the pre-insertion resistors and all values were contained between 1.4 p.u and 1.8 p.u.

The following table describes the receiving end maximum over-voltage during the 400 km line energisation with source short-circuit power of 20 GVA.

Table 4-15: Receiving end worst case over-voltage scenario

Arrester and circuit breaker details	**RΦ**	**WΦ**	**BΦ**
Arrester Current (A)	1580	-3100	-1829
Arrester Energy (MJ)	1.63	2.98	1.25
Circuit breaker closing times (s)	0.056149	0.055225	0.055795
Actual peak over-voltage (kV)	-1382.26	-2113.15	1538.34

The peak over-voltage (without arresters) at the sending end of the transmission line was 2113 kV as shown in Figure 4-13 and was almost double the magnitude of the worst case sending end over-voltage.

The maximum switching surges at the sending end for each case was evaluated to calculate the maximum expected energy dissipation for the sending end arresters. For each case, the worst case switching scenario was extracted out of the 500 recorded operations.

Each worst case is evaluated in the time domain with the exact circuit breaker operating times. The maximum arrester energy dissipation is recorded. The transient steepness is also recorded (without surge arresters)

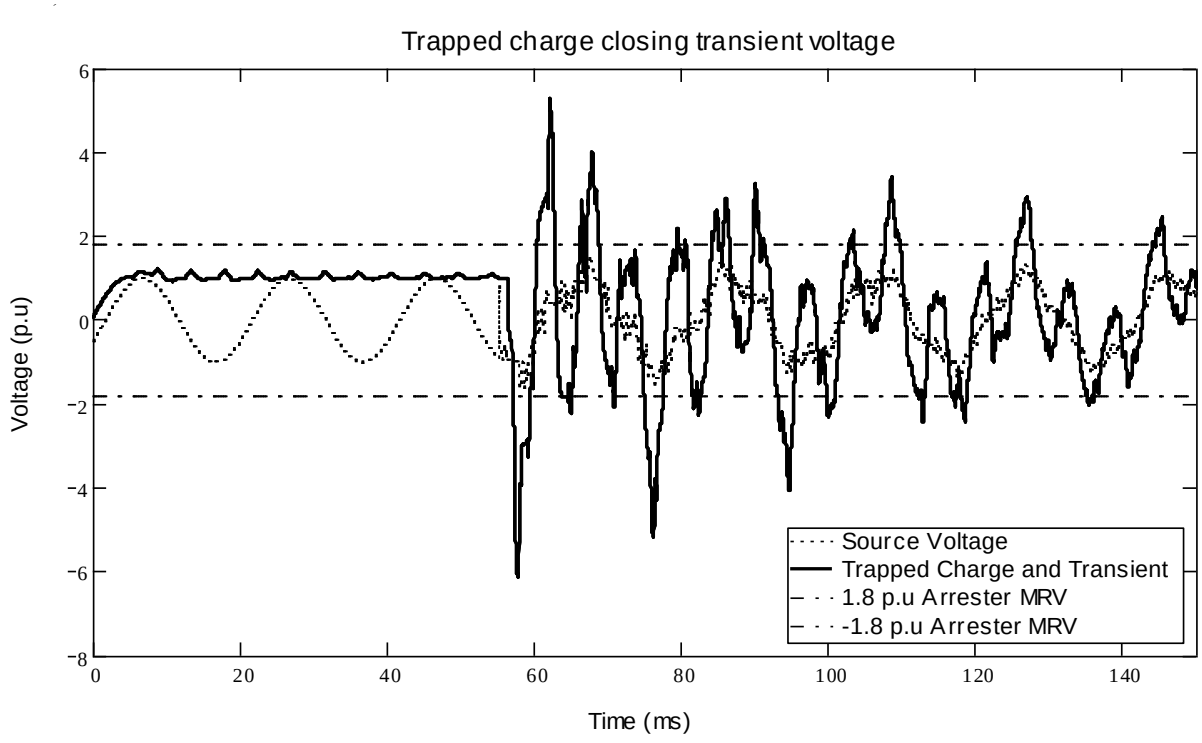


Figure 4-13: Receiving end worst case switching over-voltage.

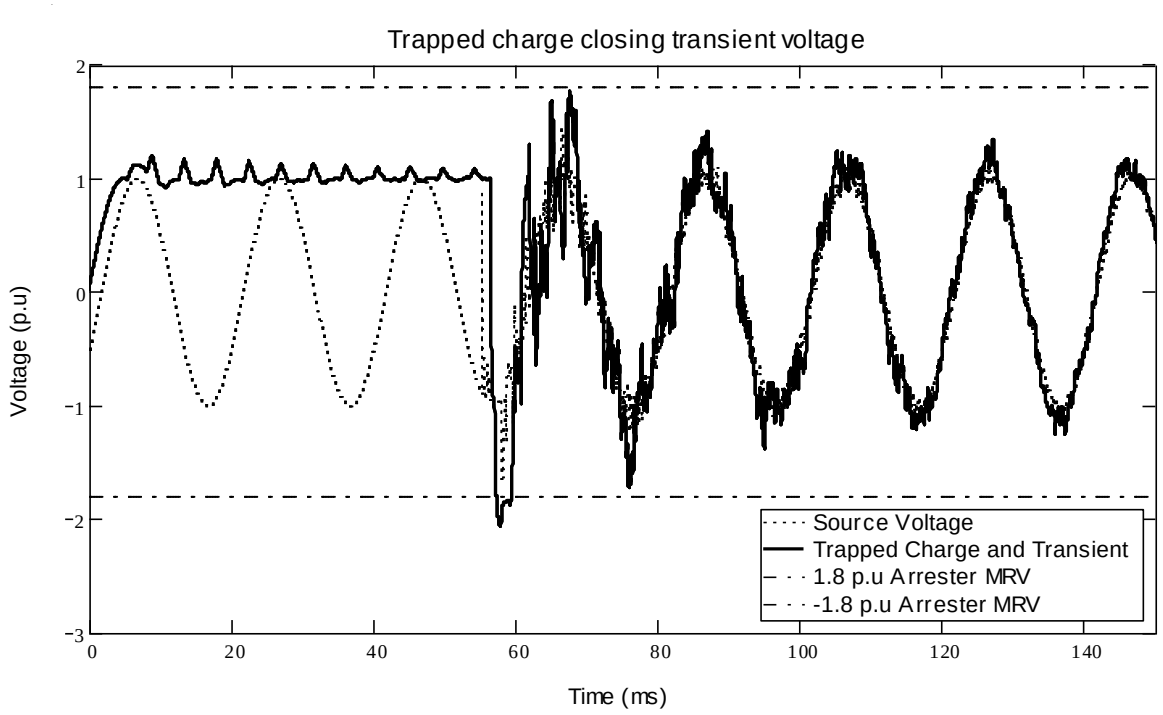


Figure 4-14: Receiving end worst case switching over-voltage (with arresters)

With surge arresters included in the simulation, the over-voltage is limited to 1.8 p.u and the damping is increased to the non-linear resistive element of the metal-oxide surge arrester in operation. This result is plotted in Figure 4-14.

Table 4-16: Receiving End Arrester Energy Analysis

Source, Line length	Circuit breaker closing time (s)			Peak Voltage (kV)			Max Peak (kV)	Max Peak (p.u)	Max Arrester Energy (MJ)	Steepness (kV / µs)
	RΦ	WΦ	BΦ	RΦ	WΦ	BΦ				
5 GVA, 50 km	0.0560	0.0564	0.0539	1339	1675	1164	1675	4.89	0.258	3.2
5 GVA, 200 km	0.0570	0.0562	0.0568	1008	1805	1117	1805	5.26	1.23	1.27
10 GVA, 50 km	0.0546	0.0559	0.0538	1048	1543	1225	1543	4.50	0.261	3.44
10 GVA, 200 km	0.0596	0.0585	0.0562	1912	1633	1636	1912	5.58	0.797	1.5
20 GVA, 50 km	0.0589	0.0571	0.0581	1223	1228	1837	1837	5.36	0.246	4.44
20 GVA 200 km	0.0587	0.0566	0.0575	1631	1540	2058	2058	6.00	1.035	1.74

From the tabulated results in Table 4-16 it is clear that the receiving end arresters are stressed to a maximum of 1.23 MJ which relates to more than 50 % of its maximum energy handling capability. Multiple re-closures could lead to excessive heat in the arrester MOV blocks and the risk of thermal runaway. However, considering the energy demand with regards to transmission line energisation with trapped charge present, the arresters are well within their limits and this is only during the worst-case simulated scenario.

Over-voltages caused by single phase-to-earth fault initiation and clearing were evaluated and were recorded with the following system configuration:

- 20 GVA, 200 km,
- 2.5 p.u switching transient,
- 1.4 p.u temporary over-voltage on healthy phases.

The over-voltage distribution contains transient values not higher than 2.5 p.u (without surge arresters). With surge arresters included at the sending and receiving end of the line, the switching over-voltages were limited to 1.69 p.u. The temporary over-voltages on the healthy phases during a single phase-to-earth fault were not expected to be a determining factor when evaluating the clearance requirement. The following simulation evaluates the arrester energy during fault initiation and fault clearing.

The fault occurred and was present for 500 ms. The back-up protection operated and cleared the fault. The Ferranti voltage rise on the longer transmission lines contributed to the overall temporary overvoltage on open-ended lines. The simulations consisted of an energised transmission line where the fault occurred at the end of the line (single phase-to-earth). The source was effectively earthed and no additional neutral impedance was included. The short-circuit resistance was neglected and was simulated as a solidly bonded short-circuit initiated and cleared with an ideal switch between one of the phases and earth.

Table 4-17: Single phase-to-earth fault over-voltage evaluation

Short-circuit Power (GVA)	Short-circuit Current at fault location (peak kA)	Line length (km)	Max Switching over-voltage (p.u)	Healthy phase TOV (p.u)	Max Arrester Energy (kJ)
5	5.2	50	Over-voltage limited to maximum residual voltage (MRV) of 1.69 p.u.	1.16	23
	3.6	100		1.25	33
	2.2	200		1.35	15
10	7.2	50		1.23	20
	4.3	100		1.30	23
	2.4	200		1.40	20
20	8.8	50		1.29	47
	4.9	100		1.34	11
	2.6	200		1.40	34

From the results obtained in Table 4-17 it is clear that the over-voltages were limited to the arrester residual voltages. The energy associated with fault initiation and clearing included both the slow-front transients and TOV on the healthy phases. The earth fault factor did not reach higher values than 1.4 and the arrester discharge currents were very small during the total 500 ms event. The highest energy value recorded was 47 kJ which is well below the maximum capability of 2400 kJ.

4.2.1.7 Surge arrester protective distance

The following equation describes the protective distance of the arrester [15]:

$$L_{max} = v.\frac{\left[\frac{SIWL}{(1+M_p)} - U_{res}\right]}{2s} - (H_{SA} + H_{struct}) \quad (4.2)$$

Where

L_{max} is the maximum allowable separation distance (m).

H_{SA} is the surge arrester height of 1.5 m.

H_{struct} is the structure height representing of 3 m.

v is the propagation velocity which is 297 m/µs.

M_p is the protective margin required of 30 %.

U_{res} is the arrester protective level of 618 kV.

s is the steepness of the incoming surge determined to be 4.44 kV/µs.

The maximum steepness obtained for switching surges was recorded at the receiving end of the 50 km line with source short-circuit power of 20 GVA. Trapped charge was included but surge arresters did not limit the measured over-voltage. A value of 4.44 kV/µs was recorded as the worst case. The maximum protective distance for the arrester to limit over-voltages and still maintain a 30 % protective margin was 6.3 km. To control the switching over-voltages on the transmission line at locations such as the mid-point and the rest of the line that is isolated from the arrester protective area, line arresters could be included of intervals of 5 km – 6 km for air clearances based on a SIWL of 1050 kV. For lower withstand levels such as 850 kV and 950 kV shorter distances are required to obtain the same protective margins.

Table 4-18: Surge arrester protective distance for slow-front switching surges

SIWL (kV)	Protective margin (%)	Protective distance (m)
850	30	1194
950	30	3767
1050	30	6340

From the results obtained in Table 4-18 it is clear that even with a required protective margin of 30 %, the arrester managed to limit the switching over-voltage with steepness in the range of 4.5 kV/µs up to 1 km for lower withstand levels such as 850 kV. This proves that for switching surges, it is very unlikely that additional surge arresters on the substation bus conductors and so forth will contribute any value. It is accepted that for higher steepness values (fast-front surges such as lightning), much smaller protective distances will be required. For non-recoverable insulation equipment such as transformers, it is standard practice to include arresters very close to the equipment terminals. For incoming surges, substation line entry arresters will operate and limit these steep-fronted surges. All non-recoverable insulation should be protected by arresters and conservative protective margins

should be applied. With regards to external insulation, fast-fronted surges are not of great concern where larger airgaps are employed. This is due to the breakdown mechanism of air and as mentioned before, the withstand of air is at its lowest value when subjected to slower-front surges where the front times are of the order of 250/300 µs.

4.2.2 Determination and selection of switching impulse withstand levels

Voltage uprating could potentially include decreasing the standard withstand levels used for specific operating voltages. For example, it is standard practice in Eskom to use 1050 kV SIWL and 1425 kV LIWL for the 400 kV substation equipment. For 275 kV equipment, 850 kV SIWL and 1050 kV for LIWL is used. The current standard used in Eskom for clearances is not based on these standard withstand levels. In fact, the current standard clearances are based on the clamping capability of the old silicon-carbide surge arresters.

It is then important to understand the withstand capability of the current clearances based on the Gallet-Leroy equation. Determining the withstand level of the standard clearances will provide vital information to use as a benchmark when comparing new clearances that are calculated from statistical switching studies.

With reference to the typical phase-to-phase gap factors, a gap factor of 1.57 is chosen for the Gallet-Leroy equation calculations. The phase-phase configuration could be envisioned as “along the span” and therefore the value is somewhat higher when compared to the phase-earth value.

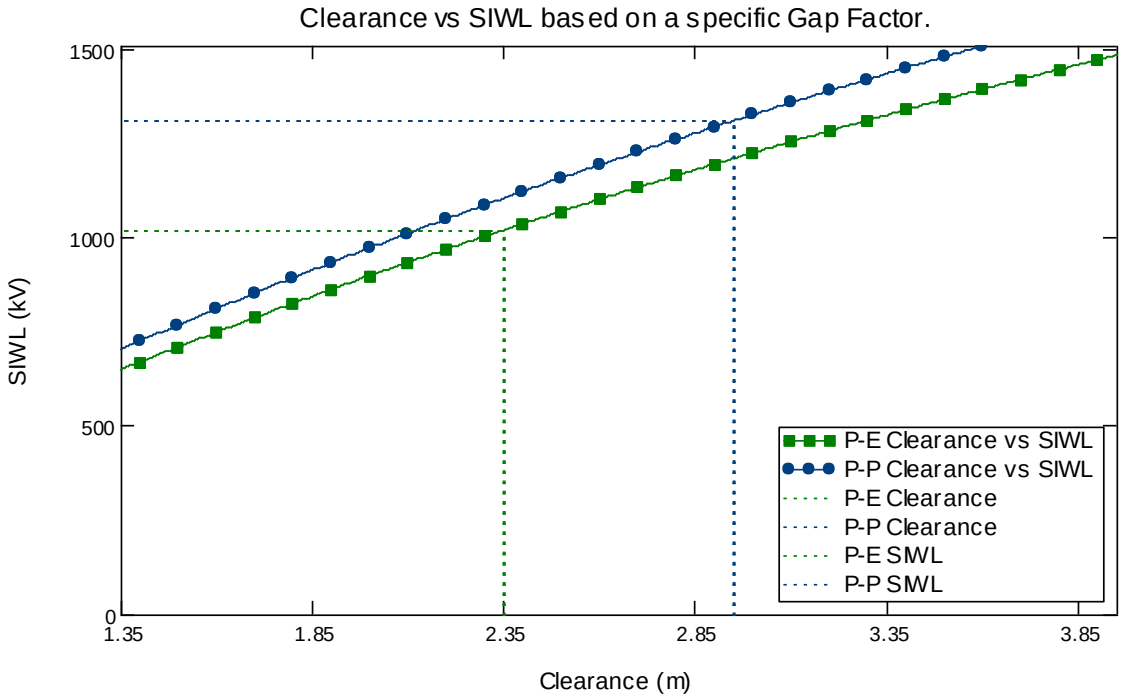


Figure 4-15: 275 kV Equivalent SIWL (based on standard clearances and specific gap factors)

For the 275 kV clearances, Figure 4-15 shows that the calculated SIWL for the phase-to-earth clearance is 1019 kV (gap factor 1.45) and for phase-to-phase is 1309 kV (gap factor 1.57). The ratio of phase-to-earth/phase-to-phase is 1.29. This is referenced to the standard clearances captured in Table 4-19.

Table 4-19: Eskom standard clearances for 275 kV and 400 kV substations

Nominal Voltage (kV)	Phase-to-Earth (mm)	Phase-to-Phase (mm)
275	2350	2950
400	3200	4000

When a substation is uprated from 275 kV to 400 kV, the airgap withstand level of 1019 kV (phase-to-earth) will be subjected to switching impulse stress. The switching over-voltages are limited by the arresters to 1.87 p.u (for a 2000 A 30/60 µs current) of the maximum peak phase-to-earth operating system voltage (in this case 343 kV).

From a typical surge arrester data sheet, the Maximum Residual Voltage (MRV) for a U_{max} of 420 kV (arrester rated voltage of 312 kV) for a 30/60 µs, 2000 A current is 642 kV. The arrester protective margin between 1019 kV and 642 kV is 58.7 % (25 % required minimum) and will decrease when a lower SIWL is selected. The available margin is 33.7 %. It is important to remember that the gap factor has a significant impact on the withstand voltage of the airgap. With the worst-case electrode configuration the gap factor is 1. The calculated phase-to-earth SIWL for a gap factor of 1 is 703 kV. The margin of protection in this case is only 9.5 %. To obtain a minimum of 25 % the gap factor should be no less than 1.14 resulting in a SIWL of 800 kV. It is also recommended that the ratio between the phase-to-earth and phase-to-phase withstand levels is 1.5. The phase-to-phase SIWL is calculated then to be 1200 kV. The corresponding phase-to-phase gap factor is 1.41. The results for these values are plotted in Figure 4-16 and tabulated in Table 4-20.

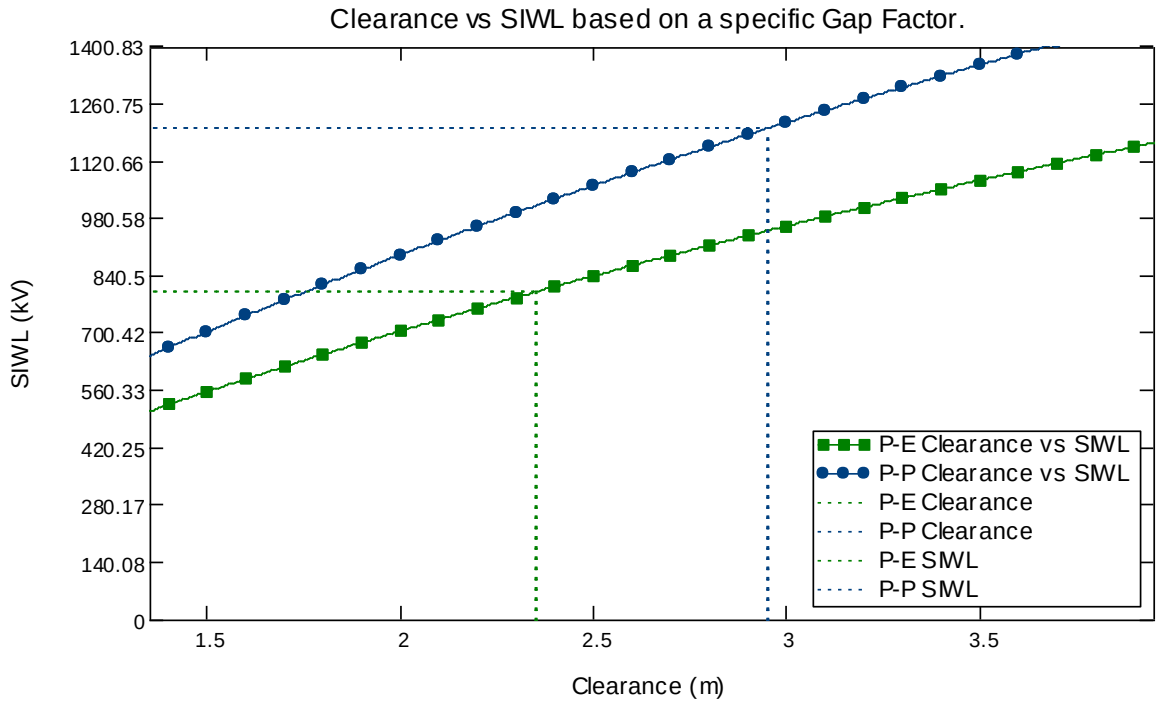


Figure 4-16: 275 kV Equivalent SIWL (smallest gap factors to obtain worst case)

Table 4-20: Standard 275 kV clearances and representative SIWL's.

275 kV clearances SIWL's	P-E SIWL	P-P SIWL	Ratio	Gap Factor		Arrester protective margin (%)
				P-E	P-P	
Case 1	1019	1309	1.29	1.45	1.57	58.7
Case 2	703	1309	1.86	1	1.57	9.5
Case 3	800	1200	1.5	1.14	1.41	25

The airgap strength for switching impulses is now defined for a minimum withstand level required to allow for a 25 % protective margin. Case 3 stipulates that for the standard clearances used in 275 kV substations, a SIWL of 800 kV represents the withstand capability of a 2.35 m airgap with a gap factor of 1.14. For phase-to-phase, the smallest gap factor allowed to maintain the clearance of 2.95 m is 1.41. The arrester protective margin for the external insulation is then 25 %. When 400 kV equipment rated for a SIWL of 1050 kV is installed, the protective margin for the internal insulation increases to 63.5 %. It is therefore important to deal with internal and external insulation separately. To calculate a clearance based on the standard SIWL relevant for internal insulation will produce grossly over conservative gap requirements for external insulation.

4.2.3 Risk of failure based on specific switching impulse withstand level

To evaluate the risk of failure for the sending and receiving end substations, a stress versus strength comparison is evaluated for each. The evaluation includes internal and external insulation.

4.2.3.1 Sending end risk evaluation

The worst-case over-voltage stress distribution for the sending end was obtained with source short-circuit power of 5 GVA and a short line of 50 km. The over-voltage distribution contained values limited by the sending end surge arresters and did not exceed 1.87 p.u as expected. As previously mentioned, a phase-to-earth SIWL of 800 kV is the reference value for the withstand capability of the standard 2.35 m airgap (used as the standard phase-to-earth clearance for 275 kV) with a gap factor of 1.14.

Table 4-21: Sending end risk calculation based on 4 different SIWL's

SIWL (kV)	Statistical safety factor (%) ($SIWL/U_{2\%}$)	Risk of failure (%)	Arrester Protective Margin (%)	Arrester Protective Margin (%)
			Discharge class 3 7.8 kJ/kV U_r MRV 642 kV	Discharge class 4 12 kJ/kV U_r MRV 630 kV
800	22.8	1.2×10^{-3}	25	27
850	30	8.1×10^{-5}	32.2	35
950	45	3.7×10^{-7}	47.8	50
1050	61	2.3×10^{-9}	63.4	66.6

The risk calculation results in Table 4-21 show that when 800 kV is selected for the external insulation SIWL, only 1 in every 100 000 switching operations could potentially result in a flashover. Selecting a standard SIWL for the internal non-recoverable insulation yields much

lower risk values and is graphically realised in Figure 4-17. Larger arrester protective margins are also achieved through the use of higher rated energy arresters. It was found that arresters with higher energy capability do not contribute significantly to additional protective margins in this case. Only a 2 – 3 % improvement is realised.

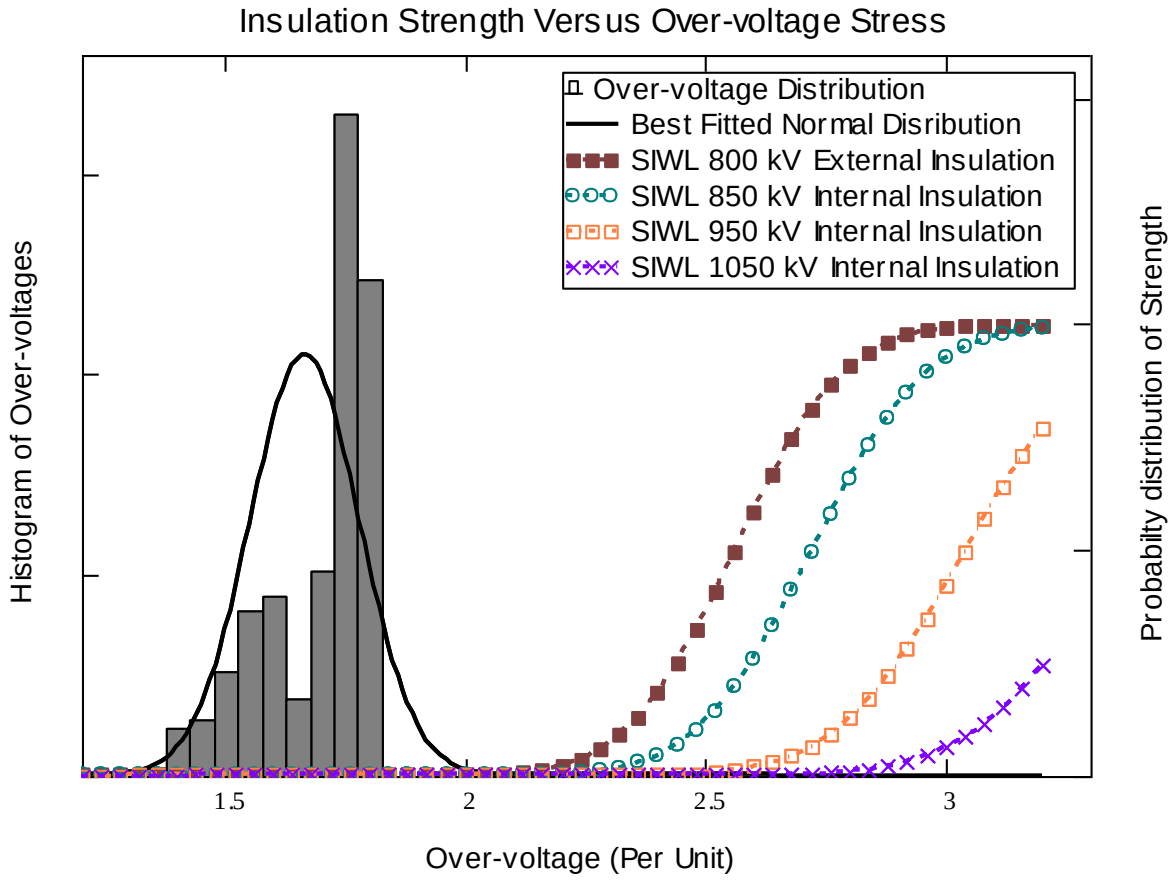


Figure 4-17: Over-voltage stress versus strength (5 GVA 50 km Sending end)

4.2.3.2 Receiving end risk evaluation

The worst-case over-voltage stress distribution for the receiving end was obtained with a source short-circuit power of 20 GVA and a long line of 400 km. The over-voltage distribution contained values limited by the sending and receiving end surge arresters and did not exceed 1.87 p.u as expected. Although similar distributions are expected for the sending and receiving ends due to the arresters limiting at almost the same per unit voltages, the distributions differed slightly.

The risk values calculated were then slightly higher for the receiving end. The same withstand levels were chosen for the calculation and the results are tabulated in Table 4-22.

Table 4-22: Receiving end risk calculation based on 4 different SIWL's

SIWL (kV)	Statistical safety factor (%) ($SIWL/U_{2\%}$)	Risk of failure (%)	Arrester Protective Margin (%) Discharge class 3 7.8 kJ/kV U_r MRV 642 kV	Arrester Protective Margin (%) Discharge class 4 12 kJ/kV U_r MRV 630
800	23.2	7.1×10^{-3}	24.6	26.9
850	30.9	4.6×10^{-4}	32.4	35
950	46.3	2.1×10^{-6}	47.9	50.6
1050	61.7	1.3×10^{-8}	63.4	66.6

For the receiving end distribution, more over-voltages are between 1.8 and 1.9 p.u as opposed to the sending end distribution with fewer values in this bracket and more values between 1.3 and 1.6 p.u. This results in a slight skewness towards higher p.u values for the receiving end and is shown in Figure 4-18.

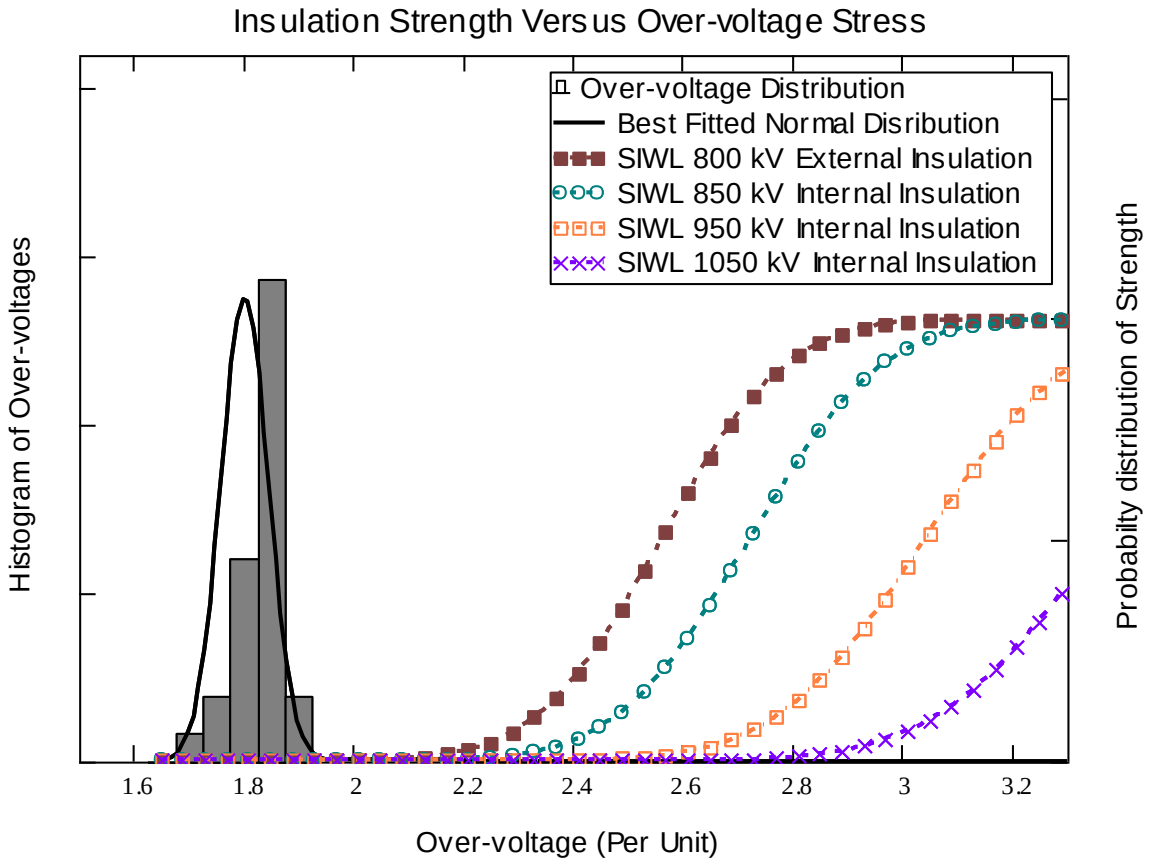


Figure 4-18: Over-voltage stress versus strength (20 GVA 400 km Receiving end)

4.2.4 Sending and receiving end clearance calculation

The risk of failure has been calculated as a function of the withstand level and over-voltage distributions obtained at the sending and receiving ends of the line. The available standard clearances (275 kV) had been defined as a function of the switching impulse withstand level where the gap factor in the Gallet-Leroy equations was selected to produce clearances (not corrected for altitude) equivalent to that of the standard clearance of 2.35 m (phase-to-earth) and 2.95 m (phase-to-phase). These gap factors were found to be 1.14 (phase-to-earth) and 1.41 (phase-to-phase). The ratio between the phase-to-phase and phase-to-earth withstand levels was 1.5, as recommended by IEC 60071 [27]. Smaller clearances are effectively possible with the same risk of failure when larger gap factors are obtained. Gap factors smaller than that of the values obtained above, will result is larger clearances required. For the calculation based on a SIWL of 800 kV as a function of the range of gap factors (1.0 – 1.8) the resulting clearance is given in Figure 4-19.

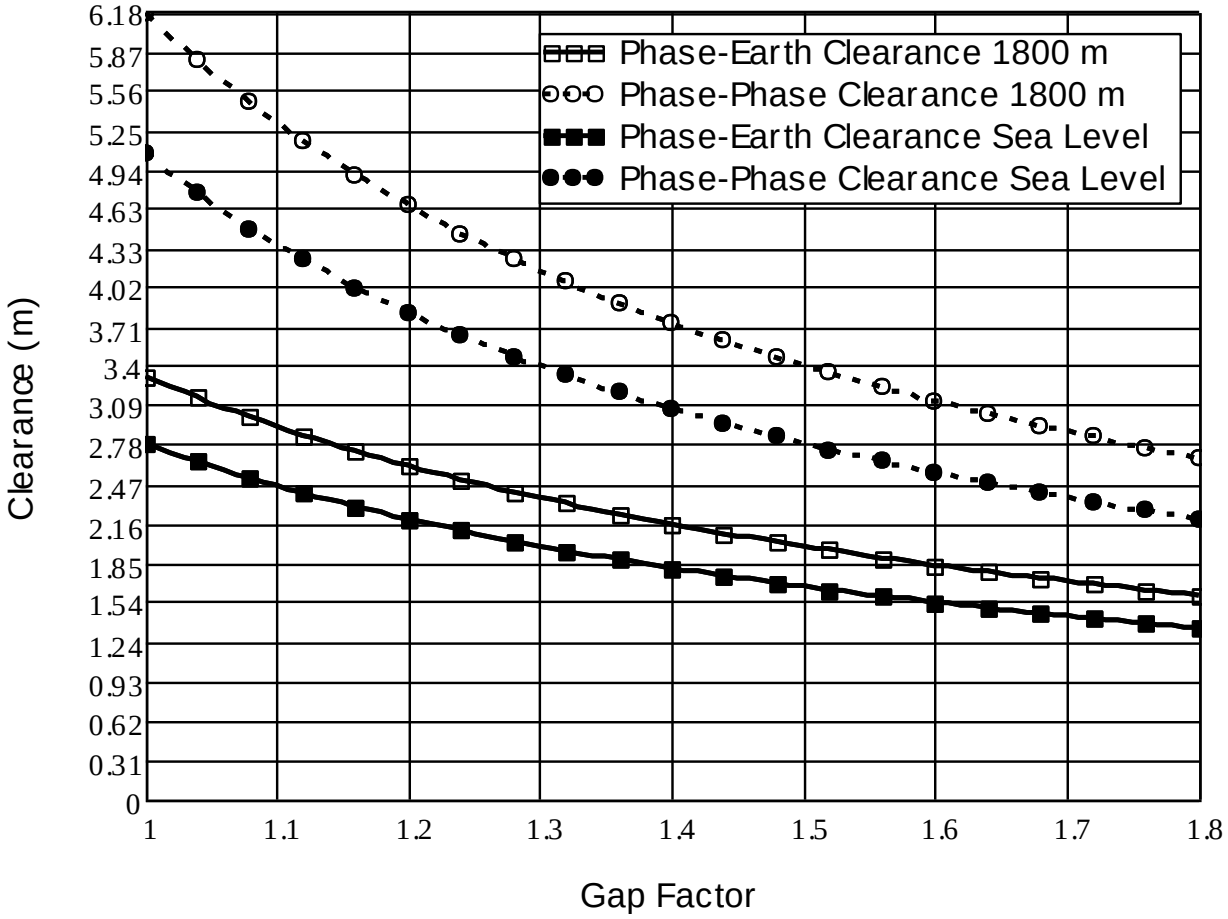


Figure 4-19: Clearance as a function of the gap factor at 800 kV SIWL

When altitude correction is considered, larger clearances are required at higher altitudes. Effectively higher values for the SIWL represents a stronger withstand capability against switching over-voltage stresses. In order to normalise the altitude corrected values (larger clearances) to values within the range of the standard clearances, the gap factor will need to be adjusted.

The larger gap factors required for the same airgap distances were 1.3 and 1.67 for phase-to-earth and phase-to-phase respectively. The results are tabulated in Table 4-23. It is

important to note that it is good practice to allow for the weaker withstand capability within the external recoverable insulation. It is better to have an external insulation failure due to lower withstand levels as opposed to having internal or non-recoverable insulation failure.

The gap factor K_g could be defined by the ratio between the positive flashover voltage for the actual gap geometry and the positive flashover voltage for a rod-plane gap. Gap factors are determined experimentally where the airgap spacing is kept constant and the gap geometry is changed. It is known that the gap factor increases slightly with the number of sub-conductors.

Table 4-23: The impact of altitude correction on preferred clearance

	Clearance (mm)		**Equivalent SIWL (kV)**		**Gap Factor**	
	***PE**	***PP**	***PE**	***PP**	***PE**	***PP**
Sea level	2350	2950	800	1200	1.14	1.41
Clearance Corrected for 1800 m	2800	3700	800	1200	1.14	1.41
Gap factor Corrected for 1800 m	2350	2950	800	1200	1.3	1.67

*PE refers to Phase-to-earth and PP refers to phase-to-phase

The electric field distribution of electrode shapes has a significant impact on the gap factor. Grading rings and hardware designs could potentially increase the gap factor to reduce the required clearances between live apparatus/conductors to the earthed structure [30].

5 CONCLUSION

5.1 Voltage range 1: 88 kV uprated to 132 kV - transient analysis

The need to investigate uprating 88 kV substations to 132 kV arises from thermal overload constraints combined with the unavailability of new servitudes. The length of 88/132 kV transmission lines evaluated within this study ranged from 10 km to 100 km.

When considering the expected over-voltages for substations in voltage range 1, lightning is considered as the dominating stress. Smaller clearances are employed within the substation and external insulation could be vulnerable to failure. The switching over-voltages were considered to be a secondary risk for external insulation. To establish confidence in the expectation of stress distributions, both lightning and switching were considered and the following was evident from the studies.

5.1.1 Fast-front transients

A typical 88 kV feeder bay layout was evaluated to establish the minimum clearances available. This feeder bay represents the typical arrangement that will be of interest when uprating is considered. The configuration and dimensions of the equipment and conductors were used for the calculation of representative surge impedances.

Cases where large distances between the equipment and the nearest surge arrester were evaluated. The stress at the equipment terminals was expected to increase as a function of the distance between its own terminals and the nearest arrester.

The results have shown that even with a very conservative approach the probability of the gap flashing over is very small. The conservative approach was modelled very simplistically where a flashover occurs when a voltage gradient of 530 kV/m is exceeded. Tower footing resistances were selected to be slightly higher than what is expected in reality. The simulations included 4 different lightning current sources, where two of the sources consisted of very high peak currents. The probability of the lightning source currents was also taken into account.

From the simulations, it was clear that for the protective margin to decrease below 25 %, the substation configuration would be impractical. Very large separation distances of 100 m to 140 m between arresters and equipment are highly unlikely in 88/132 kV substations.

It was found that additional busbar arresters installed at the bus coupler improved the arrester protective margins throughout the substation. When additional arresters were installed at both ends of the busbar the protective margins were improved significantly. It is then concluded that the inclusion of busbar arresters has a significant impact on the over-voltages and is recommended where operating configurations might include large separation distances.

For external insulation, it was clear that the stress rarely exceeded the LIWL of the equipment, which was 550 kV. Protecting the internal insulation will inherently limit the stress for external insulation failure. Additional busbar arresters will limit over-voltages further and minimise the risk even further.

The inclusion of MOV arresters on the busbars contributes to the improvement of the substation reliability. Due to the high energy content of transients initiated by severe

lightning current (such as Source 4), busbar arresters assist the line entrance arrester in dissipating the energy.

The conclusion is to coordinate the selection of insulation for the protection of the non-recoverable insulation, the probability of external insulation failing also decreases through this process. Busbar arresters will assist with the required additional energy dissipation for severe fast transient over-voltages initiated by a back-flashover close to the substation. Busbar arresters will also limit over-voltages to the maximum allowable protective margin of 25 %, where very long conductor distances separate equipment from installed arresters at the line entrances and transformers. Regarding voltage uprating in this voltage range, fast-front transient over-voltages will not be of great concern when the surge arresters are efficiently utilised within the substation.

5.1.2 Slow-front transients

It was found that the protective distance of the surge arrester during switching surges extends beyond the substation busbars. This is due to the slow surge steepness. The over-voltage stress is expected not to exceed the arrester protective level when switching surges enter the substation. The Gallet – Leroy equation yields a switching impulse withstand value of 344 kV for the airgap when the gap factors are in the range of 1.0 for phase-to-earth and 1.16 for phase-to-phase. This implies that the electrode configuration with a gap factor of 1.0 and 1.16 decreases the airgap withstand strength to its minimum. The 1 m clearance will essentially have a 90 % probability to withstand a switching surge with a peak of 344 kV.

Based on the studies performed where maximum over-voltage distributions were obtained the stress is expected not to exceed the voltage of the arrester protective level. The margin of protecting the external clearance is 52 %. It should be noted that the external clearance withstand level does not degrade over time and the smaller protective margins could be accepted.

There is significant margin of protection between the maximum stresses and the surge arrester protective level.

The internal non-recoverable insulation will be protected for switching surges by the substation MOV surge arresters. It is therefore clear that switching transients will not be of significant importance when the aim is to minimise the risk of insulation failure in an uprated substation in this voltage range.

Voltage Range 1: Summary:

- Current Eskom 88 kV clearances are expected to perform well concerning lightning and switching impulse stress when the system is uprated to 132 kV.
- Additional surge arresters will contribute significantly to limit the over-voltages throughout the whole substation.
- Protective margins should be coordinated for internal insulation levels.
- The external insulation will inherently be well protected when surge arresters are selected to protect the equipment internal insulation at 550 kV LIWL.
- Electrode configuration and grading could be enhanced to improve gap factors.
- Transmission line tower footing resistances should be measured and minimised.

5.2 Voltage range 2: 275 kV uprated to 400 kV - switching transient analysis

Multiple statistical switching studies were performed to evaluate the maximum expected over-voltage distributions. It was evident that the source parameters and transmission line lengths have a significant impact not only on the magnitude of the over-voltages, but also on the wave shapes of the over-voltages when measured from the sending end to the receiving end.

Initially a cold energisation of the line revealed that the maximum over-voltages without arresters were in the region of 2 p.u at the sending end and 3 p.u at the receiving end. The maximum expected over-voltages at the sending end occurred when the line lengths were short and source short-circuit power was weak. The opposite occurred when the maximum over-voltages were recorded on the longest line where the short-circuit power was strong.

When trapped charge was included on the transmission line, similar results but much higher magnitudes were observed. Maximum values were 3.47 p.u at the sending end and 6.32 at the receiving end.

When surge arresters were included at the sending and receiving ends of the line the over-voltages at the substation were limited to the protective level of the surge arresters. This was expected to be the case. However, the mid-point of the transmission line experienced maximum over-voltages in the range of 3 p.u.

The inclusion of pre-insertion resistors dramatically reduced the over-voltages along the line. Other alternatives should also be investigated. The addition of a maintenance burden due to more pre-insertion resistors is not recommended. Installing line arresters has proved to be a very attractive and cost effective solution. This has not been studied in detail in this work.

The maximum over-voltage scenarios were extracted from the statistical simulations to determine the following:

- Arrester energy requirement
- Arrester protective distance

It was found that the maximum switching surge steepness did not exceed values of 2.4 kV / µs at the sending end substation. For the receiving end maximum steepness the values did not exceed 4.44 kV / µs. Due to the slow-fronts, the protective distance of the arresters extends well beyond the total length of a large EHV substation. It was also found that the arrester energy demands did not exceed 1.23 MJ which relates to 50 % of its total energy capability.

Based on the Eskom standard for electrical clearances, the switching impulse withstand levels of the gaps were calculated. The results according to the Gallet – Leroy equation yielded SIWL values of 1019 kV for the phase-to-earth 2.35 m gap. When the arrester limits the voltage to 642 kV the margin of protection is in the range of 58.7 %. With the minimum protective margin required to be 25 %, and the phase-to-earth / phase-to-phase ratio required to be 1.5 the gap factors were adjusted to obtain a minimum expected SIWL for the standard air clearances. It was found that when the gap factors are reduced to 1.14 and 1.41 for phase-to-earth and phase-to-phase respectively, the SIWL values were 800 kV and 1200 kV.

This means that at sea level gap factors are not required to be larger than 1.14 and 1.41 to maintain a 25 % margin of protection within existing gaps. When at altitude of 1800 m above sea level, the withstand level is effectively reduced due to the air density being lower. But when the gap factors are increased to 1.3 and 1.67 for phase-to-earth and phase-to-phase, the same withstand levels of 800 kV and 1200 kV with a 25 % protective margin are realised.

It was found that the risk of failure for the sending and receiving end substations proved to be as low as 7 in 100000 operations when a SIWL of 800 kV was selected. For the non-recoverable insulation the standard for 400 kV SIWL is 1050 kV. The protective margin is in the range of 60.3 % with a risk of failure of 1.3×10^{-8} .

Voltage Range 2: Summary:

- Current Eskom 275 kV clearances are expected to perform well concerning switching impulse stress when the system is uprated to 400 kV.
- At sea level, gap factors of 1.14 and 1.41 produce a SIWL of 800 kV for phase-to-earth and 1200 kV for phase-to-phase.
- At 1800 m above sea level gap factors of 1.3 and 1.67 produce the required 800 kV SIWL that produces the 25 % protective margin.
- Clearance requirements should be based on the over-voltage stress and gap strength and not non-recoverable insulation withstand levels.
- Non-recoverable insulation levels are conservative considering the margins of 63 % where the required minimum is only 25 %.
- Risk of external insulation failure could be further reduced if required by improving the gap geometry to obtain larger gap factors.
- Transmission line switching and lightning performance need to be further investigated.
- Field effects such as electrostatic and electromagnetic coupling need to be further evaluated to ensure the safety of humans in uprated substations.

5.3 Recommendations and future work

When uprating is considered the following is recommended:

- Transmission line lightning and switching performance evaluations should be conducted.
- Additional over-voltage limiting methods and devices should be considered to address the stress distribution functions.
- Electromagnetic field effect studies to evaluate the intensity and exposure for humans.
- Evaluation of mechanical forces and conductor movement during short-circuits in the substation.
- Substation earth electrode optimisation.
- Electrode geometry optimisation.
- Testing of a combination of parallel external gaps to determine the gap factor of parallel gaps.
- The impact of voltage uprating on live substation work.
- Corona requirements in an uprated substation should be reviewed.

6 REFERENCES

[1] Electrical Engineering Directive Standard Insulation Levels. Electricity Supply Commission, Oct-1970.

[2] IEEE Power Engineering Society, Substations Committee, IEEE-SA Standards Board, and Institute of Electrical and Electronics Engineers, *IEEE guide for recommended electrical clearances and insulation levels in air-insulated electrical power substations*. New York, NY: Institute of Electrical and Electronics Engineers, 2007.

[3] I. Albizu, A. J. Mazon, and I. Zamora, 'Methods for increasing the rating of overhead lines', in *Power Tech, 2005 IEEE Russia*, 2005, pp. 1–6.

[4] K. Kopsidas and S. M. Rowland, 'Evaluating opportunities for increasing power capacity of existing overhead line systems', *IET Gener. Transm. Distrib.*, vol. 5, no. 1, p. 1, 2011.

[5] K. Kopsidas, S. M. Rowland, M. N. R. Baharom, and I. Cotton, 'Power transfer capacity improvements of existing overhead line systems', in *Electrical Insulation (ISEI), Conference Record of the 2010 IEEE International Symposium on*, 2010, pp. 1–5.

[6] J. R. Daconti and D. C. Lawry, 'Increasing power transfer capability of existing transmission lines', in *Transmission and Distribution Conference and Exposition, 2003 IEEE PES*, 2003, vol. 3, pp. 1004–1009.

[7] S. V. UPRATING, 'Safety aspects in substation voltage uprating', *IEEE Trans. Power Deliv.*, vol. 7, no. 3, 1992.

[8] W. J. Lannes, H. Schneider, J. A. Jones, and M. Spalding, 'Performance of uprated substations in contaminated environments', *IEEE Trans. Power Deliv.*, vol. 13, no. 4, pp. 1143–1156, 1998.

[9] J. Panek and H. Elahi, 'Substation voltage upgrading', *IEEE Trans. Power Deliv.*, vol. 4, no. 3, pp. 1715–1724, 1989.

[10] A. R. Hileman, *Insulation coordination for power systems*. CRC Press, 1999.

[11] A. C. Report, 'A Guide for Minimum Electrical Clearances for Standard Basic Insulation Levels [includes discussion]', *Power Appar. Syst. Part III Trans. Am. Inst. Electr. Eng.*, vol. 73, no. 1, 1954.

[12] I. C. Report, 'Second Interim Report-Minimum Electrical Clearances for Substations Based on Switching Surge Requirements', *Power Appar. Syst. IEEE Trans. On*, vol. 84, no. 5, pp. 415–417, 1965.

[13] P. Bellaschi, P. R. Dolan, and E. R. Taylor, 'Minimum Line-To-Ground Electrical Clearances for EHV Substations Based on Switching Surge Requirements', *Power Appar. Syst. IEEE Trans. On*, no. 5, pp. 1924–1930, 1972.

[14] Gallet, G., et al., "Switching impulse results obtained on the outdoor testing area at Renardieres," IEEE Transactions on Power Apparatus and Systems, vol. PAS-95, pp. 580–585, Mar./Apr. 1976.

[15] A.J.S Groenewald, Eskom Substation layout design guide, Insulation coordination and electrical clearances. 2011.

[16] J. R. Daconti and D. C. Lawry, 'Increasing power transfer capability of existing transmission lines', in *Transmission and Distribution Conference and Exposition, 2003 IEEE PES*, 2003, vol. 3, pp. 1004–1009.

[17] IEC Publication 71-1-1976, Insulation coordination, Part 1: Terms, definitions and rules.'

[18] IEEE Power Engineering Society, Substations Committee, IEEE-SA Standards Board, and Institute of Electrical and Electronics Engineers, *IEEE guide for recommended electrical clearances and insulation levels in air-insulated electrical power substations*. New York, NY: Institute of Electrical and Electronics Engineers, 2007.

[19] Switching overvoltages in EHV and UHV systems with special reference to closing and reclosing transmission lines. CIGRE Working Group 13.02.

[20] L. Van der Sluis, *Transients in power systems*. Chichester ; New York: Wiley, 2001.

[21] *Transmission Line Grounding Volume 1. EPRI, Palo Alto, CA: 1982. EL-2699. Volume 1.*

[22] *AC Transmission Line Reference Book – 200 kV and Above, Third edition. EPRI, Palo Alto, CA: 2005. 1011974.* .

[23] *Cigré SC33 WG 01 Guide to procedures for estimating the lightning performance of transmission lines, Cigré Brochure 63, October 1991.* .
[24] Institute of Electrical and Electronics Engineers, *IEEE guide for the application of metal-oxide surge arresters for alternating-current systems*. New York: Institute of Electrical and Electronics Engineers, 2009.
[25] Anderson, R. B. and A. J. Eriksson. 1980. Lightning parameters for engineering application. Electra 69: 65- 102. .
[26] Lightning parameters for engineering applications. CIGRE Working Group C4, Aug-2013.
[27] IEC 60071-2 (1996), Insulation coordination application guide. .
[28] A. Eriksson, J. Grandl, and O. Knudsen, 'Optimized line switching surge control using circuit-breakers without closing resistors', Sep. 1990.
[29] C4_203_2014 cigre switching paper .
[30] CIGRE Working group 07, Study Committee 33, "Guidelines for Evaluation of the Dielectric Strength of External Insulation," CIGRE Technical Brochure 72, 1992. .
[31] L. Paris and R. Cortina, 'Switching and lightning impulse discharge characteristics of large air gaps and long insulator strings', *IEEE Trans. Power Appar. Syst.*, no. 4, pp. 947–957, 1968.
[32] F. M. Couquelet *et al.*, 'Application of Insulators in a Contaminated Environment', *IEEE Trans. Power Appar. Syst.*, vol. 98, no. 5, 1979.
[33] I. Kimoto, K. Kito, and T. Takatori, 'Anti-pollution design criteria for line and station insulators', *IEEE Trans. Power Appar. Syst.*, no. 1, pp. 317–327, 1972.
[34] R. Matsuoka *et al.*, 'Assessment of basic contamination withstand voltage characteristics of polymer insulators', *IEEE Trans. Power Deliv.*, vol. 11, no. 4, pp. 1895–1900, 1996.
[35] IEEE International Committee on Electromagnetic Safety on Non-Ionizing Radiation, Institute of Electrical and Electronics Engineers, and IEEE-SA Standards Board, *IEEE standard for safety levels with respect to human exposure to electromagnetic fields, 0-3kHz*. New York, N.Y.: Institute of Electrical and Electonics Engineers, 2002.

7 APPENDICES

7.1 Voltage range 1 and 2 statistical switching study ATP model

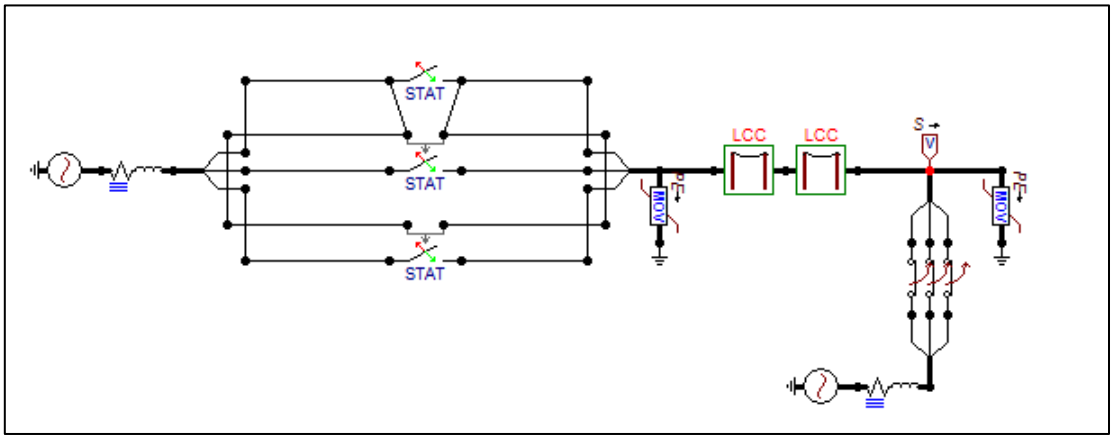


Figure 7-1: Statistical switching study ATP model.

7.2 Voltage range 2 back-flashover ATP model

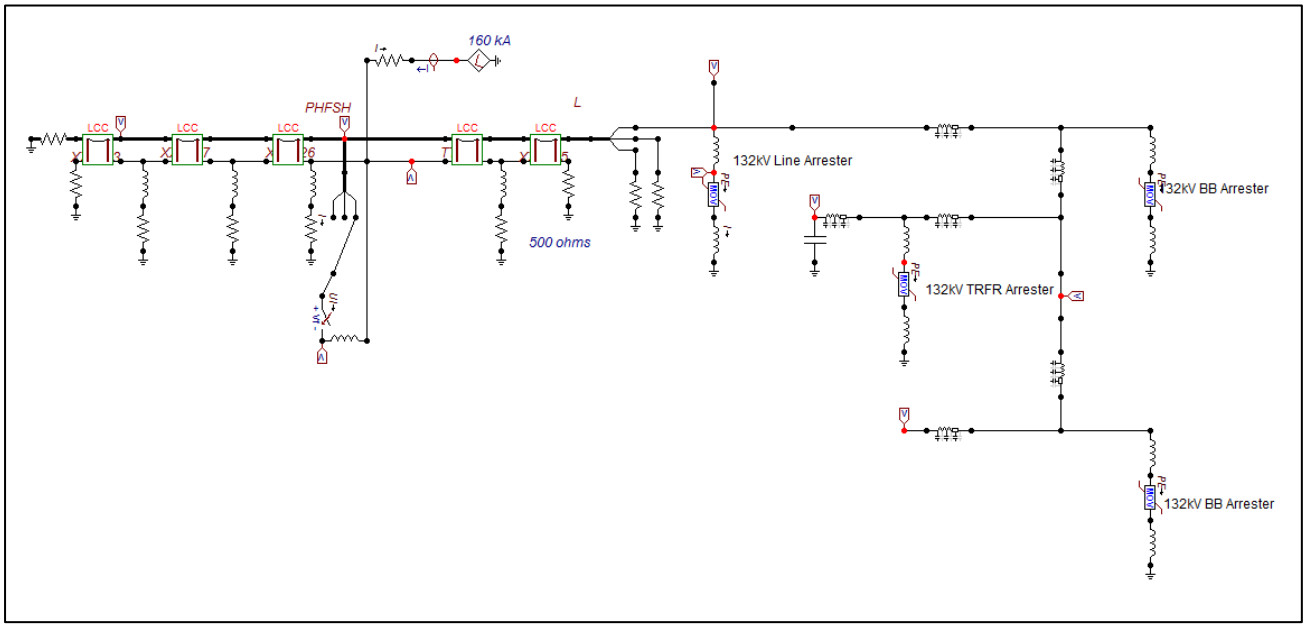


Figure 7-2: Back-flashover ATP model.